การออกแบบ สังเคราะห์ และทดสอบฤทธิ์ทางชีวภาพของตัวยับยั้งเอนไซม์ Janus Kinase 3 ที่เป็นอนุพันธ์ของ Thieno[3,2-*d*]pyrimidine

DESIGN SYNTHESIS AND BIOLOGICAL EVALUATION OF THIENO[3,2-d]PYRIMIDINE DEVIVATIVE JANUS KINASE 3 INHIBITORS

ภูวดล ฟูเกษม

POOWADON FUKASEM

วิทยานิพนธ์นี้เป็นส่วนหนึ่งของการศึกษาตามหลักสูตรปริญญาวิศวกรรมศาสตรมหาบัณฑิต

สาขาวิชาวิศวกรรมชีวการแพทย์

คณะวิศวกรรมศาสตร์

สถาบันเทคโนโลยีพระจอมเกล้าเจ้าคุณทหารลาดกระบัง

พ.ศ.2567

KMITL-2024-EN-M-317-310

DESIGN SYNTHESIS AND BIOLOGICAL EVALUATION OF THIENO[3,2-d]PYRIMIDINE DEVIVATIVE JANUS KINASE 3 INHIBITORS

POOWADON FUKASEM

A THESIS SUBMITTED IN PARTIAL FULFILLMENT
OF THE REQUIREMENT FOR THE DEGREE OF
MASTER OF ENGINEERING IN BIOMEDICAL ENGINEERING
SCHOOL OF ENGINEERING
KING MONGKUT'S INSTITUTE OF TECHNOLOGY LADKRABANG
2024

KMITL-2024-EN-M-317-310

หัวข้อวิทยานิพนธ์	การออกแบบ สังเคราะห์และทดสอบฤทธิ์ทางชีวภาพของตัวยับยั้งเอนไซม์ Janus Kinase 3 ที่เป็นอนุพันธ์ของ Thieno[3,2-d]pyrimidine
นักศึกษา	นาย ภูวดล ฟูเกษม
รหัสประจำตัว	64601112
ปริญญา	วิศวกรรมศาสตรมหาบัณฑิต
สาขาวิชา	วิศวกรรมชีวการแพทย์
พ.ศ.	2567
อาจารย์ที่ปรึกษาวิทยานิพนธ์	รศ.ดร.แมทธิว พอล กลีสัน

บทคัดย่อ

เอนไซม์ Janus Kinase 3 (JAK3) เป็นหนึ่งในเอนไซม์กลุ่ม Janus Kinase Family มีบทบาทสำคัญในวิถีการส่งสัญญาณของระบบภูมิคุ้มกัน และได้รับการระบุแล้วว่าเป็นเป้าหมายสำหรับการรักษาโรคในกลุ่มการอักเสบที่เกี่ยวข้องกับระบบภูมิคุ้มกันได้ เช่นโรคข้ออักเสบ โรคภูมิคุ้มกันบกพร่อง หรือโรคแพ้ภูมิตัวเอง ในงานวิจัยฉบับนี้ได้ทำการออกแบบสารยับยั้งเอนไซม์ JAK3 บนพื้นฐานโครงสร้างของยาสำหรับต้าน JAK3 ที่ได้รับการขึ้นทะเบียนแล้ว ร่วมกับสารยับยั้งเอนไซม์ JAK3 ในขั้นกำลังพัฒนา โดยเลือกอนุพันธ์ของ Thieno[3,2-d]pyrimidine เป็นโครงสร้างหลัก และแทนที่หมู่ฟังก์ชันในตำแหน่งที่ 2 และ 4 ในการศึกษาขั้นตอนการสังเคราะห์และหาสภาวะที่เหมาะในการสังเคราะห์พบว่าผลได้ร้อยละของสารที่สังเคราห์ได้ในขั้นสุดท้ายอยู่ในช่วงร้อยละ 10-60 จากผลการวิเคราะห์แบบจำลองโมเลกุลเชิงพลวัต (MD simulation) ระหว่าง JAK3 กับสารที่ออกแบบ พบว่าแบบจำลองสามารถทำนายได้ว่าโมเลกุลของสารที่ออกแบบสามารถจับกับ JAK3 (PDB ID: 4Z16) ได้อย่างเสถียรเมื่อเทียบกับสารอ้างอิง และจากผลการวิเคราะห์ยังสามารถทำนายได้ว่า สารหมายเลข 42 มีความเป็นไปได้ที่จะมีฤทธิ์ยับยั้ง JAK3 ได้ดีที่สุด และ จากผลการทดสอบฤทธิ์ในการยับยั้ง JAK3 ของสาร 22-49 พบว่าที่ความเข้มข้น 1 μM เกินครึ่งของสารที่ออกแบบสามารถยับยั้งการทำงานของ JAK3 ได้ร้อยละ 40-91 (%inhibition) ใกล้เคียงกับยา Tofacitinib (ร้อยละ 98) โดยสารหมายเลข 42 มีค่ายับยั้งการทำงานของ JAK3 ดีที่สุด ที่ร้อยละ 91 ยืนยันด้วยค่าความเข้มข้นต่ำสุดของสารที่ยับยั้งการทำงานของ JAK3 ได้ร้อยละ 50 (JAK3 IC_{50}) ของสารหมายเลข 42 อยู่ที่ 6.24 nM ซึ่งสูงกว่า Tofacitinib (14.11 nM) สอดคล้องกับผลการวิเคราะห์แบบจำลองโมเลกุลเชิงพลวัต

Thesis	Design Synthesis and Biological Evaluation of Thieno[3,2-d]pyrimidine Derivative Janus Kinase 3 Inhibitors
Student	Mr. Poowadon Fukasem
Student ID.	64601112
Degree	Master of Engineering
Program	Biomedical Engineering
Year	2024
Thesis Advisor	Assoc. Prof. Dr. Matthew Paul Gleeson

ABSTRACT

Janus Kinase 3 (JAK3) is one of the enzymes in the Janus Kinase Family, playing a crucial role in immune system signaling pathways. It has been identified as a key therapeutic target for immune-mediated inflammatory diseases such as arthritis, immunodeficiency disorders, and autoimmune diseases. In this study, we designed a set of 28 JAK3 inhibitors based on the structure of approval JAK3 inhibitors and inhibitors under the development compounds. Thieno[3,2-d]pyrimidine derivatives were chosen as the core structure, functional groups were substituted at positions 2 and 4. The synthesis conditions have been optimized and yielded a final product with a %yield ranging from 10-60%. Molecular Dynamics (MD) simulations were performed to study the interaction between JAK3 and the designed compounds, the result predicted that the designed molecules could bind stably to JAK3 (PDB ID: 4Z16) compared to reference compounds. The analysis also predicted that compound 42 is the most likely to exhibit the strongest inhibitory activity against JAK3. In the JAK3 inhibition assay, testing compounds 22-49 at a concentration of 1 μM showed that more than half of the designed compounds inhibited JAK3 activity by 40-91% (% inhibition), which is comparable to Tofacitinib (98%). Compound 42 demonstrated the highest inhibition at 91%, confirmed by its JAK3 IC_{50} which was found to be 6.24 nM, lower than that of Tofacitinib (14.11 nM). These results related to the MD simulation.

ACKNOWLEDGEMENT

This thesis has been successfully completed with the support and contributions from several organizations and individuals. I would like to express my deepest gratitude to Associate Professor Dr. Matthew Paul Gleeson, my thesis advisor, for his valuable knowledge and guidance throughout the experiments, data interpretation, and report writing, as well as for his financial support for living expenses. Additionally, I appreciate his permission to use the facilities at the Computational and Medicinal Chemistry Laboratory in the Department of Biomedical Engineering, KMITL, which provided fully equipped instruments, chemicals for synthesis, and a cluster computing system for modeling. I would also like to sincerely thank Professor Dr. Kiattawee Choowongkomon from the Department of Biochemistry, Faculty of Science, Kasetsart University, for allowing me to use his laboratory, equipment, and chemicals for Biochemical Assay testing. My thanks extend to Associate Professor Dr. Duangkamol Gleeson for facilitating the submission of samples for NMR analysis at the Scientific Instrument Center, Faculty of Science, KMITL. Additionally, I am grateful to Associate Professor Dr. Kanokthip Boonyaratgalin for allowing me to access the HPLC machine at the Nanotechnology and Material Analytical Instrument Service Unit, College of Material Innovation and Technology, KMITL. I also wish to acknowledge the Scientific Equipment Center, Faculty of Science, Kasetsart University, for the analysis of samples using Mass Spectrophotometry. Special thanks to all the members of CMCL for their helpful advice and support throughout my time in the laboratory, which enabled the completion of this thesis.

Lastly, this thesis would not have been possible without the knowledge and kindness of everyone mentioned. I thank fate and the extraordinary support that brought everyone's efforts together to make this thesis a success.

Poowadon Fukasem

TABLE OF CONTENTS

Page

LIST OF TABLES

LIST OF FIGURES

Figure Page

LIST OF ABBREVIATIONS AND SYMBOLS

Å	angstrom
ADP	adenosine diphosphate
ATP	adenosine triphosphate
BTK	Broton's tyrosine kinase
C	carbon
COX	cyclooxygenase
cryo-EM	cryo-electron microscopy
CYS	Cysteine
DCM	Dichloromethane
DMARDs	Disease-Modifying Antirheumatic Drugs
EGFR	epidermal growth factor receptor
EtOAc	Ethyl acetate
EtOH	Ethanol
H	Hydrogen
HPLC	High Performance Liquid Chromatography
IBD	inflammatory bowel diseases
IC50	half maximal inhibitory concentration
IFN	interferon
IL	interleukin
IMIDs	Immune-mediated inflammatory diseases
JAK	Janus Kinase
JH	JAK homology
LEU	leucine
MD	Molecular Dynamics
MET	Methionine
Mg2SO4	Magnesium sulfate
mL	milliliter
MS	multiple sclerosis
N	nitrogen
NaOH	Sodium Hydroxide
nM	nano molar

NMR	nuclear magnetic resonance
ns	Nano Second
NSAID	Non-Steroidal Anti-Inflammatory Drugs
O	oxygen
PDB	Protein data bank
RA	rheumatoid arthritis
S	sulfur
SAR	Structure Activity Relation
SBDD	Structure-Based Drug Design
SLE	systemic lupus erythematosus
STAT	signal transducer and activator of transcription
TEA	Triethylamine
TFA	trifluoroacetic acid
TNF- α	tumor necrosis factor-alpha
TYK2	Tyrosine Kinase 2
WHO	World Health Organization

CHAPTER 1

INTRODUCTION

1.1 STATEMENT AND SIGNIFICANCE OF PROBLEM

In recent decades, immune-mediated diseases have emerged as a significant health concern globally, presenting complex challenges in diagnosis and treatment in a spectrum of disorders such as rheumatoid arthritis, inflammatory bowel disease, and psoriasis [1]. These conditions were characterized by dysregulated immune responses targeting the body's own tissues in the patients. The prevalence of these conditions has seen a remarkable upsurge, affecting millions of individuals worldwide [2]. According to the World Health Organization (WHO), autoimmune diseases alone afflict over 5% of the global population, with a disproportionate impact on women [3]. This epidemiological trend underscores the pressing need for a deeper understanding of immune dysregulation and innovative therapeutic approaches to alleviate the substantial burden these diseases impose on individuals and healthcare systems globally [2]. As researchers delve deeper into the underlying mechanisms driving these disorders, the role of kinase enzymes has garnered considerable attention due to their pivotal involvement in immune system regulation and pathological processes.:

Kinases are a group of over 500 phosphate transfer enzymes that control the reduction of the phosphate group from adenosine triphosphate (ATP) into adenosine diphosphate (ADP) through the process called “phosphorylation” [4]. This occurs in various types of cells that are involved in many functions such as intracellular signaling, cell proliferation and apoptosis. The mutation or overexpression of kinases can induce some diseases in the human body such as cancer. Janus Kinase 3 (JAK3) is a non-receptor intracellular tyrosine kinase belonging to the JAK family including 4 isoforms JAK1, JAK2, JAK3 and TYK2 which can bind to type I/II cytokine receptor [5]. JAK3 expression in leukocytes and plays an important role in leucocyte downstream signaling pathways that control immunological responses, but dysregulation of JAK3 has been implicated in the development of blood cancer, inflammatory diseases, and autoimmune diseases [6]. In recent years there have emerged some medical treatments that use a small molecule inhibitor binds to a target kinase instead of ATP to inhibit the kinase activity.

Although kinase inhibitors have become more popular for disease treatment in the past few years because of known binding mode of ATP into kinases from crystallographic experiment and inhibitors were designed by using aromatic heterocycles, including pyrimidine, to mimic the structure of its natural substrate ATP [7]. The challenge in this process is to obtain a potent inhibitor with low toxicity to human normal cells and low side effects to patients by limiting the activity against other targets at the same time. This is a particular problem for JAK inhibitors targeting the ATP-binding site. A number of JAK inhibitors have been developed with FDA approval, including Tofacitinib, a pan-JAK inhibitor has a potent activity against JAK1, JAK2, and JAK3 approved for treatment of rheumatoid arthritis patients, [8] Ruxolitinib and Fedratinib were reported as JAK1/JAK2 inhibitor for myelofibrosis treatment [9]. From these examples, there is only Tofacitinib that approved the activity against JAK3. However, it also can inhibit JAK1 and JAK2 to some degree [10].

To improve the selectivity of JAK3 inhibitors, the active site of a large number of JAK3 inhibitor-enzyme structures have been identified to facilitate development. All of JAK family members have methionine residue 902 (MET902) in the back pocket, while JAK3 is the only one member that has a unique cysteine residue at position 909 (CYS909) [11]. The sulfur atom of this residue can react with electrophile of an inhibitor such as Michael acceptor resulting in covalent bond. This structure was equivalent to epidermal growth factor receptor T790M (EGFR T790M) at CYS797 and Broton's tyrosine kinase (BTK) at CYS481 which have been successfully targeted by covalent inhibitors. Olmutinib contains an acrylamide warhead that targets CYS797 in EGFR, and Ibrutinib contains 2-butynamide warhead that targets CYS481 in BTK [12, 13].

In recent years, researchers reported the development of covalent JAK3 and relevant kinase inhibitors. In 2015, Tan L et al. reported the high potent activity pyrimidine based JAK3 covalent inhibitor [14] which has benzylamine as a linker group connected to acrylamide Michael acceptor. Thorarensen et al. reported Pyrrolopyrimidine JAK3 covalent inhibitor with acrylamide substituted piperidine linker (Ritlecitinib) that have high selectivity for JAK3 [15].

In this study, we have applied structure-based design to develop new JAK3 inhibitors based on the 2,4-diaminothieno[3,2-d]pyrimidine scaffold. We have focused on exploring the effect of incorporating different electrophilic groups on JAK3 activities,

incorporation of polar moieties to improve physical properties, including lipophilicity and solubility.

In total, 28 compounds have been prepared that incorporate new smaller, more polar aromatic amines at the 2-position of pyrimidine. We modified the 4-substituted by introducing 6 different cyclic aliphatic amine linkers and modify the electrophilic groups attached, which can affect the suicidal complex formation. The SAR of compounds has then been assessed at JAK3 enzyme, and Molecular Dynamics (MD) simulation has been used to understand the behavior of the compound with different linker groups into binding site which can be related back to their JAK3 activity.

1.2 GOAL AND OBJECTIVES

We are going to discover the JAK3 inhibitors that could bind in the JAK3 ATP binding site and apply the aliphatic cyclic amine functional groups with the difference size, length and stereoisomers in order to tightly bind in active site of the protein target and solubility improvement, then synthesized the series of 30 compounds and assessed within biochemical and biological assays by our established academic collaborators.

1. To get better understanding about Structure Activity Relation (SAR) and design JAK3 inhibitors using structure-base design approach.

2. To Synthesize 30 novel compounds based on Thieno[3,2-d]pyrimidine scaffold as inhibitors to inhibit JAK3 activity.

3. To discover the new route of synthesis to make the compounds associated with JAK3 inhibitor.

4. To evaluate JAK3 inhibition activity of the compounds that we have synthesized.

1.3 SCOPE OF THE STUDY

This research emphasizes the development of methods for Janus Kinase 3 (JAK3) treatment in drug form. The research involves a multi-disciplinary study effort covering. (a) computational inhibitors target analysis, (b) Thieno[3,2-d]pyrimidine-based compounds synthesis and characterization and (c) biological assay being performed by established our collaborator at Kasetsart University, Thailand.

CHAPTER 2

THEORY AND LITERATURE REVIEW

2.1 IMMUNE MEDIATED INFLAMMATORY DISEASES (IMIDS)

Immune-mediated inflammatory diseases (IMIDs) represent a broad spectrum of chronic disorders characterized by dysregulated immune responses that result in persistent inflammation and tissue damage. IMIDs encompass a diverse group of diseases, including rheumatoid arthritis (RA), psoriasis, systemic lupus erythematosus (SLE), inflammatory bowel diseases (IBD) such as Crohn's disease and ulcerative colitis, and multiple sclerosis (MS) [16]. The hallmark feature of IMIDs is the breakdown of immune tolerance, which leads to the inappropriate activation of both the innate and adaptive immune systems [17].

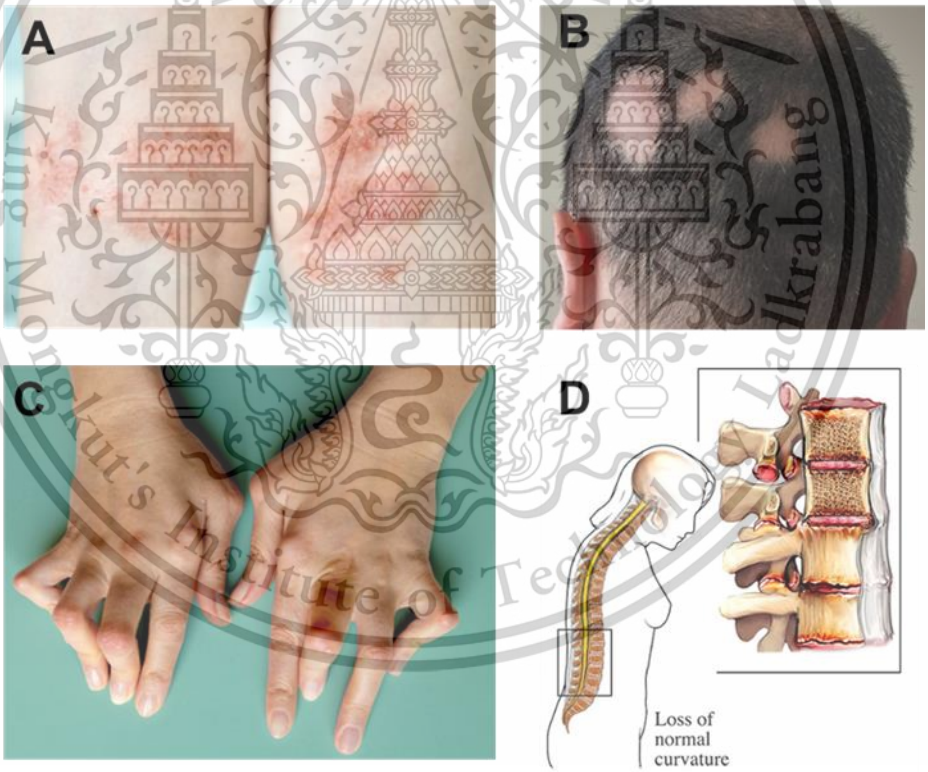

Figure 1 Examples of IMIDs represented in (A) Atopic dermatitis, (B) Alopecia areata, (C) Rheumatoid arthritis and (D) Ankylosing-spondylitis [17].

2.1.1 Pathophysiology of IMIDs This section includes:

The pathogenesis of IMIDs is driven by a complex interplay between genetic predispositions, environmental factors, and immune system abnormalities. A common feature across IMIDs is the aberrant activation of immune cells, particularly T-cells, B-cells, macrophages, and dendritic cells (Figure 2). These cells contribute to the production of pro-inflammatory cytokines, including tumor necrosis factor-alpha (TNF- α), interleukins (ILs) such as IL-1, IL-6, and IL-17, and interferons (IFNs). These cytokines amplify the inflammatory response, leading to tissue damage in affected organs [18].

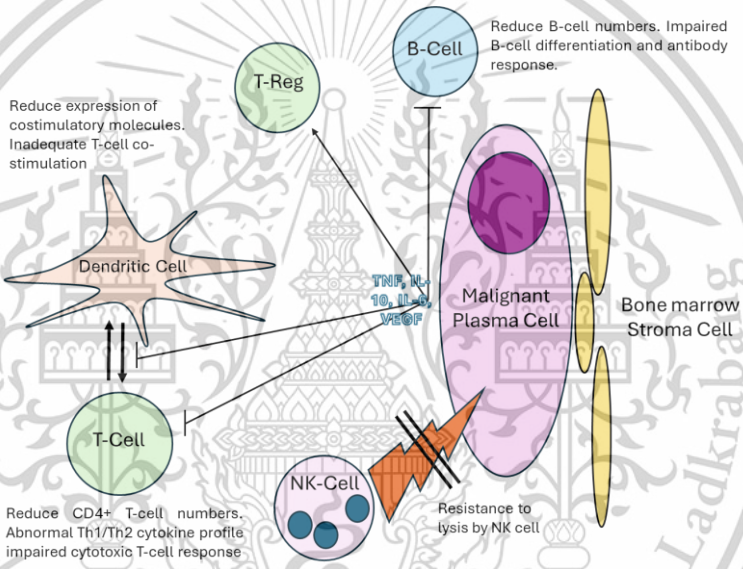

Figure 2 Multiple Myeloma induces immunoparesis. Plasma cell derived cytokines including transforming growth factor (TGF)- b, interleukin (IL)-10, IL-6 and VEGF mediate suppression of B and T lymphocytes and impair T-cell co-stimulation by dendritic cells (DC), ultimately leading to poor tumor-specific immune response [19].

For example, in rheumatoid arthritis, activated T-cells and macrophages infiltrate the synovium of joints, leading to the production of cytokines like TNF-α, which in turn promotes cartilage and bone destruction. In psoriasis, dysregulation of the IL-23/IL-17 axis has been shown to drive the excessive proliferation of keratinocytes, resulting in the characteristic plaques. Similarly, in IBD, immune cells infiltrate the intestinal mucosa, contributing to chronic inflammation and ulceration [20].

2.1.2 Genetic and Environmental Factors

While the exact etiology of IMIDs remains unknown, genetic susceptibility plays a significant role in disease onset. Polymorphisms in genes associated with immune regulation, such as those encoding for HLA molecules, cytokine receptors, and signaling proteins, have been linked to the development of IMIDs [21, 22]. For example, specific HLA-DR alleles are associated with an increased risk of developing rheumatoid arthritis and type 1 diabetes [23].

Environmental factors also contribute to the pathogenesis of IMIDs. Infections, smoking, and alterations in the microbiome have all been implicated in triggering or exacerbating immune responses in genetically predisposed individuals. In particular, the hygiene hypothesis suggests that reduced exposure to pathogens in early life can lead to an increased risk of autoimmune and inflammatory diseases [3].

2.1.3 Epidemiology and Clinical Presentation

IMIDs are prevalent worldwide, affecting millions of individuals. Their incidence varies by disease and population, with some IMIDs more common in certain geographic regions and ethnic groups. Rheumatoid arthritis, for example, has a global prevalence of approximately 1%, while psoriasis affects about 2-3% of the population [24]. IMIDs are often associated with significant morbidity, leading to a reduced quality of life and increased healthcare burden due to their chronic nature [25].

The clinical presentation of IMIDs depends on the organs involved and the extent of inflammation [26]. In rheumatoid arthritis, patients typically experience joint pain, swelling, and stiffness [27]. In IBD, symptoms include abdominal pain, diarrhea, and weight loss [28]. Psoriasis presents with red, scaly skin lesions, while multiple sclerosis is characterized by neurological deficits such as muscle weakness and visual disturbances [29]. Despite their differences, IMIDs share overlapping immune mechanisms, suggesting that therapeutic approaches targeting these common pathways may be effective across multiple diseases [30].

2.1.4 Advances in IMID Research

Recent advances in molecular and genetic research have enhanced our understanding of IMIDs. The discovery of cytokine signaling pathways, such as the TNF, IL-6, and JAK-STAT pathways, has opened new avenues for therapeutic intervention [31].

In summary, IMIDs are a group of chronic disorders driven by dysregulated immune responses, resulting in persistent inflammation and tissue damage. Although each disease presents with distinct clinical features, they share common immune mechanisms, making them suitable targets for immunomodulatory therapies.

2.2 IMIDS THERAPEUTICS

The therapeutic landscape for immune-mediated inflammatory diseases (IMIDs) has undergone significant transformations in recent decades, shifting from broad-spectrum anti-inflammatory drugs to targeted biologics and small molecules. The primary goal of IMID therapies is to reduce inflammation, alleviate symptoms, and prevent disease progression [32]. However, the heterogeneity of IMIDs in terms of their immune pathways requires a diverse set of therapeutic strategies. Current treatments can be broadly categorized into traditional therapies, biologic agents, and small molecule inhibitors, each with distinct mechanisms of action [25].

2.2.1 Traditional Therapies for IMIDs

Historically, the management of IMIDs relied on non-specific anti-inflammatory and immunosuppressive agents, including Non-Steroidal Anti-Inflammatory Drugs (NSAIDs) [33]. NSAIDs, such as ibuprofen and naproxen, are commonly used to manage pain and inflammation in diseases like rheumatoid arthritis and ankylosing spondylitis. These drugs inhibit cyclooxygenase (COX) enzymes, reducing prostaglandin synthesis and thereby alleviating inflammation [34]. However, they do not modify disease progression and can have gastrointestinal and cardiovascular side effects with prolonged use.

Corticosteroids, such as prednisone, have potent anti-inflammatory and immunosuppressive effects by inhibiting multiple inflammatory pathways [35], including cytokine production and leukocyte recruitment. Despite their

effectiveness in quickly controlling inflammation, long-term use is associated with significant adverse effects, including osteoporosis, hyperglycemia, and increased infection risk [36].

Conventional Disease-Modifying Antirheumatic Drugs (DMARDs): DMARDs, such as methotrexate, sulfasalazine, and hydroxychloroquine, are used to slow the progression of IMIDs like rheumatoid arthritis by interfering with immune cell function and cytokine production [37]. Methotrexate, a folate antagonist, remains the gold standard for many IMIDs due to its efficacy and relatively favorable safety profile [38]. However, its slow onset of action and variable patient response often necessitate the use of more targeted therapies [39].

2.2.2 Biologic Therapies in IMIDs

The advent of biologic agents has revolutionized the treatment of IMIDs by offering highly targeted approaches that modulate specific components of the immune system. Biologics are typically monoclonal antibodies or recombinant proteins that neutralize pro-inflammatory cytokines or inhibit immune cell function [40]. The most prominent classes of biologics include:

TNF Inhibitors: Tumor necrosis factor-alpha (TNF-α) plays a central role in the inflammatory processes of many IMIDs [41]. TNF inhibitors, such as infliximab, etanercept, and adalimumab, block the interaction between TNF-α and its receptors, thereby reducing inflammation and halting disease progression [42]. TNF inhibitors have demonstrated efficacy in conditions such as rheumatoid arthritis, ankylosing spondylitis, psoriasis, and Crohn's disease. However, they are associated with an increased risk of infections, particularly tuberculosis, as TNF-α is critical for immune responses against intracellular pathogens [43].

IL-6 Inhibitors: Interleukin-6 (IL-6) is a cytokine involved in the acute-phase response and chronic inflammation in IMIDs. Tocilizumab, an IL-6 receptor antagonist, has been approved for the treatment of rheumatoid arthritis and other inflammatory diseases [44]. By inhibiting IL-6 signaling, tocilizumab effectively reduces joint damage and systemic inflammation, with

some studies showing its superiority to TNF inhibitors in specific patient populations [45].

IL-12/23 and IL-17 Inhibitors: IL-12, IL-23, and IL-17 are cytokines implicated in the pathogenesis of psoriasis, psoriatic arthritis, and Crohn's disease [46]. Ustekinumab (an IL-12/23 inhibitor) and secukinumab (an IL-17 inhibitor) are biologics that specifically target these cytokines, reducing inflammation and skin lesions in patients with moderate to severe psoriasis. These therapies have shown long-term efficacy in controlling disease symptoms with relatively fewer side effects compared to earlier biologics [47].

B-cell and T-cell Modulators: B-cells and T-cells play critical roles in autoimmunity and inflammation [48]. Rituximab, a monoclonal antibody that depletes CD20+ B-cells, is used in the treatment of rheumatoid arthritis and other B-cell-mediated diseases such as systemic lupus erythematosus [49]. Similarly, abatacept, a T-cell co-stimulation blocker, prevents the activation of T-cells by inhibiting the interaction between CD80/86 on antigen-presenting cells and CD28 on T-cells. These therapies target key immune cells involved in the autoimmune response and are effective in patients who do not respond to TNF inhibitors [50].

2.2.3 Small Molecule Inhibitors

Small molecule inhibitors, particularly Janus kinase (JAK) inhibitors, represent a newer class of oral therapies for IMIDs. These drugs target intracellular signaling pathways involved in cytokine-mediated immune responses, offering a convenient alternative to injectable biologics [51].

Janus Kinase (JAK) Inhibitors: JAK inhibitors, such as tofacitinib, baricitinib, and upadacitinib, selectively inhibit one or more JAK enzymes (JAK1, JAK2, JAK3, and TYK2), which are essential for the signaling of several pro-inflammatory cytokines. By blocking JAK-STAT signaling, these inhibitors reduce cytokine-driven inflammation [52]. JAK inhibitors are approved for the treatment of rheumatoid arthritis, psoriatic arthritis, and ulcerative colitis, offering a promising oral option for patients who prefer non-biologic therapies [53]. However, concerns about adverse effects, such as increased risk of

infections and thrombosis, have necessitated ongoing monitoring and risk mitigation strategies.

2.2.4 Combination Therapy and Personalized Medicine

In clinical practice, combination therapy, involving the use of DMARDs alongside biologics or small molecules, is often employed to enhance therapeutic efficacy and prevent disease progression. For example, methotrexate is commonly used in combination with TNF inhibitors in rheumatoid arthritis to improve outcomes and reduce the development of anti-drug antibodies [54].

The future of IMID therapeutics is moving towards personalized medicine, where treatment is tailored to the individual patient based on their genetic, molecular, and clinical characteristics. Advances in pharmacogenomics and biomarker discovery may soon enable clinicians to predict a patient's response to specific therapies, minimizing trial-and-error approaches and improving long-term outcomes.

2.2.5 Limitations and Future Directions

Despite the availability of numerous therapeutic options, many IMID patients experience suboptimal responses or develop resistance to treatment over time [54]. Additionally, the long-term safety of biologics and JAK inhibitors remains a concern, particularly with regard to infection risk and malignancy. There is a need for new therapeutic strategies that provide sustained efficacy with fewer side effects.

Ongoing research is focused on developing next-generation biologics, including bispecific antibodies that target multiple cytokines simultaneously, as well as cell-based therapies, such as CAR-T cells, for refractory cases [55]. The discovery of novel pathways involved in immune regulation, such as those associated with the microbiome, offers exciting opportunities for future drug development.

2.3 JANUS KINASE (JAK)

Janus kinases (JAKs) are a family of non-receptor tyrosine kinases that play a critical role in mediating intracellular signaling for numerous cytokines and growth factors involved in immune regulation, hematopoiesis, and inflammation [56]. The JAK family consists of four members: JAK1, JAK2, JAK3, and TYK2 (Tyrosine Kinase 2), all of which function by transducing signals from cell surface cytokine receptors to the nucleus, where they regulate gene expression via the STAT (Signal Transducer and Activator of Transcription) family of proteins [57]. The JAK-STAT pathway is integral to the regulation of immune responses, and dysregulation of this pathway has been implicated in the pathogenesis of various immune-mediated inflammatory diseases (IMIDs).

2.3.1 Structure and Function of JAK Proteins

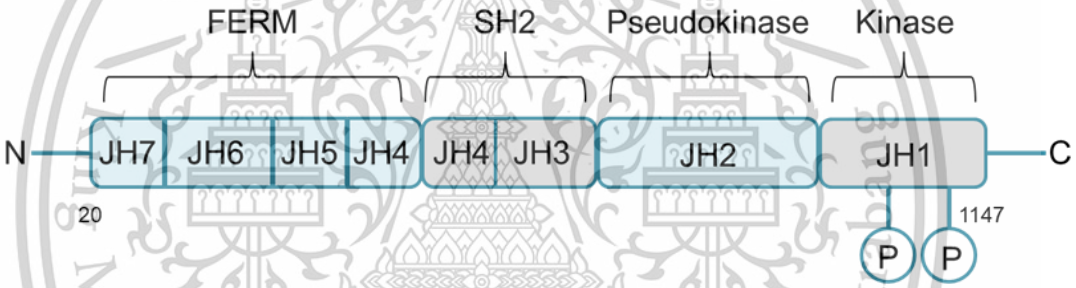

Figure 3 Structure and conserved phosphorylation sites of the JAK family [58].

Each JAK protein contains seven JAK homology (JH) domains that are crucial for its activity. These domains include:

JH1: The catalytic kinase domain responsible for phosphorylating target proteins, including STATs.

JH2: A pseudokinase domain that regulates the activity of the JH1 domain through intramolecular interactions.

JH3-JH7: Domains responsible for mediating interactions with cytokine receptors and other signaling molecules.

JAKs are associated with type I and type II cytokine receptors, which lack intrinsic kinase activity. Upon cytokine binding, the receptor undergoes dimerization, which brings two JAK molecules into close proximity, leading to their activation through trans-phosphorylation. Activated JAKs then

phosphorylate specific tyrosine residues on the receptor, creating docking sites for STAT proteins. STAT proteins are subsequently phosphorylated by JAKs, dimerize, and translocate to the nucleus, where they bind to specific DNA sequences and regulate gene transcription [59].

2.3.2 The JAK-STAT Signaling Pathway

The JAK-STAT signaling pathway is one of the most well-characterized mechanisms by which cytokines exert their effects on immune cells. It is involved in the signaling of numerous cytokines [60], including:

1. Interleukins: IL-2, IL-6, IL-10, and IL-12, which are critical for immune cell differentiation and function.
2. Interferons: IFN-α, IFN-β, and IFN-γ, which are involved in antiviral responses and immunomodulation.
3. Growth Factors: Such as erythropoietin (EPO) and thrombopoietin (TPO), which regulate hematopoiesis.

Dysregulation of the JAK-STAT pathway can lead to aberrant cytokine signaling, resulting in immune system hyperactivity and chronic inflammation. In particular, mutations or overactivation of JAK proteins have been associated with various hematological malignancies, such as polycythemia vera (a result of JAK2 V617F mutation), and autoimmune diseases like rheumatoid arthritis, psoriasis, and inflammatory bowel diseases (IBDs) [61].

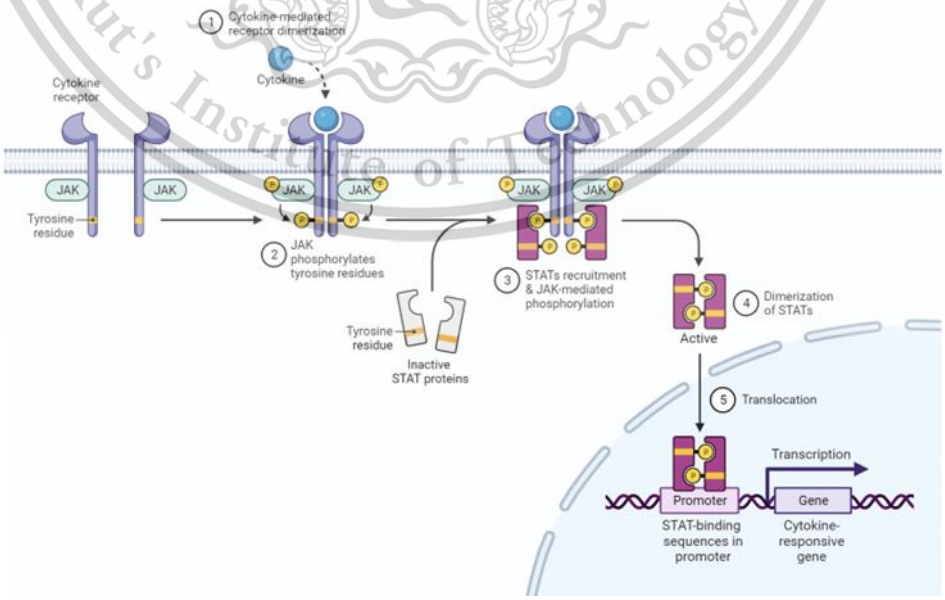

Figure 4 JAK/STAT signaling pathway. Illustrated by BioRender.

2.3.3 Role of JAKs in IMIDs

Aberrant JAK-STAT signaling has been identified as a key driver in the pathogenesis of multiple IMIDs. Cytokines that signal through the JAK-STAT pathway, such as IL-6, IL-12, and IFN-γ, are involved in maintaining the inflammatory milieu seen in these diseases.[62] For example, in rheumatoid arthritis (RA), excessive production of IL-6 activates JAK1/3 and STAT3 signaling, promoting the differentiation of Th17 cells, which are potent drivers of autoimmunity. Similarly, in ulcerative colitis, JAK-mediated signaling through IL-23 contributes to intestinal inflammation [63].

- JAK1: Primarily mediates signals from cytokines involved in both innate and adaptive immunity, including type I and II interferons and several interleukins (e.g., IL-6 and IL-12).[64]
- JAK2: Plays a central role in hematopoiesis by transducing signals from EPO, TPO, and granulocyte colony-stimulating factor (G-CSF), in addition to immune-related cytokines such as IL-12 and IFN-γ. [65]
- JAK3: Is exclusively associated with the γ-chain family of cytokine receptors, which include IL-2, IL-4, IL-7, IL-9, IL-15, and IL-21, all of which are important for lymphocyte function and development [66].
- TYK2: Is involved in signaling by cytokines such as IL-12 and IL-23, both of which are implicated in autoimmune diseases, particularly psoriasis and Crohn's disease [67].

The overactivation of JAK-STAT signaling in IMIDs has led to the development of targeted therapies aimed at inhibiting specific JAK family members, thereby reducing cytokine-driven inflammation and ameliorating disease symptoms.

2.3.4 JAK Mutations and Disease

In addition to their role in chronic inflammation, mutations in JAK genes have been identified in several hematologic malignancies and immunodeficiencies. For example:

- JAK2 V617F Mutation: This mutation results in constitutive activation of JAK2 and is a key driver of myeloproliferative

disorders such as polycythemia vera, essential thrombocythemia, and myelofibrosis [68].

- Loss-of-Function Mutations in JAK3: These mutations are associated with severe combined immunodeficiency (SCID), characterized by a lack of functional T and NK cells due to impaired cytokine signaling through the common **γ**-chain [69].

The identification of these mutations has paved the way for the development of selective JAK inhibitors as therapeutic agents, not only for IMIDs but also for hematological malignancies.

2.3.5 Therapeutic Targeting of JAKs

Given the central role of JAKs in cytokine signaling and immune regulation, targeting these kinases with small molecule inhibitors has emerged as a promising therapeutic strategy. JAK inhibitors, also known as JAKinibs, selectively block the activity of one or more JAK family members, preventing the phosphorylation and activation of STAT proteins. This, in turn, reduces the transcription of pro-inflammatory genes and helps to restore immune homeostasis [70].

The development of JAK inhibitors has primarily focused on JAK1, JAK2, and JAK3 due to their involvement in the pathogenesis of various IMIDs. These inhibitors are orally available, providing a convenient alternative to biologic therapies, which are typically administered via injection or infusion [71].

2.4 JAK INHIBITORS

Janus kinase (JAK) inhibitors, often referred to as JAKinibs, represent a class of targeted small molecule therapeutics designed to inhibit the activity of one or more Janus kinases (JAK1, JAK2, JAK3, and TYK2) [72]. These inhibitors have emerged as a powerful treatment option for various immune-mediated inflammatory diseases (IMIDs) due to their ability to modulate dysregulated cytokine signaling [73]. By blocking the JAK-STAT signaling pathway, JAK inhibitors reduce the production and activity of pro-inflammatory cytokines, which are often overactive in IMIDs such as rheumatoid arthritis, psoriasis, and inflammatory bowel diseases (IBD) [74].

2.4.1 Mechanism of Action

JAK inhibitors function by competitively binding to the ATP-binding site of JAKs, thereby preventing the phosphorylation and activation of downstream signal transducer and activator of transcription (STAT) proteins. Inhibition of STAT phosphorylation halts the transcription of cytokine-regulated genes that drive inflammation and immune cell activation. Since many cytokines rely on the JAK-STAT pathway for signal transduction—particularly interleukins (IL-6, IL-12, IL-23), interferons (IFN-α, IFN-γ), and growth factors—JAK inhibitors provide a broad anti-inflammatory effect [70].

By selectively inhibiting specific JAK family members, it is possible to tailor the therapeutic approach to target specific cytokine pathways while minimizing off-target effects [56].

JAK1 Inhibitors: Primarily interfere with cytokine signaling related to immune regulation, including IL-6, IL-10, and IFN-γ. Selective JAK1 inhibition is advantageous in diseases like rheumatoid arthritis and atopic dermatitis, where these cytokines play a prominent role [75].

JAK2 Inhibitors: Inhibit cytokine signaling involved in hematopoiesis and immune responses, such as IFN-γ and IL-12. JAK2 inhibitors are also useful in treating hematological disorders like polycythemia vera, as well as IMIDs.[68]

JAK3 Inhibitors: Primarily affect the common γ- chain cytokines (e.g., IL-2, IL-4, IL-7, IL-15, IL-21) that regulate lymphocyte development and function, making JAK3 inhibitors potentially beneficial in autoimmune conditions driven by lymphocyte dysregulation [14].

2.4.2 Approved JAK Inhibitors for IMIDs

Several JAK inhibitors (Figure 6-10) have received approval for the treatment of IMIDs, offering oral alternatives to biologic agents that are administered via injection or infusion. These drugs have shown efficacy in patients who do not respond adequately to conventional DMARDs (disease-modifying antirheumatic drugs) or biologics and have expanded therapeutic options for managing chronic inflammatory conditions.

2.4.2.1 Baricitinib

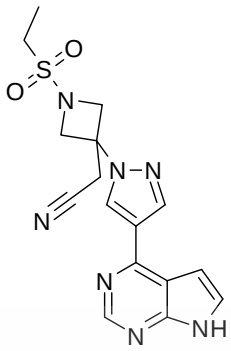

Figure 5 Baricitinib structure

- Targets: JAK1 and JAK2 [76].
- Indications: Approved for moderate to severe rheumatoid arthritis in patients with an inadequate response to TNF inhibitors. It has also been investigated for use in atopic dermatitis and systemic lupus erythematosus (SLE) [76].
- Mechanism: By targeting both JAK1 and JAK2, baricitinib effectively reduces IL-6-mediated inflammation, which is a key driver of RA. The dual inhibition also affects hematopoiesis, which necessitates monitoring for hematological side effects.
- Adverse Effects: Similar to tofacitinib, baricitinib increases the risk of infections and may lead to elevated cholesterol levels and thrombosis [77].

2.4.2.2 Delgocitinib

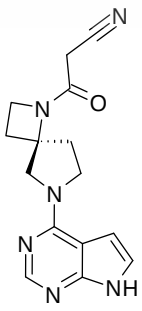

Figure 6 Delgocitinib Structure

- Target: JAK1, JAK2, JAK3, TYK2 (Pan-JAK inhibitor) [78].
- Indications: Atopic dermatitis (AD) (topical) [78].
- Mechanism: By inhibiting multiple JAK isoforms, Delgocitinib suppresses cytokines involved in inflammatory skin responses, particularly IL-4, IL-13, and IFN- γ [79].
- Adverse Effects: Local skin irritation, folliculitis, and susceptibility to skin infections [79].

2.4.2.3 Fedratinib

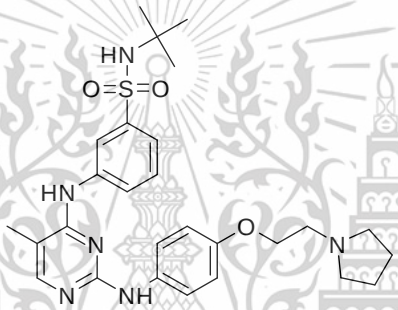

Figure 7 Fedratinib Structure

- Target: JAK2
- Indications: Myelofibrosis (MF).
- Mechanism: Inhibits JAK2, which is implicated in abnormal JAK-STAT signaling in myeloproliferative disorders like myelofibrosis, reducing disease progression and symptoms such as splenomegaly [75].
- Adverse Effects: Gastrointestinal disturbances (e.g., diarrhea, nausea), anemia, thrombocytopenia, and risk of serious infections [75].

2.4.2.4 Filgotinib

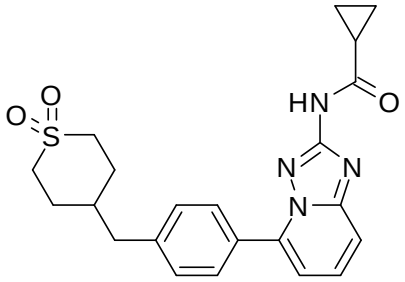

Figure 8 Filgotinib Structure

- Targets: Selective JAK1 inhibitor [80].
- Indications: Approved for rheumatoid arthritis in some regions and under investigation for ulcerative colitis and Crohn's disease [81].
- Mechanism: Filgotinib provides targeted inhibition of JAK1-driven inflammatory pathways, particularly IL-6, IL-23, and IFN-γ signaling, offering a promising option for autoimmune diseases [82].
- Adverse Effects: Filgotinib has shown a favorable safety profile compared to other JAK inhibitors, with fewer serious infections and less impact on hematological parameters [81].

2.4.2.5 Peficitinib

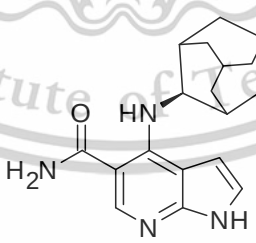

Figure 9 Peficitinib Structure

- Target: JAK1, JAK2, JAK3, TYK2 (Pan-JAK inhibitor)
- Indications: Rheumatoid arthritis (RA) (approved in Japan) [83].

- Mechanism: Broad inhibition of JAK isoforms, leading to reduced signaling of inflammatory cytokines like IL-6, IL-12, and IL-23 [83].
- Adverse Effects: Infections (particularly upper respiratory tract infections), neutropenia, and liver enzyme elevation [84].

2.4.2.6 Ruxolitinib

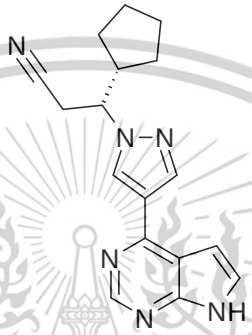

Figure 10 Ruxolitinib Structure

- Target: JAK1, JAK2
- Indications: Myelofibrosis (MF), polycythemia vera (PV), and graft-versus-host disease (GVHD) [85].
- Mechanism: Inhibits JAK1 and JAK2 to suppress the overactive JAK-STAT signaling pathway in conditions such as myelofibrosis and GVHD, reducing cytokine-driven inflammation [85].
- Adverse Effects: Anemia, thrombocytopenia, increased risk of infections, and weight gain [86].

2.4.2.7 Tofacitinib

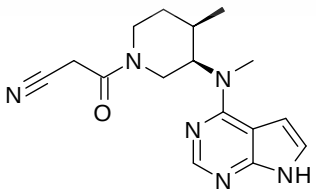

Figure 11 Tofacitinib Structure

- Targets: JAK1 and JAK3 (with lesser activity against JAK2).

- Indications: Approved for the treatment of rheumatoid arthritis (RA), psoriatic arthritis, and ulcerative colitis (UC). Tofacitinib was the first oral JAK inhibitor approved for RA and has shown significant efficacy in reducing disease activity and joint damage [87].
- Mechanism: By inhibiting JAK1 and JAK3, tofacitinib blocks cytokine signaling critical for T-cell activation and pro-inflammatory cytokine production [87].
- Adverse Effects: Increased risk of infections, particularly herpes zoster (shingles), and thrombosis. Careful patient monitoring is required for long-term use [88].

2.4.2.8 Upadacitinib

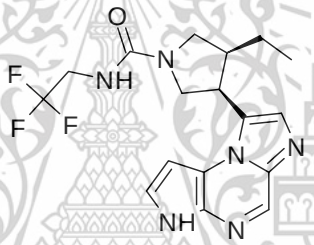

Figure 12 Upadatinib Structure

- Targets: Selective JAK1 inhibitor.
- Indications: Approved for the treatment of rheumatoid arthritis, ankylosing spondylitis, and psoriatic arthritis. It has demonstrated superior efficacy compared to some biologics in RA, offering a potent option for patients with refractory disease [89].
- Mechanism: Upadacitinib selectively inhibits JAK1, reducing cytokine signaling involved in immune cell recruitment and inflammation without significantly affecting hematopoiesis [89].
- Adverse Effects: Similar to other JAK inhibitors, there is an increased risk of infections, though JAK1 selectivity

may reduce some of the hematologic side effects seen with JAK2 inhibition [90].

Table 1 Summary of approved JAK Inhibitors for IMIDs.

Drug	Target selectivity	Indication
Baricitinib	JAK1/JAK2: high	Rheumatoid arthritis
	TYK2: moderate	Atopic dermatitis
	JAK3: minor	COVID-19
Delgocitinib	Pan-JAK: high	Atopic dermatitis
Fedratinib	JAK2: high	Myelofibrosis
Filgotinib	JAK1: high	Rheumatoid arthritis
Peficitinib	JAK3 :moderate	Rheumatoid arthritis
	JAK1/JAK2/TYK2: minor	
Ruxolitinib	JAK1/JAK2 :high	Myelofibrosis
		Polycythemia vera
		Essential thrombocythemia
		Graft vs host disease
Tofacitinib	JAK1/JAK3: high	Rheumatoid arthritis
	JAK2/TYK2: minor	Psoriatic arthritis
		Juvenile idiopathic arthritis
		Systemic JIA
Upadacitinib	JAK1: high	Rheumatoid arthritis
		Psoriatic arthritis
		Ankylosing spondylitis

2.4.3 Advantages and Limitations of JAK Inhibitors

2.4.3.1 Advantages

- Oral Administration: Unlike biologics, which require injection or infusion, JAK inhibitors are orally administered, providing greater convenience and patient compliance [1].
- Broad Cytokine Targeting: By inhibiting multiple cytokine pathways simultaneously, JAK inhibitors offer a comprehensive approach to reducing inflammation,

particularly in patients who do not respond well to more targeted biologics [17].

- Rapid Onset of Action: JAK inhibitors tend to have a quicker onset of action compared to biologics, offering faster relief of symptoms in conditions like rheumatoid arthritis and ulcerative colitis [53].

2.4.3.2 Limitations

- Safety Concerns: Long-term use of JAK inhibitors has been associated with an increased risk of serious infections (e.g., tuberculosis, herpes zoster) due to their broad immunosuppressive effects. Thrombosis and elevated cholesterol levels are also notable side effects, and patients require regular monitoring [52].
- Cost: While generally less expensive than biologics, JAK inhibitors are still costly, and access may be limited in certain healthcare settings.
- Patient Response Variability: Not all patients respond to JAK inhibitors, and some may develop secondary resistance, necessitating a switch to other therapeutic options [52].

2.4.4 Future Directions for JAK Inhibitors

The development of next-generation JAK inhibitors with improved selectivity and safety profiles is ongoing. Researchers are focusing on reducing off-target effects by designing inhibitors that selectively target specific JAK isoforms associated with disease pathogenesis. For example, TYK2 inhibitors, which specifically target IL-12 and IL-23 signaling, are being developed for psoriasis and Crohn's disease, offering more refined approaches with potentially fewer side effects [63].

Moreover, combination therapies involving JAK inhibitors alongside biologics or conventional DMARDs are being explored to enhance therapeutic efficacy while minimizing adverse effects. Personalized medicine approaches,

where JAK inhibitors are tailored to individual genetic or molecular profiles, also represent a promising direction for optimizing treatment outcomes [64].

2.5 STRUCTURE-BASED DRUG DESIGN

Structure-Based Drug Design (SBDD) is a rational approach to drug discovery that leverages the three-dimensional (3D) structures of biological targets, typically proteins, to design new therapeutic compounds. This methodology aims to optimize the interaction between a small molecule drug and its target, typically by fitting the molecule into the binding site of the protein. SBDD has become a pivotal technique in modern drug discovery, significantly enhancing the precision and efficiency of identifying drug candidates, especially in fields like oncology, immunology, and infectious diseases [93].

2.5.1 Fundamentals of Structure-Based Drug Design

The foundation of SBDD lies in the knowledge of the 3D structure of the target protein, which can be obtained through techniques such as X-ray crystallography, nuclear magnetic resonance (NMR) spectroscopy, or, more recently, cryo-electron microscopy (cryo-EM). Once the structure is determined, computational tools are used to visualize the target and identify potential binding sites for small molecule [9].

The SBDD process generally follows a systematic approach:

1. Target Selection: The first step in SBDD is the selection of a suitable biological target, typically a protein whose activity is implicated in the pathogenesis of a disease. Proteins such as enzymes, receptors, and ion channels are common targets for therapeutic intervention [10].
2. Structural Characterization: The 3D structure of the target protein must be elucidated, usually in complex with a ligand or co-factor. X-ray crystallography and cryo-EM are widely used to obtain high-resolution structures, allowing for detailed analysis of the active or binding site [10].
3. Lead Compound Identification: Once the structure is known, the design of small molecules begins. The goal is to identify “lead”

compounds that interact favorably with the protein's binding site. These compounds can be identified using various techniques [11], including:

- Virtual Screening: Computational docking of a large library of small molecules against the protein structure to identify potential binders.
- Fragment-Based Drug Design (FBDD): A method that involves screening small fragments of molecules that bind weakly to the target. These fragments are then chemically modified or combined to generate lead compounds with higher affinity.
- De Novo Design: A strategy where new chemical entities are designed from scratch based on the structure of the target binding site, often using algorithms to suggest potential drug-like molecules.

4. Lead Optimization: Once lead compounds are identified, they undergo iterative cycles of chemical modification and testing to improve their binding affinity, selectivity, pharmacokinetics, and toxicity profiles. Structure-activity relationship (SAR) studies are essential during this phase, as they provide insights into how structural changes in the compound affect its biological activity.
5. Validation: The designed drug candidates are tested in vitro (e.g., using biochemical assays) and in vivo (e.g., animal models) to validate their efficacy and safety. Molecular dynamics simulations, discussed in more detail later, are often used to confirm the stability of the drug-target interaction.

2.5.2 Types of Structure-Based Drug Design

Two primary strategies are employed in structure-based drug design: ligand-based and receptor-based design.

1. Ligand-Based Drug Design (LBDD): When the structure of the target protein is unavailable, LBDD uses known ligands (compounds that bind to the protein) to predict new molecules

that could bind in a similar manner. This approach relies on the knowledge of the physicochemical properties and structural features of known ligands to design new drugs.

2. Receptor-Based Drug Design (RBDD): This is the classic form of SBDD, where the known 3D structure of the protein receptor is used to design small molecules. RBDD allows for direct visualization of the binding pocket and enables rational optimization of small molecules to improve their fit and interaction with the target.

2.5.3 Applications of Structure-Based Drug Design in Drug Discovery

Structure-Based Drug Design has revolutionized the development of drugs across several therapeutic areas, particularly in cancer, neurodegenerative diseases, and infectious diseases. Some of the notable applications of SBDD include:

Kinase Inhibitors: Many cancer therapies target kinases, enzymes that are key regulators of cell signaling. SBDD has been instrumental in designing small molecule kinase inhibitors that fit precisely into the ATP-binding pocket of kinases, thereby inhibiting their activity. For example, imatinib (Gleevec®), a tyrosine kinase inhibitor used to treat chronic myelogenous leukemia (CML), was developed using SBDD techniques [93].

Antiviral Agents: The design of antiviral drugs, such as inhibitors of the HIV protease and reverse transcriptase, has greatly benefited from SBDD. The availability of structural information about these viral enzymes allowed for the precise design of drugs like saquinavir and ritonavir, which block viral replication [94].

Autoimmune Diseases: SBDD has played a critical role in the development of JAK inhibitors, which are used to treat various immune-mediated inflammatory diseases. By targeting the JAK family of enzymes, drugs like tofacitinib were designed to fit into the ATP-binding site of JAKs, preventing the activation of the JAK-STAT signaling pathway that drives inflammation [11].

2.5.4 Tools and Techniques in SBDD

Advances in computational power and software have made SBDD more accessible and efficient. Several tools and methodologies are integral to this process:

Molecular Docking: Docking algorithms predict the preferred orientation of a small molecule when it binds to a protein. By simulating different binding poses, researchers can estimate the binding affinity and select the most promising candidates for further optimization [11].

Molecular Dynamics (MD) Simulations: While docking provides a static snapshot of the interaction between the drug and its target, MD simulations allow researchers to observe the dynamic behavior of the complex over time. This is crucial for understanding the flexibility of the binding site and the stability of the drug-target interaction [95].

Homology Modeling: When experimental structures of the target protein are unavailable, homology modeling can be used to build a 3D model based on the sequence similarity to a known structure. This modeled structure can then be used for virtual screening and drug design [11].

Fragment-Based Drug Design (FBDD): This method involves screening small molecular fragments that weakly bind to the target protein. These fragments are then optimized or linked together to create potent lead compounds. FBDD has been particularly successful in the design of kinase inhibitors and other enzyme modulators [11].

2.5.5 Challenges and Future Directions in SBDD

While SBDD has achieved notable successes, several challenges remain. One major limitation is the availability of high-quality 3D structures of protein targets. Many important drug targets are difficult to crystallize, limiting the application of SBDD in these cases. Additionally, protein flexibility and conformational changes during binding are difficult to capture using static crystallographic data, although advances in molecular dynamics simulations are helping to address this limitation [92].

The future of SBDD lies in further integration with machine learning and artificial intelligence (AI) technologies. AI-driven drug discovery platforms can

analyze vast amounts of structural and chemical data, potentially identifying new drug candidates faster and more accurately than traditional methods. Additionally, the ongoing development of cryo-EM and other high-resolution imaging techniques will expand the range of druggable targets and improve the accuracy of SBDD models.

2.6 MOLECULAR DOCKING AND MOLECULAR DYNAMICS (MD) SIMULATION

Molecular Docking and Molecular Dynamics (MD) Simulation are two fundamental computational techniques used in drug discovery and structure-based drug design (SBDD). These methods provide critical insights into the interactions between small molecules and their protein targets, helping to identify and optimize potential drug candidates [95].

2.6.1 Molecular Docking

Molecular Docking is a computational technique used to predict the preferred orientation and binding affinity of a small molecule (ligand) when it binds to a protein (receptor). The primary goal of docking is to determine the best-fit pose of the ligand within the protein's binding site, which helps in understanding how the ligand interacts with the protein and assists in optimizing drug candidates [92].

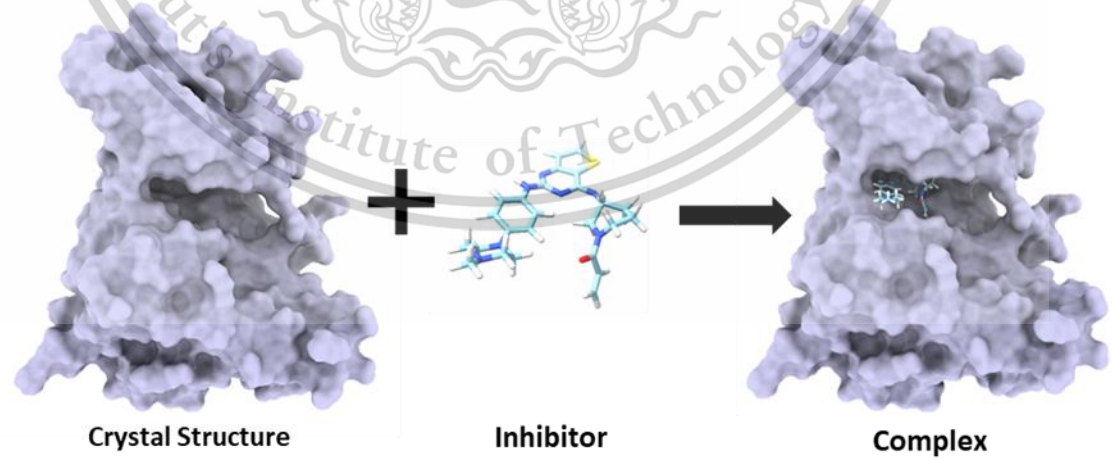

Figure 13 Molecular Docking Concept of PDB structure from RCSB database and self-created inhibitor molecule. illustrated by PyMol.

2.6.1.1 Key Concepts in Molecular Docking

1. Docking Algorithms [11]
   - Rigid Docking: Assumes that both the protein and ligand remain fixed in their conformations during the docking process. This approach is faster but less accurate for flexible ligands or binding sites.
   - Flexible Docking: Allows for conformational changes in both the protein and ligand. This approach is more accurate as it accounts for the flexibility of the binding site and the ligand, but it is computationally more demanding.
   - Induced Fit Docking: Combines aspects of rigid and flexible docking by allowing the protein's binding site to adapt to the ligand. This approach is useful for capturing the dynamic nature of protein-ligand interactions.
2. Scoring Functions: Scoring functions are used to evaluate the quality of the predicted ligand-protein interactions. They estimate the binding affinity based on various factors, such as van der Waals interactions, electrostatic interactions, and solvation effects. Common scoring functions [11], including:
   - Grid-Based Scoring Functions: Use pre-computed grids to quickly calculate interactions between the ligand and protein.
   - Empirical Scoring Functions: Based on experimental data to predict binding affinities.
   - Knowledge-Based Scoring Functions: Use statistical data from known protein-ligand complexes to score interactions.
3. Applications

- Virtual Screening: Docking is used to screen large libraries of compounds to identify potential drug candidates based on their predicted binding affinities. [92]
- Lead Optimization: Helps in optimizing lead compounds by predicting how structural modifications affect binding affinity and specificity.
- Pose Prediction: Provides insights into the possible binding modes of a ligand, which aids in understanding the mechanism of action.

2.6.2 Molecular Dynamics (MD) Simulation

Molecular Dynamics (MD) Simulation is a computational technique used to study the physical movements of atoms and molecules over time. It provides a dynamic view of protein-ligand interactions by simulating the time-dependent behavior of the system, allowing researchers to observe conformational changes, binding dynamics, and stability of the drug-target complex [91].

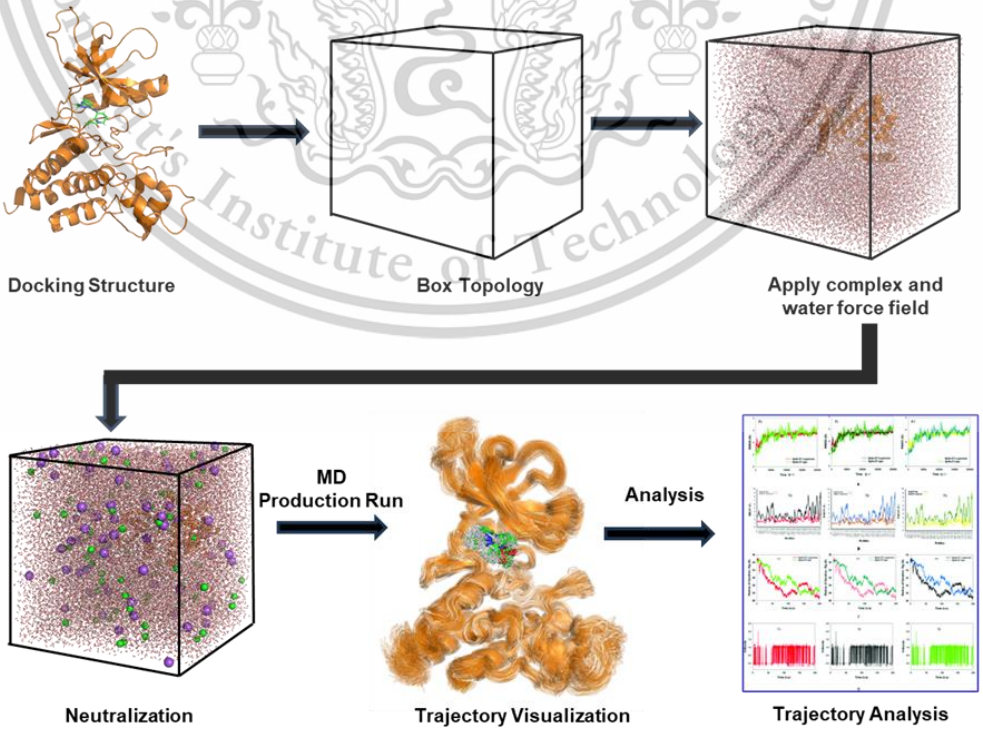

Figure 14 The Overall process of MD simulation preparation, production and analysis.

2.6.2.1 Key Concepts in Molecular Dynamics Simulation

1. MD Simulation Workflow [95].
   - Preparation: Involves setting up the initial coordinates, defining the force field parameters, and preparing the system for simulation. This includes solvation of the protein-ligand complex in a water box and adding ions to neutralize the system.
   - Energy Minimization: Reduces steric clashes and adjusts the structure to a more stable conformation before running the simulation.
   - Equilibration: Ensures that the system reaches a stable state under the desired conditions (e.g., temperature and pressure) before starting the production run.
   - Production Run: The core simulation phase where the system is run for a specified duration to collect data on the dynamics of the protein-ligand complex.
2. Force Fields: Force fields are mathematical models used to describe the potential energy of the system, including bond stretching, angle bending, torsional rotations, and non-bonded interactions. Common force fields[99] include:
   - AMBER: Widely used for biomolecules, providing accurate descriptions of protein-ligand interactions.
   - CHARMM: Often used for large-scale simulations and provides detailed force field parameters.
   - GROMOS: Used for both proteins and nucleic acids, focusing on large-scale systems.

3. Analysis [92].
   - Binding Affinity: MD simulations provide insights into the binding stability and dynamics of the ligand in the binding site.
   - Conformational Changes: Helps in understanding how the protein and ligand conformations change over time, providing a dynamic view of the interaction.
   - Free Energy Calculations: Techniques such as Molecular Mechanics Poisson-Boltzmann Surface Area (MM-PBSA) and Thermodynamic Integration (TI) are used to estimate the free energy of binding, offering insights into the affinity and stability of the complex.
4. Applications
   - Refinement of Docking Results: MD simulations can be used to validate and refine docking results by exploring the dynamic behavior of the protein-ligand complex [14].
   - Understanding Binding Mechanisms: Provides insights into how ligands interact with their targets, including details on binding modes, induced fit, and conformational changes.
   - Predicting Drug Resistance: Helps in understanding how mutations in the target protein affect drug binding and resistance mechanisms [15].

2.6.3 Integration of Docking and MD Simulations

Combining molecular docking and MD simulations provides a comprehensive approach to drug discovery. Docking offers initial predictions of binding modes and affinities, while MD simulations provide a dynamic view of these interactions, helping to validate and refine the docking results. This

integrated approach enhances the accuracy of predicting drug-target interactions and aids in the development of more effective and specific therapeutics [92].

Example Workflow:

1. Docking: Perform virtual screening to identify potential lead compounds.
2. MD Simulation: Simulate the protein-ligand complex to observe binding dynamics and stability.
3. Analysis: Analyze simulation results to confirm binding modes, stability, and potential interactions not captured in static docking models.

The integration of advanced computational methods, such as machine learning and AI, with docking and MD simulations is paving the way for more efficient and accurate drug discovery processes. These technologies enhance the predictive power of simulations, allowing for better identification of drug candidates and optimization of their properties.

Additionally, the development of more accurate and faster computational tools will continue to improve the efficiency of docking and MD simulations, facilitating the discovery of novel therapeutics for a wide range of diseases.

2.7 KINASE INHIBITION ACTIVITY ASSESSMENT

Kinase inhibition activity assessment is a crucial step in drug discovery, particularly for targeting protein kinases, which play a central role in various cellular processes, including growth, differentiation, and metabolism. Accurate evaluation of kinase inhibition is essential for the development of effective therapeutic agents, especially in oncology and inflammatory diseases where kinases are often dysregulated [15].

2.7.1 Methods for Kinase Inhibition Activity Assessment

Several methodologies are employed to evaluate the efficacy and potency of kinase inhibitors. These methods can be broadly categorized into biochemical assays, cellular assays, and structural approaches [102].

2.7.1.1 Biochemical Assays

Biochemical assays measure the direct interaction between a kinase and its substrate in vitro. These assays provide insights into the inhibition potency and mechanism of kinase inhibitors

1. Enzyme-Linked Immunosorbent Assay (ELISA) [47].
   - Description: ELISA can be used to quantify the phosphorylation of substrates in kinase assays. The assay involves immobilizing the substrate on a plate, adding the kinase and inhibitor, and detecting the phosphorylated substrate using specific antibodies.
   - Advantages: High sensitivity and specificity for detecting phosphorylation events.
   - Limitations: Can be affected by non-specific binding and may require optimization for different kinds of kinases.
2. Radioactive Kinase Assays [48]:
   - Description: Uses radiolabeled ATP to measure the phosphorylation of substrates. The amount of radioactivity incorporated into the substrate correlates with kinase activity.
   - Advantages: Provides quantitative data on kinase activity and inhibition.
   - Limitations: Requires handling of radioactive materials and may involve complex assay setups.
3. Fluorescent or Chemiluminescent Assays [71]:
   - Description: These assays use fluorescent or chemiluminescent substrates to detect

phosphorylation. Fluorescent resonance energy transfer (FRET) or time-resolved fluorescence resonance energy transfer (TR-FRET) can be employed for high-throughput screening.

- Advantages: non-radioactive, allowing for safer and more scalable assays.
- Limitations: May require specific reagents and can be influenced by background fluorescence.

4. Kinase Profiling [102]:
   - Description: Involves screening inhibitors against a panel of kinases to determine their selectivity. This helps to identify off-target effects and potential interactions with other kinds of kinases.
   - Advantages: Provides a comprehensive view of inhibitor selectivity and potential side effects.
   - Limitations: Requires a diverse kinase panel and may be expensive.

2.7.1.2 Cellular Assays

Cellular assays assess the impact of kinase inhibitors on cellular processes and signaling pathways, providing information on their efficacy in a more physiologically relevant context.

1. Western Blotting [14].
   - Description: Measures the levels of phosphorylated proteins within cells. After treating cells with inhibitors, proteins are extracted, separated by SDS-PAGE, and probed with antibodies specific for the phosphorylated forms.
   - Advantages: Provides information on the inhibition of specific pathways and downstream effects.
   - Limitations: Requires optimization for different proteins and can be time-consuming.

2. Flow Cytometry [14].
   - Description: Allows for the quantitative analysis of phosphorylated proteins in individual cells using fluorescently labeled antibodies. This technique can be used to monitor changes in kinase activity within cell populations.
   - Advantages: Enables the analysis of large cell numbers and can provide data on cellular heterogeneity.
   - Limitations: Requires specialized equipment and expertise.
3. Reporter Gene Assays [3].
   - Description: Utilizes cell lines with reporter genes under the control of kinase-responsive promoters. The activity of the reporter (e.g., luciferase) indicates the impact of the inhibitor on kinase signaling pathways.
   - Advantages: Provides a real-time assessment of kinase activity and downstream effects.
   - Limitations: May not fully represent the complexity of endogenous signaling pathways.
4. Cell Viability and Proliferation Assays [15].
   - Description: Measures the effects of kinase inhibitors on cell growth and survival. Common assays include MTT, CellTiter-Glo, and XTT assays.
   - Advantages: Useful for assessing the overall impact of inhibitors on cell health and proliferation.
   - Limitations: May not provide detailed mechanistic insights into the inhibition of specific kinases.

2.7.1.3 Structural Approaches

Structural approaches involve analyzing the interaction between kinase inhibitors and their targets at the atomic level.

1. X-ray Crystallography [9].
   - Description: Provides high-resolution structures of kinase-inhibitor complexes, revealing the binding mode and interactions within the active site [9].
   - Advantages: Offers detailed structural information and insights into the mechanism of inhibition.
   - Limitations: Requires crystallization of the protein-ligand complex, which can be challenging.
2. Nuclear Magnetic Resonance (NMR) Spectroscopy [14].
   - Description: Allows for the study of protein-ligand interactions in solution, providing information on binding kinetics and conformational changes.
   - Advantages: Captures dynamic aspects of binding and can provide data on protein flexibility.
   - Limitations: Limited to smaller proteins and complexes and can be technically demanding.
3. Cryo-Electron Microscopy (cryo-EM) [9].
   - Description: Provides high-resolution structures of protein-ligand complexes in a near-native state, offering insights into the binding interactions and conformational changes.
   - Advantages: Suitable for large complexes and provides structural information without the need for crystallization.
   - Limitations: Requires specialized equipment and expertise.

2.7.2 Evaluation and Interpretation

The assessment of kinase inhibition activity involves analyzing data from various assays to determine the potency, selectivity, and mechanism of inhibition [14, 15]. Key metrics include:

1. IC_{50} (Half-Maximal Inhibitory Concentration): The concentration of the inhibitor required to achieve 50% inhibition of kinase activity. Lower IC_{50} values indicate higher potency.
2. Selectivity: The ability of the inhibitor to target a specific kinase while minimizing interactions with other kinases. Profiling data helps to assess selectivity.
3. Binding Mode: Insights into how the inhibitor binds to the kinase, including interactions with key residues and the impact on the kinase's active site.

Assessing kinase inhibition activity presents several challenges, including the need for accurate and reproducible assay conditions, potential interference from other cellular components, and the complexity of kinase signaling networks.

CHAPTER 3

MATERIAL AND METHODS

3.1 MATERIAL

3.1.1 Instruments

^{1}H-NMR and ^{13}C-NMR spectra were recorded on a Jeol spectrometer model: ECZ500/S1 at 500 MHz (^{1}H-NMR), 125 MHz (^{13}C-NMR). Chemical shifts (δ) and coupling constants are quoted in parts per million (ppm) and Hertz (Hz), respectively, with the residual DMSO-d6 solvent line acting as the internal standard.

Mass spectra were obtained from an LC-MSD-Trap mass spectrometer, ion source type ESI(+) mode. High-resolution mass spectra (HRMS) were determined on Bruker Daltonics - micrOTOF-Q III in source ESI(+) mode.

3.1.2 Chromatography

Thin-layer chromatography (TLC) was performed on TLC aluminum/silica gel plate (Silicycle UltraPure Silica gels) with UV light visualization.

Purification of the compounds by column chromatography was performed using silica gel G60 (60-200 µm) as a stationary phase. The mixture of ethyl-acetate/hexane (80:20 %v/v) was used as mobile phase for the purification of intermediate compounds and the mixture of dichloromethane/methanol (99:1 to 95:5 %v/v) was used as mobile phase for the purification of final compounds.

The purity of compounds was confirmed ≥95% based on a UV absorbance HPLC chromatogram (HITACHI/Chromaster HPLC with a Poroshell 120 EC-C8 2.7 µM column using a mobile phase consisting of (a) 0.1% formic acid in water and (b) acetonitrile: 99:1% to 1:99% gradient run in 8 minutes).

3.1.3 Chemical and Reagents

All reagents and solvents were purchased from commercial suppliers and were used without further purification.

3.2 COMPUTATIONAL METHODS

3.2.1 Molecular Docking

A crystal structure of JAK3 was obtained from RCSB protein data bank (PDB ID: 5LWM, resolution of 1.55 Å) [92]. This structure contains a complete amino acid sequence and non-covalent bonding inhibitor. A 2nd lower resolution structure containing a structurally related covalently bound benzylamine linker pyrimidine inhibitor (PDB ID: 4Z16, resolution 2.90 Å) [14] was also obtained. This structure lacked coordinates for 6 amino acids in the N-terminal domain (residue 891-897), and 6 residues in the activation loop (residue 984-990), and a small helix of C-terminal domain (residue 1038-1046). The missing residues of 4Z16 were completed by homology modeling using the coordinates of 5LWM.

All mol2 format of ligand 3D structure were created in Discovery Studio Visualizer software and binding mode of ligands in both 4Z16 and 5LWM were generated from molecular docking using a manual pharmacophore-based superimposition and run calculation by GOLD docking. The protonation state of amino acid residues was defined based on the predicted pKa using Propka3.0 [93, 94].

3.2.2 Molecular Dynamics (MD) Simulation

All simulations were carried out using GROMACS v.2019.6 software in conjunction with the AMBER99SB forcefield [95, 96]. The restrained electrostatic potential (RESP) charge of all ligands was determined from the Hartree-Fock calculation with the 6-31G(d) basis set [97]. Ligand topology files were generated using the ACPYPE script with GAFF force field [98, 99]. The protein was immersed in a box of TIP3P water molecules [100]with a minimum distance of 12 Å between the protein and box edge. The concentration of 0.15 M Sodium chloride (NaCl) ions was added to neutralize the system. Then the system was minimized to an RMS gradient of 10 kJ mol^{-1} nm^{-1} to relax any steric conflict and heated from 0 to 300 K over 100 ps by NVT scheme followed by equilibration for 500 ps [101]. The system underwent production dynamics using NPT ensemble for 10 ns [91].

3.3 SYNTHESIS

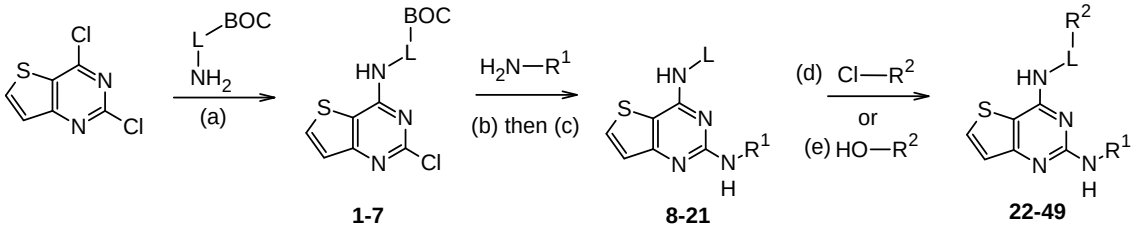

Figure 15 (a) EtOH, TEA, 80°C, 6 hrs. [14], (b) i-PrOH, TFA, 90°C, 18 hrs. [15], (c) DCM, TFA, rt, 2 hrs. [15], (d) DCM, $NaHCO_3$, 0°C, 1 hr. [14] and (e) DCM, DCC, rt , 1 hr. [11]

3.3.1 General Route (a)

2,4-Dichlorothieno[3,2-d]pyrimidine (1 equivalent) and Boc-protected amine linker (1.2 equivalent) and TEA (2 equivalent) was dissolved in EtOH (4 mL for 500 mg). The reaction was stirred at 80°C for 4-18 hrs. After the reaction period, the reaction mixture was extracted with Ethyl acetate (EtOAc)/ DI water (1:1 %v/v). The organic layer was dried over Mg_2SO_4 anhydrous and removed organic solvents under vacuum by using rotary evaporator. The crude solid was purified by silica gel column chromatography using 1:1 EtOAc/Hexane and the product was evaporated to obtain a solid product compound **1-7**

3.3.2 General Route (b) and (c)

Compound **1-7** (1 equivalent) were dissolved in iso-propanol (2 mL) then 4-(4-Methylpiperazino)aniline or 1-Methyl-1h-pyrazol-4-ylamine (1.2 equivalent) and 300µL of trifluoroacetic acid (TFA) were added. The mixture was heated to 90 °C, for overnight. The solvent from the reaction mixture was removed under reduced pressure. Then crude material was used for deprotection step directly without any purification process. crude compounds 8-20 in DCM and then add TFA (1:1). To stir the solution at 60 °C 1-2 hrs. The reaction was diluted with DI water and DCM, then neutralized by adding 2M NaOH. Then extracted with DCM and dried with Mg_2SO_4 anhydrous. The solvent of the organics layer was removed under reduced pressure and the crude material was purified by column chromatography on silica gel with CH_2Cl_2/CH_3OH in a 9:1 (%v/v) ratio as eluent, to afford compounds **8-21**.

3.3.3 General Route (d)

Condition 1: Intermediate compound **8-21** (1 equivalent) and Saturated $NaHCO_3$ (2 equivalent) were mixed in anhydrous DCM and stirred at 0°C for 30 mins. Then added the Acryloyl chloride or Propionyl chloride (1.75 equivalent) dropwise. The reaction was continue stirred at 0°C for 1 hour. After the reaction period the reaction mixture was diluted with DI water and extracted with DCM/6 M NaOH 1:1 (%v/v). The organic extracts were dried over Mg_2SO_4 anhydrous and purified by silica gel column chromatography (CH_2Cl_2/CH_3OH 99:1 to 95:5

3.3.4 General Route (e)

Condition 2: Intermediate compound **8-21** (1 equivalent) and N,N'-Dicyclohexylcarbodiimide (DCC, 2 equivalent) were mixed in anhydrous DCM and stirred at room temperature for 30 mins. Then added 2-butynoic acid (1.75 equivalent). The reaction was continue stirred at room temperature for 1 hour. After the reaction period the reaction mixture was diluted with DI water and extracted with DCM/6 M NaOH 1:1 (%v/v). The organic extracts were dried over Mg2SO4 anhydrous and purified by silica gel column chromatography (CH2Cl2/CH3OH 99:1 to 95:5 %v/v).

3.4 JAK3 INHIBITION ACTIVITY

All synthesized compounds were tested for their inhibitory activity against JAKs, and EGFR-TK using the ADP-Glo™ Kinase Assay (Promega). The experimental process was performed according to the method described by the manufacturer. The reaction mixture (25 µL) contained 5 µL of kinase buffer (20 mM Tris-HCl (pH 7.5), 20 mM MgCl2, 0.1 mg/mL BSA), 5µL of 25 µM ATP, 5 µL of 12.5 µg/mL poly (Glu: Tyr) substrate, 5 µL of 2 ng/µL JAK3 (diluted in kinase buffer), and 5 µL of various compounds concentrations. Tofacitinib, Fedratinib and Olmutinib (NCI, USA), were used as control kinase-inhibitor. The reactions were performed in a 384-well plate (Greiner Bio-One Lumitrac plate, solid white) and incubated at room temperature for 1 hr. Afterward, 5 µL of ADP-Glo reagent was added to terminate the kinase reaction and deplete the remaining ATP at room temperature for 40 min. Next, 10 µL of ADP-Glo detection reagent was added for 30 min to simultaneously convert ADP to ATP and to allow the newly synthesized ATP to be measured using a luciferase/luciferin reaction.

Luminescence measurements were made using a microplate spectrophotometer (Synergy HTX Multi-Mode reader, BioTek, VT, USA). The half-maximal inhibitory concentration (IC_{50}) values of inhibitors were determined using the nonlinear regression curve fit in GraphPad Prism (GraphPad Software Inc., San Diego, CA, USA). All assays were done in triplicate. Experiments will be conducted at the Department of Biochemistry, Kasetsart University.

CHAPTER 4

RESULTS AND DISCUSSION

4.1 STRUCTURE-BASED DESIGN

4.1.1 Structure Screening

The FAD approval JAK inhibitor and JAK development compound structure and their JAK activity data were extracted from CHEMBL (Figure 16 A-D). Some of the structure related kinase inhibitors were also extracted in order to compare the molecule structure and inhibition activity (Figure 16 E-F) [8, 9, 11, 14]. All inhibitors had a common pyrimidine ring as a core structure to mimic the binding of ATP and substituted the functional group at both 2 and 4-position on the pyrimidine core. The substitution of various types of aniline at 2-position were found in many kinase inhibitors. The role of this position was to improve the compound physical property (solubility and molecular weight). The substitution at 4-position on the pyrimidine core with the hydrogen bond formation group such as cyanoacetamide sulfonamide or acrylamide with extended linker that would make the compound more active.

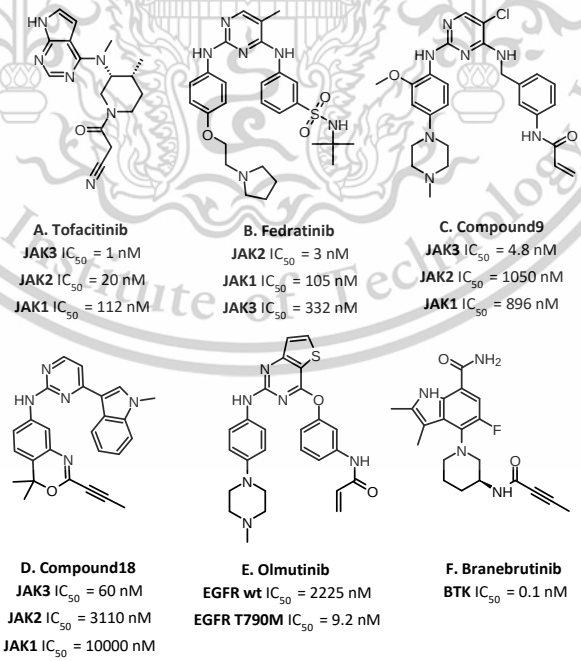

Figure 16 JAKs inhibitor (A) Tofacitinib, (B) Fedratinib, (C) Compound9, (D) Compound18, (E) related EGFR T790M inhibitor Olmutinib and (F) Branebrutinib the BTK inhibitor.

4.1.2 Binding Mode Analysis

The experimental x-ray crystal structure of JAK3 with an inhibitor was obtained from RCSB in protein data bank format (PDB). The JAK3 structure PDB ID 4Z16 was selected to be study for the binding position, inhibitor conformation and bond distances.

In the JAK3 binding pocket, there were 3 amino acid residues that make the strong interaction with the inhibitor (Figure 17). At the hinge region, The Leucine no. 905 (LEU905) formed 2 hydrogen bonds (HB) with the inhibitor, the first one was a hydrogen bond doner (HB1) donated H atom of LEU 905 amino group to the N atom on pyrimidine of inhibitor. The second hydrogen bond (HB2) was formed between LEU905 hydrogen bond acceptor (O atom of LEU905 carbonyl) and N-atom of inhibitor amino group at 2-position.[102] The functional group that connected to 2-position of pyrimidine was faced to the solvent front of the binding pocket. The 4-position on pyrimidine was substituted with benzyl group with the acrylamide at the end of the ring. The inhibitor was covalently bound with Cysteine no. 909 (CYS909) by formed a covalent bond between acrylamide and S atom of CYS909 [15].

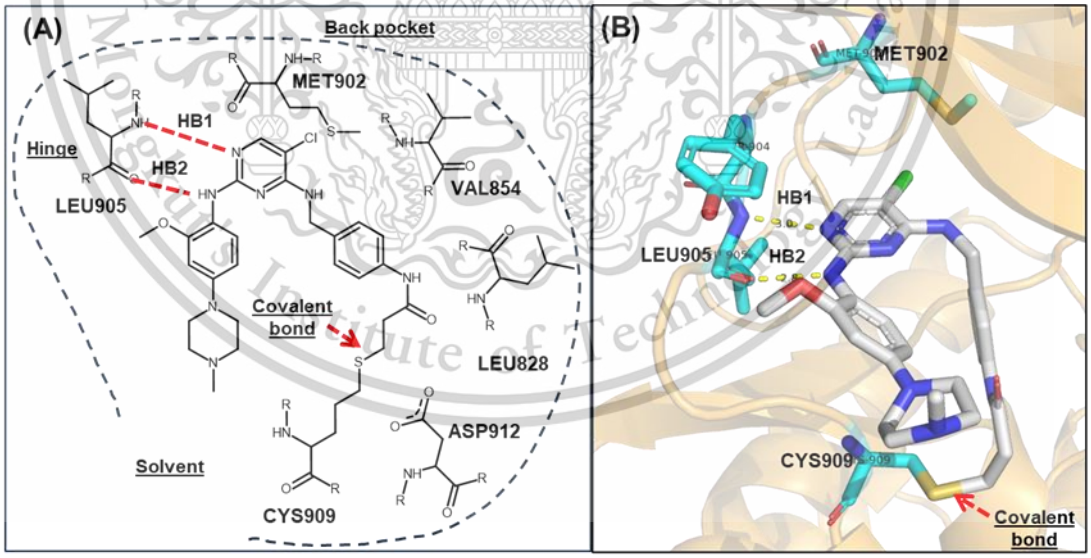

Figure 17 illustration of compound 9 in JAK3 binding site (PDB: 4Z16) represented in 2D (A) and 3D (B).

4.1.3 Design Scope

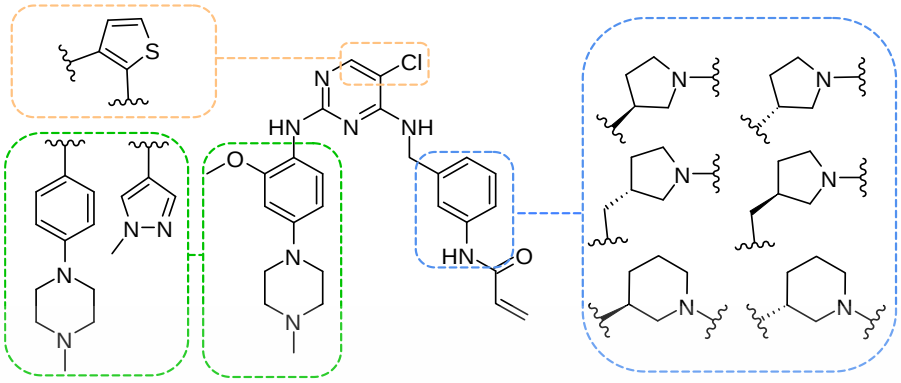

Figure 18 Scope of scaffold of modification (Thiophene replacement at 5-cl position: yellow label, 2 anilines replacement at 2-polition: green label, the replacement of benzylamine with aliphatic cyclic amine at 4-position).

Our JAK3 inhibitors were designed based on the modification of JAK3: 4Z16 original inhibitor (Figure 16) by performing the pharmacophore superimposition and taking the inspiration from structural screening data shown in Figure 18.

The thiophene ring was substituted on 5-position of pyrimidine and applied for all compound call thieno[3,2-d]pyrimidine. Two types of aniline were substituted at 2-position (Met-Piperazine and Met-Pyrazole). The major change of 4 position linker was a substitution with aliphatic cyclic amine instated of the aromatic (R-pyrrolidine: 5R, S-pyrrolidine: 5S, R-Met-pyrrolidine: 5RCH2, S-Met-pyrrolidine: 5SCH2, R-piperidine: 6R and S-piperidine: 6S).

Overall structure of JAK3 inhibitors designed in this study are divided into 4 main parts (Figure 19) based on Olmutinib and A. The first part, thieno[3,2-d]pyrimidine core structure was taken from Olmutinib (Figure 16-E) [12] which replaced the A scaffold 5-pyrimidine Cl with thiophene group, a low lipophilicity Sulfur containing heterocyclic 5-memberd ring novel for JAK3 inhibitor. A further advantage of this modification is an almost 1 log unit drop in predicted logP.

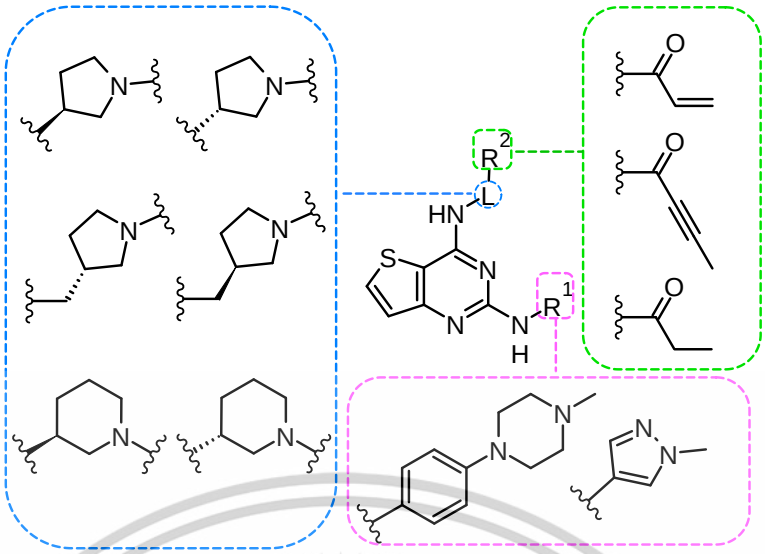

Figure 19 Scope of the scaffold modification (L: 4-position linker substitution, R1: 2-position substitution and R2: electrophilic and non-reactive amide)

The second part of the design was a 2-position substitution on a pyrimidine with 2 types of heterocyclic aromatic amine (R1: basic and neutral) which are 4-(4-methylpiperazin-1-yl)aniline and 1-methyl-1H-pyrazol-4-amine. The change of this position also assigned the overall molecular weight and overall lipophilicity of the inhibitor into two intrinsic groups due to the molecular weight of these two amines. The role of this R1 group is to react with the solvent at the front of the binding pocket [9]. The third part of design scope was a modification on the 4-position of pyrimidine, substituted with the fragments called “linker” (L). Roles of the linker was to connect core structure and reactive amide group together and assign the reaction distance between electrophilic Cβ atom of Michael acceptor and nucleophilic sulfur atom of CYS909 residue in JAK3 binding site to form a covalent bond [15, 102]. First, the O-link atom of Olmutinib was replaced by N-link atom that are commonly found in JAKs inhibitors. The reason behind this change was the angle of C-NH-C obtained in 120 degree was optimal for JAK3 (4Z16) while C-O-C angle was 110 degree was optimal for EGFR (5X2K). Then 3 different types of aliphatic cyclic amines have been included in the design which included pyrrolidine, methyl-pyrrolidine and piperidine, those all have 2 stereoisomers (R) and (S), Resulting in 6 groups in total were selected to understanding how chiral, sizing and length of aliphatic ring effected to their inhibition activity.

The most important part which made the molecule become an irreversible inhibitor was indicated at the R2 position. We have incorporated different electrophilic groups that can react with the nucleophilic CYS909 residue. This includes acrylamide, one of the most common suicidal inhibitor electrophiles, as well as 2-butynamide but novel for JAKs inhibitor [11]. The unreactive propenamide moiety was also prepared for the purpose of comparison.

4.1.4 Molecular Dynamics Simulation

A total of 8 MD simulations were run in this study (Table 2) produced using NPT conditions for a period of 10 ns, after which, the results were extracted from system trajectory.

Table 2 The designed compound that subjected to perform MD simulation.

ID	L	R1	R2
22 (5R)		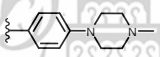	
28 (5S)		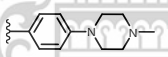	
32 (5RCH2)		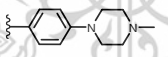	
36 (5SCH2)	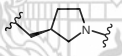	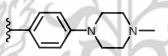	
40 (6R)	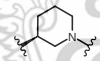	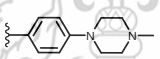	
42 (6R)			
44 (6S)	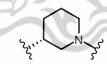	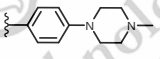	
46 (6S)	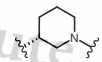		

4.1.4.1 Effect of Binding Pocket Volume

Simulations were initially run to compare the effect of using two different JAK3 structures, the more complete structure represented by 5LWM,[92] or the structure e.g., 4Z16, which had a more relevant inhibitor bound. A key observation between the two structures was that the latter pocket was larger in volume (5LWM: 709 $Å^3$ and 4Z16: 746 $Å^3$) and the position of glycine rich loop was more conductive to interaction

between the inhibitor electrophile and the CYS909 nucleophile. Our results showed no sizeable difference between the two models for inhibitor 5R and 5S (Figure 20), so we focused on the 4Z16 only.

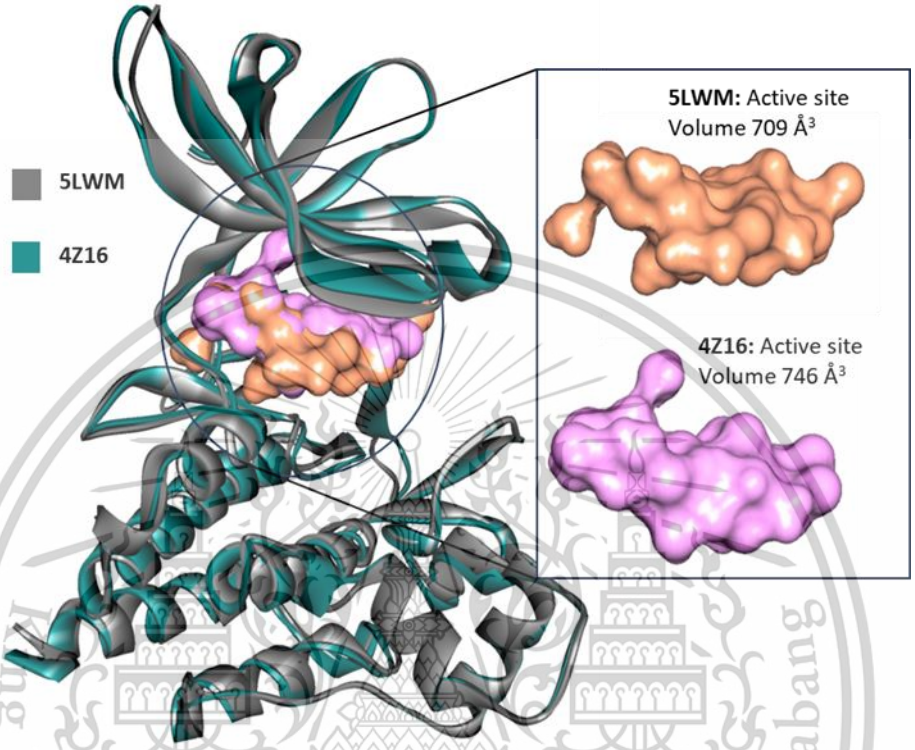

Figure 20 The superimposition of 2 JAK3 structures (5LWM: gray, 4Z16: dark green) after energy minimization (EM) calculation, the calculated binding site pocket volume represented in orange: 5LWM and pink 4Z16.

Two simulations with the H atom of the chiral linkers pointed up or down in the pocket were investigated. Thus, two simulations were obtained for Pyrrolidine (5R and 5S) and Piperidine (6R and 6S) and 3-methyl-pyrrolidine (5RCH2 and 5SCH2). Simulations of the inhibitor containing a benzyl linker originally found in the PDB structure 4Z16 were also undertaken for the purpose of comparison.

4.1.4.2 Trajectory Analysis

The relative stability of the protein and ligand conformations in the complex can be assessed from the root mean square deviation (RMSD) from the starting structure, and root mean square fluctuation (RMSF) of the residues from their mean position. The ability of the inhibitor to binding within the active site can be studied from the strength of the hydrogen bond (HB) distance formed between the nitrogen (N4) atom on pyrimidine of ligand and H atom of Leucine residue 905 (LEU905), and HB forming between the H3 atom of ligand and oxygen (O) atom of LEU 905 (indicated by HB1: Ligand-N4:---H-LEU905, and HB2: Ligand-H3---:O-LEU905). The ability of the inhibitor to form a suicidal inhibitor with the protein can be considered from the distance and angle between carbon (C32) atom of ligand (electrophilic atom) and sulfur (SG) atom of CYS909, i.e., the nucleophile, as given by the ligand-C32---SG-CYS909 (C-S) as shown in Figure 21.

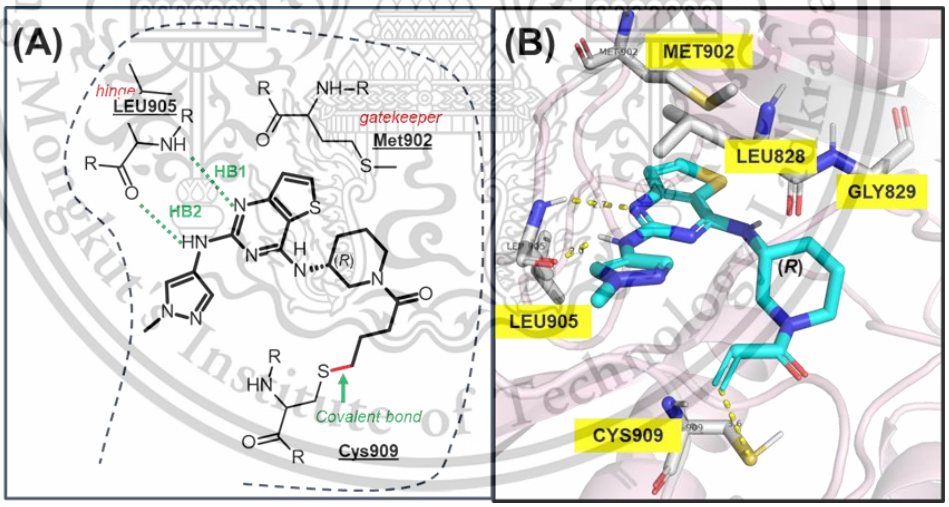

Figure 21 illustration of **42** in **4Z16** binding site (A) and snapshot of 42 in 4Z16 at 10 ns from MD trajectory represented in 3D (B).

4.1.4.3 Effect of Stereoisomer and Solvent Contacting Group

A total of 8 MD simulation of 10 ns were run in this study to understand the dynamics binding behavior of compound in JAK3 (PDB: 4Z16) complexes including the original inhibitor as a reference.

Table 3 Summary of MD Simulation Trajectory Results

ID	L	R1	R2	RMSD (Å)		Bond distance (Å)			Angle (θ°)
				backbone	ligand	hb1	hb2	C-S	C-S
22 (5R)		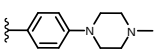		1.52	1.74	2.55	2.13	4.28	81.14
28 (5S)		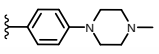		1.52	2.75	2.08	2.07	7.17	102.19
32 (5RCH2)	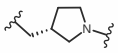	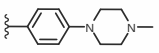		1.71	2.03	2.56	2.10	5.86	83.27
36 (5SCH2)	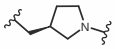	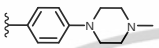		1.55	2.46	2.50	2.18	7.82	88.99
40 (6R)		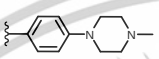		1.68	2.40	2.55	2.08	4.02	84.42
42 (6R)		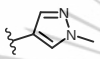		1.34	1.19	2.57	2.05	3.75	94.50
44 (6S)		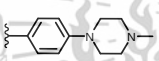		1.47	1.98	2.50	2.11	4.74	74.50
46 (6S)		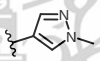		1.57	1.28	2.54	2.05	5.21	74.57

First, the preferred conformation of 6 ligands (**22, 28, 32, 36 40** and **44**) were selected to run MD simulation for study the chiral effect of the linker group at 4-position (including Amino Pyrrolidine, Amino Methyl-Pyrrolidine and Amino Piperidine with (R) and (S) stereoisomer). All complexes showed the same stability during the whole simulation period in terms of backbone RMSD 1.47-1.71 Å on average. The stability of the complex was agreed with the strength of HB forming at the hinge, both ligands formed two strong HB with LEU905 in the length of 2.08-2.50 Å (HB1) and 2.07-2.18 Å (HB2). Although the RMSD and HB distance showed that all ligands could bind stable in the binding site with strong binding ability at the hinge, linker with (R) stereoisomer could maintained the optimum length of C-S distance shorter than (S) stereoisomer. The results indicated that the ligand which has (R) linker preferred to have more JAK3 activity than (S) linker and **40** which has (R)-Amino Piperidine linker obtained the most stable C-S distance.

Next, the preferred conformation of 2 ligands (both have an amino piperidine linker at 4-position: **42** (S) and **46** (R)) were selected to run MD simulation with the same JAK3 structure and simulation condition as the previous simulation. The effects of solvent contacting group at 2-position were studied by changing the basic amine (methyl-piperazine aniline) to the neutral amine (methyl-pyrazole amine) with has the lower molecular weight and lower cLogD. The results showed both ligands **42** and **46** could bind stable in the binding site (**42**-Backbone RMSD =1.34 ± 0.14 Å, 46-Backbone RMSD =1.57 ± 0.21 Å) (Figure 22a).

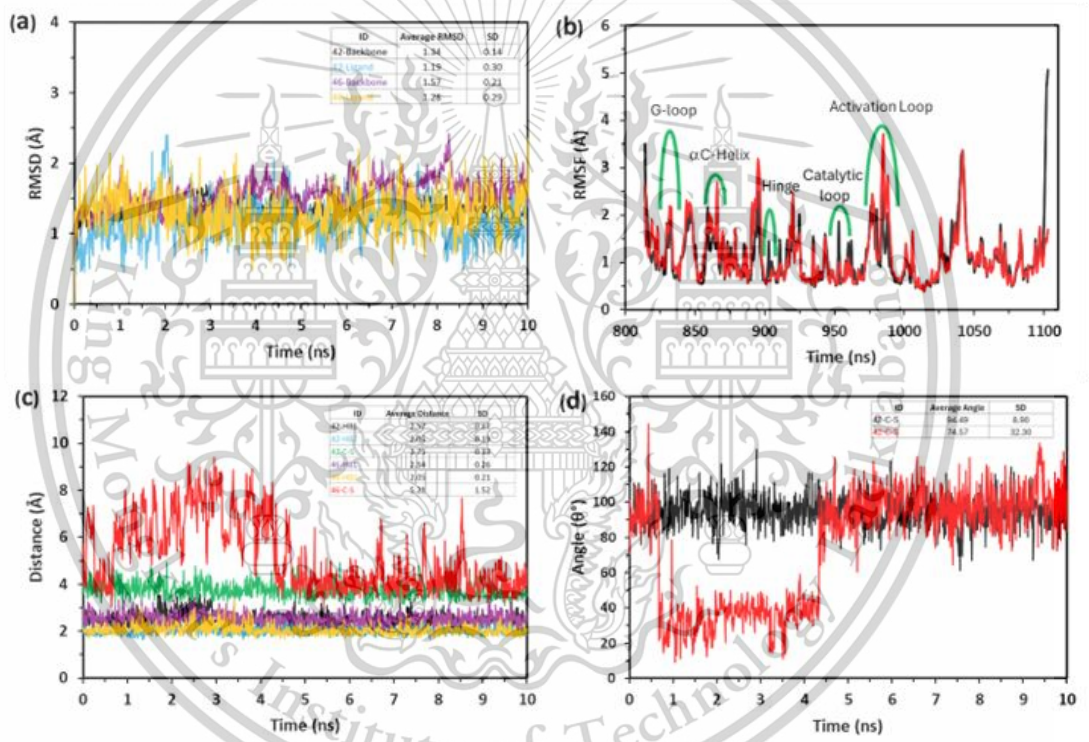

Figure 22 MD trajectory plot comparing between **42** and **46**, (a) backbone and ligand RMSD, (b) RMSF of protein, (c) distances from ligand to key amino acid residue, (d) electrophile-nucleophile angle

Agree with the stability of both ligands was confirmed by ligand RMSD values (**42**-Ligand RMSD =1.19 ± 0.30 Å, 46-Ligand RMSD =1.28 ± 0.29 Å) and the RMSF of two complexes showed a similar fluctuation pattern (Figure 22b). The HB forming at hinge of both ligands were in the same range with all simulations (Figure 21c). Indicating that all ligands

will be a good JAK3 binder. In addition, both **42** and **46** have a significantly lower ligand RMSD value than **40** and **44** which contained the same 4-position linker and methyl-piperazine aniline at 2-position due the lower steric effect of methyl-pyrazole amine. Even though the stability of complex and ligand between **42** and **46** were observed as no different, 42 could maintained the most stable C-S distance of 3.75 ± 0.33 Å with no fluctuation while 46 have a huge fluctuation from 1 to 4 ns and maintained C-S distance of 5.21 ± 1.52 Å through the simulation period (Figure 22c), correlated to their angle (Figure 22d)

The snapshot of complex was taken from both MD trajectory results at 1, 5 and 10 ns (Figure 23) to compare the binding pose and conformational change throughout the simulation period between **42** and **46** which is (R) and (S) stereoisomer.

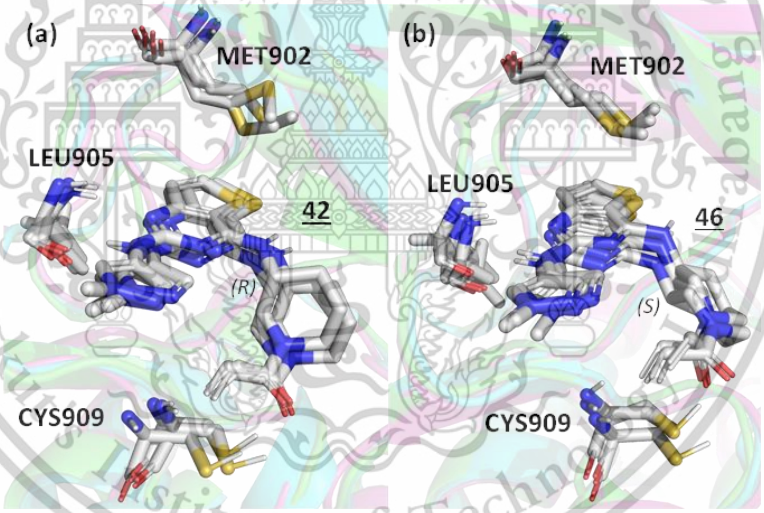

Figure 23 MD simulation Snapshots at 1 ns (Green), 5 ns (Cyan) and 10 ns (Magenta) of **42** (a) and **46** (b)

In conclusion, MD simulation can give the information that how ligand binds into the binding site, how strong of the HB forming at hinge and the possibility to form a nucleophile-electrophile interaction between nucleophilic CYS909 residue and ligand Michael-acceptor. Our simulation suggested that all ligand we design have a potential to bind in JAK3 binding site with no difference and 42 will be the most JAK3 active compound due to the stability of the

predicted nucleophile-electrophile interaction. However, we decided to synthesize all the compounds in order to compare in-vitro activity against JAK3 and the structure activity relationship (SAR) of our design will be explained in a further section.

4.2 SYNTHESIS AND CHARACTERIZATION

All compounds were prepared according to the synthetic route described in Figure 15. Briefly, intermediate **1**-**6** were prepared from the reaction of 2,4-dichlorothieno [3,2-d] pyrimidine and **6** amine linkers with triethylamine (TEA) in ethanol (EtOH), at 80 ℃, for 6 hrs., with a yield of 74-85%. **1**-**7** were then reacted with aniline or amino pyrazole by performed under Trifluoro acetic acid (TFA) as the acidic condition in iso-propyl alcohol (i-PrOH) at 90 ℃ overnight and directly used for de-protection reaction under condition (c) TFA in dichloromethane (DCM) to give intermediates **8**-**21** with yields ranging from 50-80%. Final compounds **22**-**49** were prepared by reacting to the acid chloride and carboxylic acid with different conditions. For Acryloyl Chloride and Propionyl Chloride, (d) DIPEA in anhydrous DCM at 0℃, for 30 mins., with 3-5%yield., or (e) Sodium bicarbonate ($NaHCO_3$) in anhydrous DCM at 0℃, for 1 hour with the yield from 10-20%. For 2-butynoic acid, (f) N,N'-Dicyclohexylcarbodiimide (DCC) in anhydrous DCM at room temperature for 1 hour, with yields ranging from 24-61%. Overall yields ranged from 7.0-21.8 %.

4.2.1 Final Compounds Characterization

Compounds were characterized by HPLC to confirm purity and retention time, Mass spectrophotometer (LC-QTOF and HRMS) to confirm the molecular mass, ^{1}H-NMR to confirm the total number of unique protons. ^{13}C-NMR was used to confirm the total number of unique carbon atoms. See Appendix B for all characterization data.

4.3 BIOLOGICAL ACTIVITY

All compounds have been evaluated for the relative inhibition (%inhibition) against JAK3 at a concentration of 1 μM (Table 4). The compound which obtained %inhibition more than 40% have been confirmed for their activity against JAK3, reported as IC_{50} values. Tofacitinib was used as a positive control, Fedratinib (JAK2 inhibitor) and Olmutinib (EGFR inhibitor) were used as a comparison inhibitor.

Table 4 Compound **22-49** and standard assessed in this study. Reported are L-groups, R-groups, physical properties and JAK3 activities (%Inhibition at 1 mM and IC_{50})

ID	L	R^1	R^2	MW	%inhibition at 1 μM	JAK3 IC_{50} (nM)
22	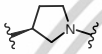	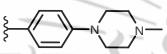		463.598	58±2.1	126.30±7.04
23	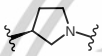	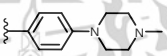		475.609	23±8.0	-
24	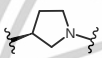	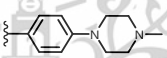		465.614	17±3.8	-
25	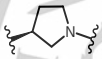			369.444	31±4.5	10189±4
26	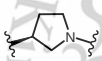			381.454	16±1.1	-
27	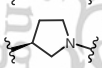			371.459	29±10.3	-
28	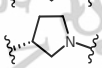	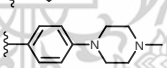		463.598	39±15.9	812.60±4.74
29	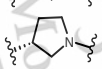	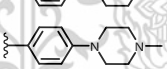		475.609	19±2.4	-
30	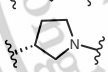			369.444	86±8.1	37.24±5.68
31	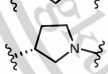			381.454	43±10.8	119.5±4.3
32	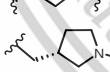	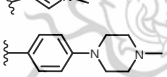		477.624	72±1.9	29.27±2.54
33	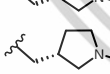	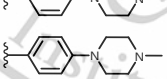		489.635	16±1.1	-
34	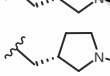			383.47	85±2.5	31.72±3.54
35	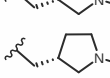			395.481	7±2.0	-
36				477.624	87±5.1	33.96±3.47
37				489.635	19±2.8	-
38				383.47	69±6.4	36.31±2.40
39				395.481	26±4.3	-
40				477.624	63±4.1	48.44±4.45
41				489.635	56±3.5	101.5±5.74
42				383.47	91±7.3	6.24±6.13

ID	L	R^1	R^2	MW	%inhibition at 1 μM	JAK3 IC_{50} (nM)
43	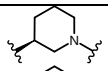		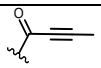	395.481	55±7.9	79.00±3.06
44	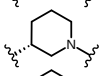	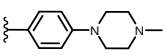		477.624	42±0.5	133.6±6.9
45	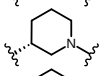	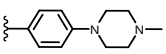		489.635	56±15.5	125.4±2.98
46	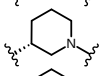			383.470	85±0.4	32.27±3.37
47	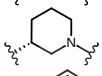			395.481	65±3.8	46.03±3.68
48	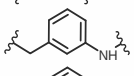	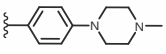		499.630	10±10.3	-
49	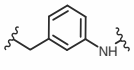	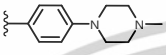		511.641	9±1.9	-
Tofacitinib					98±0.9	14.11±5.42
Fedratinib					49±30.4	99.57±4.41
Olmutinib					52±6.5	101.1±4.2

The screening of relative JAK3 %inhibition of the comparison compounds showed Tofacitinib (JAK3 inhibitor) obtained the highest JAK3 %inhibition (98±0.9%) while Fedratinib and Olmutinib obtained half of Tofacitinib activity, 49±30.4% and 52±6.5% respectively. The %inhibition cut – off value has been set at 40% due to the range of references activity. There were 15 compounds (out of 28) in our design obtained %inhibition greater than 40% (Figure 24) including all compounds with piperidine at L-position, 4 compounds with met-pyrrolidine and 3 compounds with pyrrolidine. On the other hand, compounds which contained benzylamine as a linker (**48** and **49**) exhibited the lowest activity against JAK3.

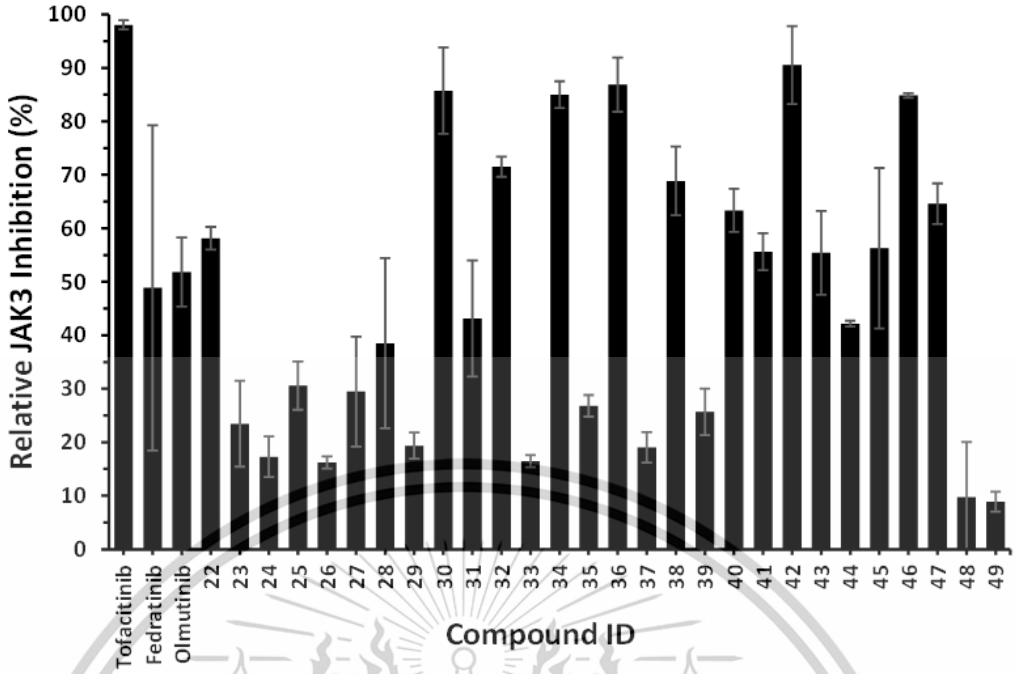

Figure 24 Relative JAK3 inhibition (%) of **22-49** at 1 μM including Tofacitinib Fedratinib and Olmutinib as a reference.

At L position, all compounds which substituted the amino piperidine at 4-position (**40-47**) exhibited the higher average %inhibition (64%), while the compound that have amino methyl-pyrrolidine (**32-39**) had average %inhibition = 50% and the compound with amino pyrrolidine (**22-31**) obtained the lowest activity (36% in average). However, when compared to the compound which substituted the benzylamine at 4-position (**48-49**), the amino piperidine compounds (**40-47**) showed more activity than **48-49** (9.5% in average).

At R2 position focused on the modification of 2 different Michael-acceptors (Acrylamide and 2-Butynamide) by compared with non-Michael-acceptors (Propenamide). The amino pyrazole compound with 2-butynamine attachment had 2-times lower activity than amino pyrazole compound with acrylamide at R2 (**22-31**). Agree with the methyl pyrazole compounds the 2-butynamine showed a 3 to 4-times lower activity than acrylamide (**32-39**). Among the comparison, all the compounds with amino piperidine had higher activity than 50% in both acrylamide and 2-butynamide (**40-47**). From the screening of JAK3 %inhibition, **42** had the activity as the same range as Tofacitinib (91±7.3% and 98±0.9%).

The top 15 compounds which obtained the activity against JAK3 more than 40% were subjected to measure the JAK3 IC_{50} to confirm their JAK3 inhibitory activity as shown in table 5 (from 60000 to 0.0002 nM: 4-fold serial dilution for 14-point concentration).

Table 5 The Key Compounds JAK3 Inhibition Activity Summary

ID	L	R1	R2	%inhibition at 1 μM	JAK3 IC_{50} (nM)	pIC_{50}
22	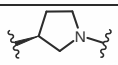	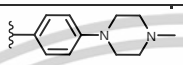	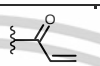	58	126.3	6.90
25	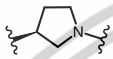			31	10189	4.99
28	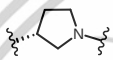	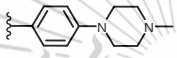		39	812.6	6.09
30	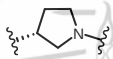	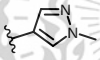		86	37.24	7.43
31	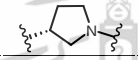	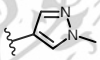	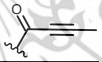	43	119.5	6.92
32	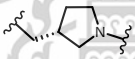	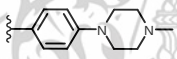		72	29.27	7.53
34		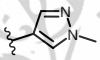		85	31.72	7.50
36	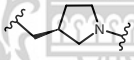	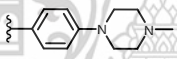		87	33.96	7.47
38	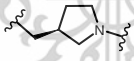	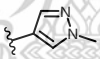		69	36.31	7.44
40	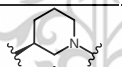	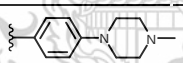		63	48.44	7.31
41	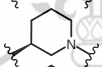	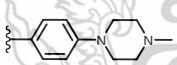	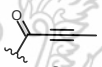	56	101.5	6.99
42	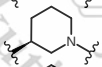	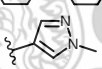		91	6.24	8.20
43	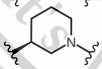		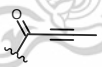	55	79	7.10
44	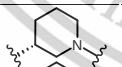			42	133.6	6.87
45				56	125.4	6.90
46				85	32.27	7.49
47				65	46.03	7.34
Tofacitinib				98	14.11	7.85
Fedratinib				49	99.57	7.00
Olmutinib				52	101.1	7.00

The JAK3 IC_{50} results from table 5 suggested that all 15 compounds were a JAK3 active compound in a nanomolar concentration (6.24- 812.60 nM, **25** and **28** was also selected for comparison). The IC_{50} results were related with the %inhibition when compared with pIC_{50}. The correlation between %inhibition and pIC_{50} values was 0.68 (Figure 25), confirmed that our reported data was reliable

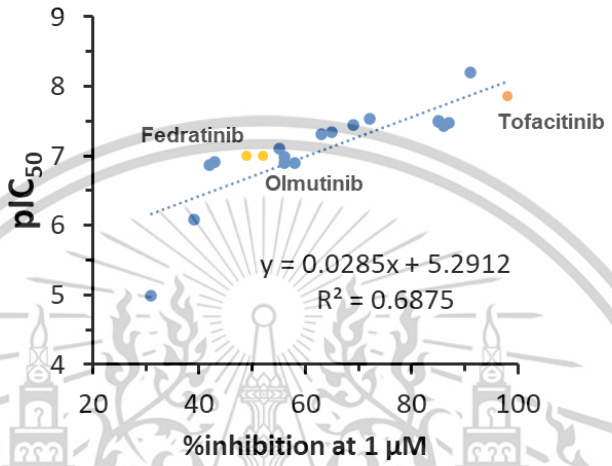

Figure 25 Correlation plot between %inhibition vs pIC_{50}

The results confirmed that 10 compounds were more active than Fedratinib and the best 5 compounds (**32 34 36 42** and **46**) were observed the JAK3 IC_{50} lower than 35 nM, only **42** (6.24 nM) obtained JAK3 IC_{50} lower than Tofacitinib (14.11 nM). However, the compound with amino pyrrolidine at L position (**22 25** and **28**) display the lowest JAK3 inhibition activity (126.30 10189 and 812.60 nM) when compared to other compounds with different linker group.

The analysis of JAK3 pIC50 was used for the Structure Activity Relationship (SAR) study that explained in Figure 26. The results indicated that the change of R1 position from piperazine to pyrazole effectively increased the compound JAK3 inhibition activity (Figure 26a). The change of Linker position from pyrrolidine to methyl-pyrrolidine and piperidine with R-stereoisomer significantly increased the overall JAK3 inhibition activity (Figure 26b and 26c). In the same way, acrylamide at R2 position could potentially increase the JAK3 inhibition activity of the compounds more than compounds with 2-butynamide (Figure 26d).

However, there was no statistical difference between pIC50 and all parameters in the analysis except the effect of linker position.

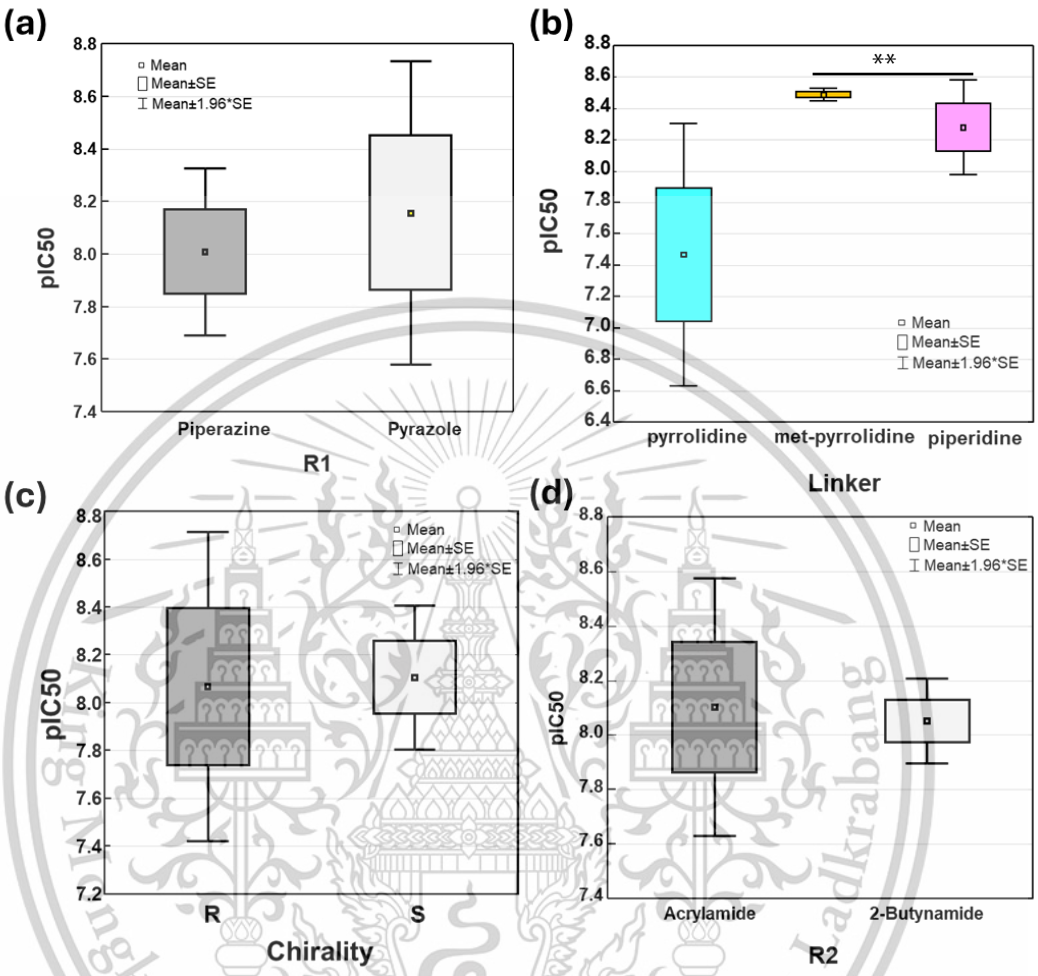

Figure 26 Structure Activity Relationship Study Based on compound's pIC50 including: (a) the changing of R1 position, (b) the difference aliphatic linker group with (c) the difference chirality and (d) the changing of R2 position. All boxplots created by paired T-test (** means p=0.04 significant difference at $p < 0.05000$)

Among all compounds, **42** which contained R-piperidine at L position, Pyrazole at R1 and acrylamide at R2 exhibited the highest JAK3 inhibition activity and become the most JAK3 active compound in this study.

The result was agreed with MD simulation when focused on R1 position, methyl-pyrazole had more active than methyl-piperazine (Table 6). The compound with amino piperidine (**40**-**47**), (R)-piperidine (**40**-**43**) had more active than (S)-piperidine (**45**-**48**).

Table 6 Summary of MD result compared with their JAK3 activity

ID	L	R1	R2	JAK3 IC_{50} (nM)	RMSD (Å)		Bond distance (Å)			Angle (θ°)
					backbone	ligand	hb1	hb2	C-S	C-S
22 (5R)		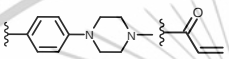		126.3	1.52	1.74	2.55	2.13	4.28	81.14
28 (5S)		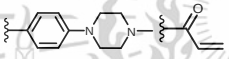		812.6	1.52	2.75	2.08	2.07	7.17	102.19
32 (5RCH2)	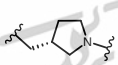	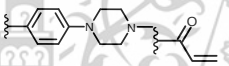		29.27	1.71	2.03	2.56	2.10	5.86	83.27
36 (5SCH2)	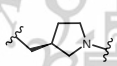	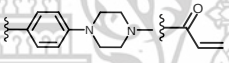		33.96	1.55	2.46	2.50	2.18	7.82	88.99
40 (6R)		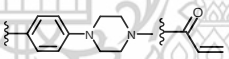		48.44	1.68	2.40	2.55	2.08	4.02	84.42
42 (6R)				6.24	1.34	1.19	2.57	2.05	3.75	94.50
44 (6S)		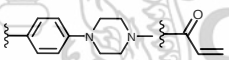		133.6	1.47	1.98	2.50	2.11	4.74	74.50
46 (6S)				32.27	1.57	1.28	2.54	2.05	5.21	74.57

MD simulation was used to determine whether molecules fit within the pocket and the results showed all the compound could bind in JAK3 binding pocket. However, there was no statistical correlation between JAK3 IC_{50} and any MD-parameter.

CHAPTER 5

CONCLUSION

A set of 28 compounds was designed as JAK3 inhibitors using a structure-based drug design approach. The core structure of Olmutinib – EGFR inhibitor was selected and modified to enhance affinity for JAK3. The general route of synthesis has been optimized to get a good yield of final compounds. All compounds have been synthesized with an acceptable yield ranging from 10-60% for the final step.

The relative inhibition activity of compounds has been screened in JAK3 and reported as %inhibition. The results indicated that there were 15 compounds active against JAK3 (%inhibition higher than 40%). This result was confirmed by JAK3 IC_{50} (correlation coefficient 0.68). Compound **42** obtained the highest JAK3 activity (**42**: JAK3 IC_{50} = 6.24 nM) and exhibited better activity than the JAK3 approved drug – Tofacitinib (Tofacitinib: JAK3 IC_{50} = 14.11 nM).

The future study will be on the identification of 5 compounds (**32, 34, 36, 42** and **46**) for the determination of solubility, lipophilicity and the selectivity over EGFR and JAK2.

REFERENCES

1. Ortega, M.A., et al. *Immune-Mediated Diseases from the Point of View of Psychoneuroimmunoendocrinology*. Biology, 2022. **11**, DOI: 10.3390/biology11070973.
2. McInnes, I.B. and E.M. Gravallese, *Immune-mediated inflammatory disease therapeutics: past, present and future.* Nature Reviews Immunology, 2021. **21**(10): p. 680-686.
3. David, T., S.F. Ling, and A. Barton, *Genetics of immune-mediated inflammatory diseases.* Clinical and Experimental Immunology, 2018. **193**(1): p. 3-12.
4. Lahiry, P., et al., *Kinase mutations in human disease: interpreting genotype-phenotype relationships.* Nat Rev Genet, 2010. **11**(1): p. 60-74.
5. O'Shea, J.J., M. Gadina, and R.M. Siegel, *Cytokines and Cytokine Receptors*, in *Clinical Immunology*. 2019. p. 127-155.e1.
6. Solimani, F., K. Meier, and K. Ghoreschi, *Emerging Topical and Systemic JAK Inhibitors in Dermatology.* Front Immunol, 2019. **10**: p. 2847.
7. Sharma, V. and M. Gupta, *Designing of kinase hinge binders: A medicinal chemistry perspective.* Chem Biol Drug Des, 2022. **100**(6): p. 968-980.
8. Changelian, P.S., et al., *Prevention of Organ Allograft Rejection by a Specific Janus Kinase 3 Inhibitor.* Science, 2003. **302**(5646): p. 875-878.
9. Wernig, G., et al., *Efficacy of TG101348, a Selective JAK2 Inhibitor, in Treatment of a Murine Model of JAK2V617F-Induced Polycythemia Vera.* Cancer Cell, 2008. **13**(4): p. 311-320.
10. Davis, R.R., et al., *Structural Insights into JAK2 Inhibition by Ruxolitinib, Fedratinib, and Derivatives Thereof.* J Med Chem, 2021. **64**(4): p. 2228-2241.
11. Casimiro-Garcia, A., et al., *Identification of Cyanamide-Based Janus Kinase 3 (JAK3) Covalent Inhibitors.* J Med Chem, 2018. **61**(23): p. 10665-10699.
12. Wang, S., S. Cang, and D. Liu, *Third-generation inhibitors targeting EGFR T790M mutation in advanced non-small cell lung cancer.* J Hematol Oncol, 2016. **9**: p. 34.
13. Dhillon, S., *Tirabrutinib: First Approval.* Drugs, 2020. **80**(8): p. 835-840.
14. Tan, L., et al., *Development of Selective Covalent Janus Kinase 3 Inhibitors.* J Med

Chem, 2015. **58**(16): p. 6589-606.

15. Thorarensen, A., et al., *Design of a Janus Kinase 3 (JAK3) Specific Inhibitor 1-((2S,5R)-5-((7H-Pyrrolo[2,3-d]pyrimidin-4-yl)amino)-2-methylpiperidin-1-yl)prop-2-en-1-one (PF-06651600) Allowing for the Interrogation of JAK3 Signaling in Humans.* J Med Chem, 2017. **60**(5): p. 1971-1993.
16. Monteleone, G., et al., *Immune-mediated inflammatory diseases: Common and different pathogenic and clinical features.* Autoimmunity Reviews, 2023. **22**(10): p. 103410.
17. Schett, G., B. McInnes Iain, and F. Neurath Markus, *Reframing Immune-Mediated Inflammatory Diseases through Signature Cytokine Hubs.* New England Journal of Medicine, 2021. **385**(7): p. 628-639.
18. Kuek, A., B.L. Hazleman, and A.J.K. Östör, *Immune-mediated inflammatory diseases (IMIDs) and biologic therapy: a medical revolution.* Postgraduate Medical Journal, 2007. **83**(978): p. 251-260.
19. Quach, H., et al., *Mechanism of action of immunomodulatory drugs (IMiDS) in multiple myeloma.* Leukemia, 2010. **24**(1): p. 22-32.
20. Wong, M., et al., *TNF α blockade in human diseases: Mechanisms and future directions.* Clinical Immunology, 2008. **126**(2): p. 121-136.
21. Lee, H.J., et al., *Immunogenetics of autoimmune thyroid diseases: A comprehensive review.* Journal of Autoimmunity, 2015. **64**: p. 82-90.
22. Reveille, J.D. and G.S. Bruce, *4 - MHC CLASS II AND NON-MHC GENES IN THE PATHOGENESIS OF SYSTEMIC LUPUS ERYTHEMATOSUS*, in *Systemic Lupus Erythematosus (Fourth Edition)*, R.G. Lahita, Editor. 2004, Academic Press: San Diego. p. 109-151.
23. Kumar, V., C. Wijmenga, and R.J. Xavier, *Genetics of immune-mediated disorders: from genome-wide association to molecular mechanism.* Current Opinion in Immunology, 2014. **31**: p. 51-57.
24. Vernero, M., et al. *Prevalence and Clinical Impact of Immune-Mediated Inflammatory Diseases in Patients with Inflammatory Bowel Disease: Results from a Large Retrospective Observational Study*. Journal of Clinical Medicine, 2024. **13**, DOI: 10.3390/jcm13041019.
25. Holstein, S.A. and P.L. McCarthy, *Immunomodulatory Drugs in Multiple Myeloma:*

Mechanisms of Action and Clinical Experience. Drugs, 2017. **77**(5): p. 505-520.

26. Kallinich, T. and M.A. Mall, *Immune-mediated inflammatory diseases (IMIDs) in children: key research questions and some answers.* Molecular and Cellular Pediatrics, 2024. **11**(1): p. 5.
27. Padyukov, L., *Genetics of rheumatoid arthritis.* Seminars in Immunopathology, 2022. **44**(1): p. 47-62.
28. Alavinejad, P., et al., *Inflammatory bowel disease evolution in the past two decades: a chronological multinational study.* eClinicalMedicine, 2024. **70**.
29. Raharja, A., S.K. Mahil, and J.N. Barker, *Psoriasis: a brief overview.* Clinical Medicine, 2021. **21**(3): p. 170-173.
30. Kopp, K.O., et al. *A New Generation of IMiDs as Treatments for Neuroinflammatory and Neurodegenerative Disorders*. Biomolecules, 2023. **13**, DOI: 10.3390/biom13050747.
31. O'Shea, J.J., M. Gadina, and Y. Kanno, *Cytokine Signaling: Birth of a Pathway.* The Journal of Immunology, 2011. **187**(11): p. 5475-5478.
32. Bird, S. and C. Pawlyn, *IMiD resistance in multiple myeloma: current understanding of the underpinning biology and clinical impact.* Blood, 2023. **142**(2): p. 131-140.
33. Gandhi, K., J.W. Heitz, and E.R. Viscusi, *CHAPTER 61 - TREATMENT OF PAIN*, in *Pharmacology and Therapeutics*, S.A. Waldman, et al., Editors. 2009, W.B. Saunders: Philadelphia. p. 883-893.
34. Hui, D.S., et al., *The role of adjuvant immunomodulatory agents for treatment of severe influenza.* Antiviral Research, 2018. **150**: p. 202-216.
35. Williams, D.M., *Clinical Pharmacology of Corticosteroids.* Respiratory Care, 2018. **63**(6): p. 655.
36. Coutinho, A.E. and K.E. Chapman, *The anti-inflammatory and immunosuppressive effects of glucocorticoids, recent developments and mechanistic insights.* Molecular and Cellular Endocrinology, 2011. **335**(1): p. 2-13.
37. Kim, G., et al., *Examining Time to Initiation of Biologic Disease-modifying Antirheumatic Drugs and Medication Adherence and Persistence Among Texas Medicaid Recipients With Rheumatoid Arthritis.* Clin Ther, 2016. **38**(3): p. 646-54.
38. Cronstein, B.N. and T.M. Aune, *Methotrexate and its mechanisms of action in*

inflammatory arthritis. Nature Reviews Rheumatology, 2020. **16**(3): p. 145-154.

39. Hamed, K.M., et al., *Overview of Methotrexate Toxicity: A Comprehensive Literature Review.* Cureus, 2022. **14**(9): p. e29518.
40. Al-Qahtani, A.A., F.S. Alhamlan, and A.A. Al-Qahtani *Pro-Inflammatory and Anti-Inflammatory Interleukins in Infectious Diseases: A Comprehensive Review*. Tropical Medicine and Infectious Disease, 2024. **9**, DOI: 10.3390/tropicalmed9010013.
41. Cummings, J.R., S. Keshav, and S.P. Travis, *Medical management of Crohn's disease.* Bmj, 2008. **336**(7652): p. 1062-6.
42. Monaco, C., et al., *Anti-TNF therapy: past, present and future.* Int Immunol, 2015. **27**(1): p. 55-62.
43. Palladino, M.A., et al., *Anti-TNF- α therapies: the next generation.* Nature Reviews Drug Discovery, 2003. **2**(9): p. 736-746.
44. Nada, H., et al., *Perspective for Discovery of Small Molecule IL-6 Inhibitors through Study of Structure–Activity Relationships and Molecular Docking.* Journal of Medicinal Chemistry, 2023. **66**(7): p. 4417-4433.
45. Scott, L.J., *Tocilizumab: a review in rheumatoid arthritis.* Drugs, 2017. **77**: p. 1865-1879.
46. Gargiulo, L., et al., *Drug survival of IL-12/23, IL-17 and IL-23 inhibitors for moderate-to-severe plaque psoriasis: a retrospective multicenter real-world experience on 5932 treatment courses – IL PSO (Italian landscape psoriasis).* Frontiers in Immunology, 2024. **14**.
47. Bai, F., et al., *Short-Term Efficacy and Safety of IL-17, IL-12/23, and IL-23 Inhibitors Brodalumab, Secukinumab, Ixekizumab, Ustekinumab, Guselkumab, Tildrakizumab, and Risankizumab for the Treatment of Moderate to Severe Plaque Psoriasis: A Systematic Review and Network Meta-Analysis of Randomized Controlled Trials.* J Immunol Res, 2019. **2019**: p. 2546161.
48. Lund, F.E. and T.D. Randall, *Effector and regulatory B cells: modulators of CD4+ T cell immunity.* Nature Reviews Immunology, 2010. **10**(4): p. 236-247.
49. Pescovitz, M.D., *Rituximab, an Anti-CD20 Monoclonal Antibody: History and Mechanism of Action.* American Journal of Transplantation, 2006. **6**(5, Part 1): p. 859-866.

50. Larsen, C.P., et al., *A New Look at Blockade of T-cell Costimulation: A Therapeutic Strategy for Long-term Maintenance Immunosuppression.* American Journal of Transplantation, 2006. **6**(5, Part 1): p. 876-883.
51. Clark, J.D., M.E. Flanagan, and J.-B. Telliez, *Discovery and Development of Janus Kinase (JAK) Inhibitors for Inflammatory Diseases.* Journal of Medicinal Chemistry, 2014. **57**(12): p. 5023-5038.
52. Shawky, A.M., et al., *A Comprehensive Overview of Globally Approved JAK Inhibitors.* Pharmaceutics, 2022. **14**(5).
53. Tampa, M., et al., *A New Horizon for Atopic Dermatitis Treatments: JAK Inhibitors.* J Pers Med, 2023. **13**(3).
54. Witte, T., *Methotrexate as combination partner of TNF inhibitors and tocilizumab. What is reasonable from an immunological viewpoint?* Clin Rheumatol, 2015. **34**(4): p. 629-34.
55. Samuel, C., et al., *A Review on the Safety of Using JAK Inhibitors in Dermatology: Clinical and Laboratory Monitoring.* Dermatol Ther (Heidelb), 2023. **13**(3): p. 729-749.
56. Laux, J., et al., *Selective Inhibitors of Janus Kinase 3 Modify Responses to Lipopolysaccharides by Increasing the Interleukin-10-to-Tumor Necrosis Factor α Ratio.* ACS Pharmacology & Translational Science, 2023. **6**(6): p. 892-906.
57. Yao, L., et al., *Design and Synthesis of Ligand Efficient Dual Inhibitors of Janus Kinase (JAK) and Histone Deacetylase (HDAC) Based on Ruxolitinib and Vorinostat.* Journal of Medicinal Chemistry, 2017. **60**(20): p. 8336-8357.
58. Hu, X., et al., *The JAK/STAT signaling pathway: from bench to clinic.* Signal Transduction and Targeted Therapy, 2021. **6**(1): p. 402.
59. Bach, J., et al., *Identification of 2-Imidazopyridine and 2-Aminopyridone Purinones as Potent Pan-Janus Kinase (JAK) Inhibitors for the Inhaled Treatment of Respiratory Diseases.* Journal of Medicinal Chemistry, 2019. **62**(20): p. 9045-9060.
60. Vadivel, C.K., et al., *JAK3 Is Expressed in the Nucleus of Malignant T Cells in Cutaneous T Cell Lymphoma (CTCL).* Cancers (Basel), 2021. **13**(2).
61. Zhu, H., et al., *Chlorinated Organophosphate Flame Retardants Impair the Lung Function via the IL-6/JAK/STAT Signaling Pathway.* Environmental Science & Technology, 2022. **56**(24): p. 17858-17869.

62. Tanaka, Y., *Systemic lupus erythematosus.* Best Practice & Research Clinical Rheumatology, 2022. **36**(4): p. 101814.
63. Mascarenhas, J.O., N.C.P. Cross, and R.A. Mesa, *The future of JAK inhibition in myelofibrosis and beyond.* Blood Reviews, 2014. **28**(5): p. 189-196.
64. Zheng, J., et al., *Small molecule approaches to treat autoimmune and inflammatory diseases (Part I): Kinase inhibitors.* Bioorganic & Medicinal Chemistry Letters, 2021. **38**: p. 127862.
65. Levine, R.L., et al., *Role of JAK2 in the pathogenesis and therapy of myeloproliferative disorders.* Nature Reviews Cancer, 2007. **7**(9): p. 673-683.
66. Field, S.D., et al., *Selective Downregulation of JAK2 and JAK3 by an ATP-Competitive pan-JAK Inhibitor.* ACS Chemical Biology, 2017. **12**(5): p. 1183-1187.
67. Liu, C., et al., *Discovery of BMS-986202: A Clinical Tyk2 Inhibitor that Binds to Tyk2 JH2.* Journal of Medicinal Chemistry, 2021. **64**(1): p. 677-694.
68. Jekarl, D.W., et al., *JAK2 V617F mutation in myelodysplastic syndrome, myelodysplastic syndrome/myeloproliferative neoplasm, unclassifiable, refractory anemia with ring sideroblasts with thrombocytosis, and acute myeloid leukemia.* Korean J Hematol, 2010. **45**(1): p. 46-50.
69. Robinette, M.L., et al., *Jak3 deficiency blocks innate lymphoid cell development.* Mucosal Immunology, 2018. **11**(1): p. 50-60.
70. Tanaka, Y., et al., *Janus kinase-targeting therapies in rheumatology: a mechanisms-based approach.* Nature Reviews Rheumatology, 2022. **18**(3): p. 133-145.
71. Singh, S. and S. Singh, *JAK-STAT inhibitors: Immersing therapeutic approach for management of rheumatoid arthritis.* International Immunopharmacology, 2020. **86**: p. 106731.
72. Taylor, P.C., et al., *Differential properties of Janus kinase inhibitors in the treatment of immune-mediated inflammatory diseases.* Rheumatology, 2024. **63**(2): p. 298-308.
73. Bonelli, M., et al., *Selectivity, efficacy and safety of JAKinibs: new evidence for a still evolving story.* Annals of the Rheumatic Diseases, 2024. **83**(2): p. 139.
74. Liu, C., et al., *A Decade of JAK Inhibitors: What Have We Learned and What May Be the Future?* Arthritis & Rheumatology, 2021. **73**(12): p. 2166-2178.

75. Quintas-Cardama, A., et al., *Preclinical characterization of the selective JAK1/2 inhibitor INCB018424: therapeutic implications for the treatment of myeloproliferative neoplasms.* Blood, 2010. **115**(15): p. 3109-17.
76. King, B., et al., *Two Phase 3 Trials of Baricitinib for Alopecia Areata.* New England Journal of Medicine, 2022. **386**(18): p. 1687-1699.
77. Assadiasl, S., et al., *Baricitinib: From Rheumatoid Arthritis to COVID-19.* J Clin Pharmacol, 2021. **61**(10): p. 1274-1285.
78. Nakagawa, H., et al., *Safety, efficacy, and pharmacokinetics of delgocitinib ointment in infants with atopic dermatitis: A phase 3, open-label, and long-term study.* Allergology International, 2024. **73**(1): p. 137-142.
79. Bissonnette, R., et al., *Efficacy and safety of delgocitinib cream in adults with moderate to severe chronic hand eczema (DELTA 1 and DELTA 2): results from multicentre, randomised, controlled, double-blind, phase 3 trials.* The Lancet, 2024. **404**(10451): p. 461-473.
80. Chandran, V., et al., *Pharmacodynamic effects of filgotinib treatment driving clinical improvement in patients with active psoriatic arthritis enrolled in the EQUATOR trial.* RMD Open, 2023. **9**(4).
81. Tanaka, Y., et al., *Safety and efficacy of filgotinib for Japanese patients with RA and inadequate response to MTX: FINCH 1 52-week results and FINCH 4 48-week results.* Modern Rheumatology, 2023. **33**(4): p. 668-679.
82. Burmester, G.R., et al., *Integrated safety analysis of filgotinib in patients with moderate-to-severe rheumatoid arthritis over a treatment duration of up to 8.3 years.* Annals of the Rheumatic Diseases, 2024. **83**(9): p. 1110.
83. Takeuchi, T., et al., *Efficacy and safety of peficitinib (ASP015K) in patients with rheumatoid arthritis and an inadequate response to methotrexate: results of a phase III randomised, double-blind, placebo-controlled trial (RAJ4) in Japan.* Annals of the Rheumatic Diseases, 2019. **78**(10): p. 1305.
84. Tanaka, Y. and H. Izutsu, *Peficitinib for the treatment of rheumatoid arthritis: an overview from clinical trials.* Expert Opinion on Pharmacotherapy, 2020. **21**(9): p. 1015-1025.
85. Arana Yi, C., C.S. Tam, and S. Verstovsek, *Efficacy and safety of ruxolitinib in the treatment of patients with myelofibrosis.* Future Oncol, 2015. **11**(5): p. 719-33.

86. Pemmaraju, N., et al., *Ten years after ruxolitinib approval for myelofibrosis: a review of clinical efficacy.* Leukemia & Lymphoma, 2023. **64**(6): p. 1063-1081.
87. Vélez, P., et al., *Tofacitinib, an oral Janus kinase inhibitor, in patients from Colombia with rheumatoid arthritis: Pooled efficacy and safety analyses of data from phase III studies.* Revista Colombiana de Reumatología (English Edition), 2018. **25**(4): p. 233-244.
88. Ytterberg Steven, R., et al., *Cardiovascular and Cancer Risk with Tofacitinib in Rheumatoid Arthritis.* New England Journal of Medicine, 2022. **386**(4): p. 316-326.
89. Sanmartí, R. and H. Corominas, *Upadacitinib for Patients with Rheumatoid Arthritis: A Comprehensive Review.* J Clin Med, 2023. **12**(5).
90. Burmester, G.R., et al., *Upadacitinib in Rheumatoid Arthritis and Inadequate Response to Conventional Synthetic Disease-Modifying Antirheumatic Drugs: Efficacy and Safety Through 5 Years (SELECT-NEXT).* The Journal of Rheumatology, 2024. **51**(7): p. 663.
91. De Vivo, M., et al., *Role of Molecular Dynamics and Related Methods in Drug Discovery.* J Med Chem, 2016. **59**(9): p. 4035-61.
92. Forster, M., et al., *Selective JAK3 Inhibitors with a Covalent Reversible Binding Mode Targeting a New Induced Fit Binding Pocket.* Cell Chem Biol, 2016. **23**(11): p. 1335-1340.
93. Olsson, M.H.M., et al., *PROPKA3: Consistent Treatment of Internal and Surface Residues in Empirical pKa Predictions.* Journal of Chemical Theory and Computation, 2011. **7**(2): p. 525-537.
94. Sondergaard, C.R., et al., *Improved Treatment of Ligands and Coupling Effects in Empirical Calculation and Rationalization of pKa Values.* J Chem Theory Comput, 2011. **7**(7): p. 2284-95.
95. Abraham, M.J., et al., *GROMACS: High performance molecular simulations through multi-level parallelism from laptops to supercomputers.* SoftwareX, 2015. **1-2**: p. 19-25.
96. Hornak, V., et al., *Comparison of multiple Amber force fields and development of improved protein backbone parameters.* Proteins, 2006. **65**(3): p. 712-25.
97. Wang, J., et al., *Automatic atom type and bond type perception in molecular mechanical calculations.* J Mol Graph Model, 2006. **25**(2): p. 247-60.

98. Sousa da Silva, A.W. and W.F. Vranken, *ACPYPE - AnteChamber PYthon Parser interfacE.* BMC Research Notes, 2012. **5**(1): p. 367.
99. Wang, J., et al., *Development and testing of a general amber force field.* J Comput Chem, 2004. **25**(9): p. 1157-74.
100. Price, D.J. and C.L. Brooks, 3rd, *A modified TIP3P water potential for simulation with Ewald summation.* J Chem Phys, 2004. **121**(20): p. 10096-103.
101. Thompson, E.J., et al., *Evaluating molecular mechanical potentials for helical peptides and proteins.* PLoS One, 2010. **5**(4): p. e10056.
102. Telliez, J.B., et al., *Discovery of a JAK3-Selective Inhibitor: Functional Differentiation of JAK3-Selective Inhibition over pan-JAK or JAK1-Selective Inhibition.* ACS Chem Biol, 2016. **11**(12): p. 3442-3451.

Appendix A

MD SIMULATION RESULTS

MD Simulation of 22

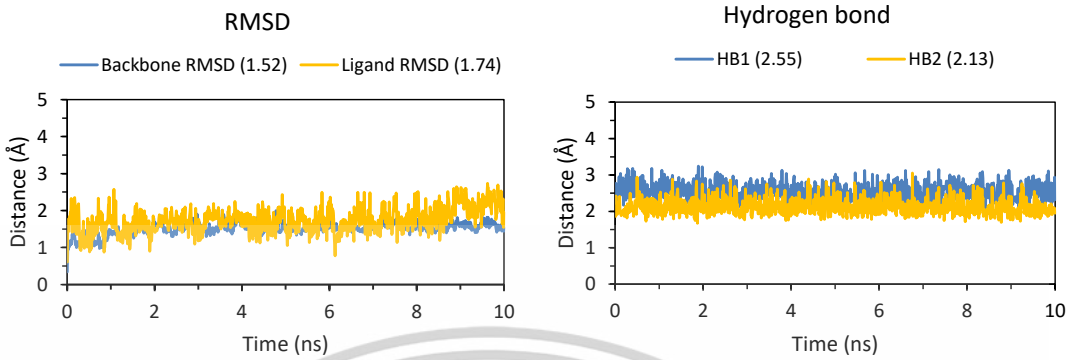

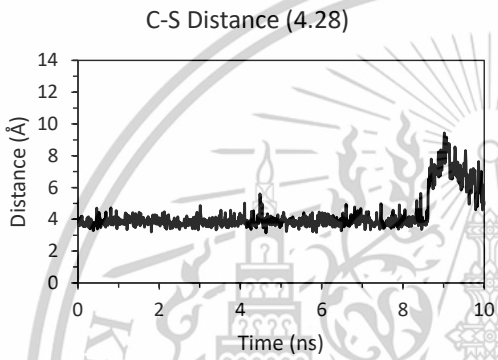

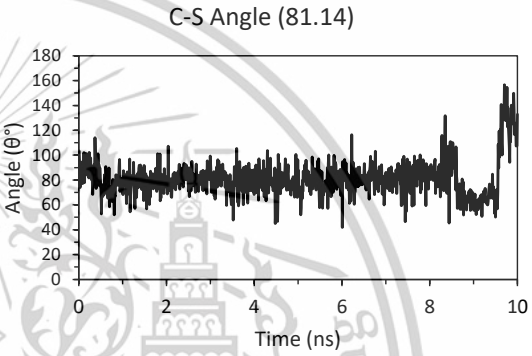

MD Simulation of 28

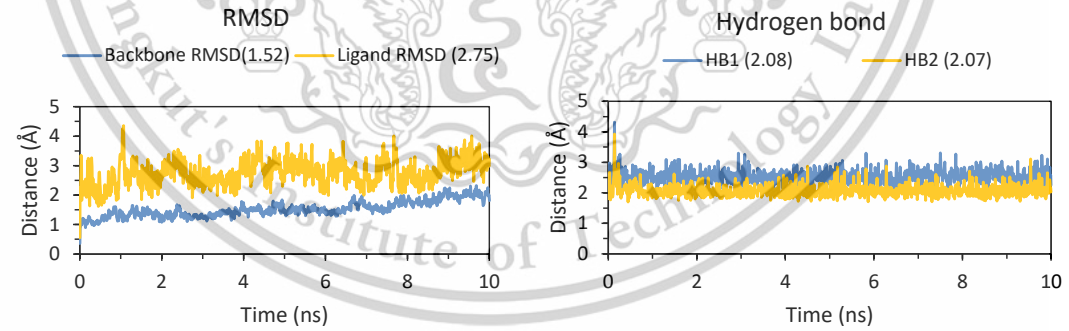

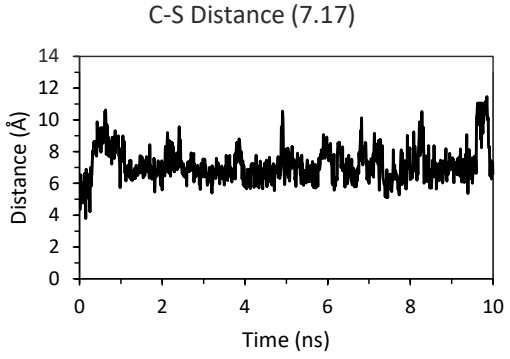

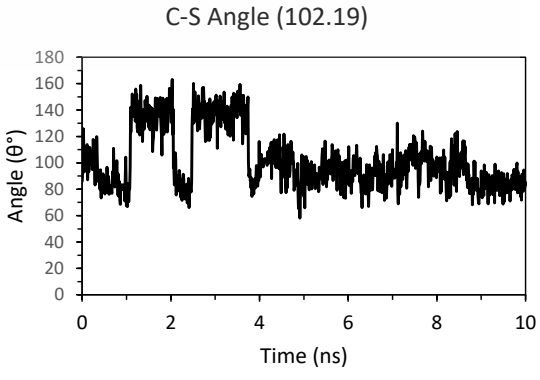

MD Simulation of 32

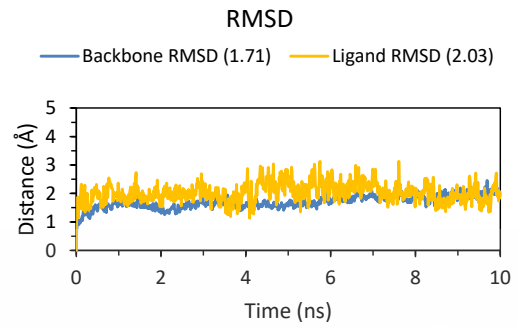

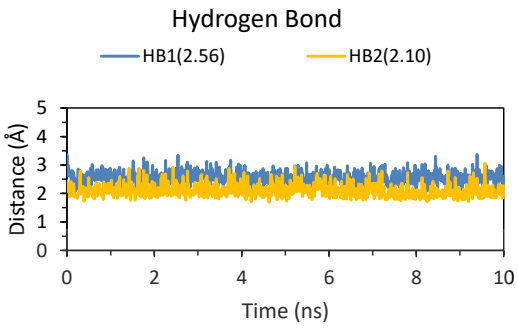

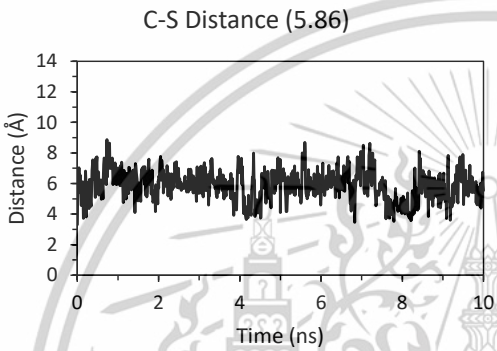

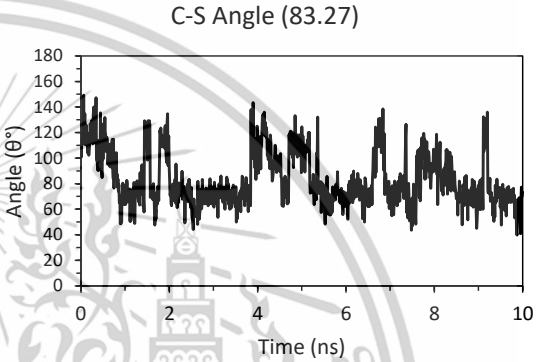

MD Simulation of 36

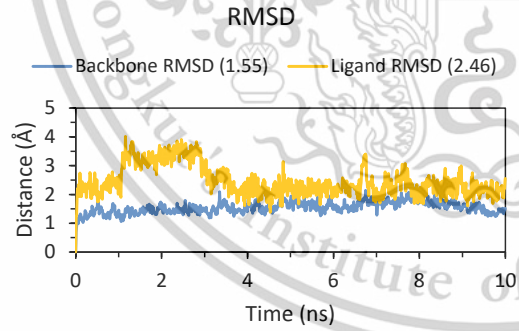

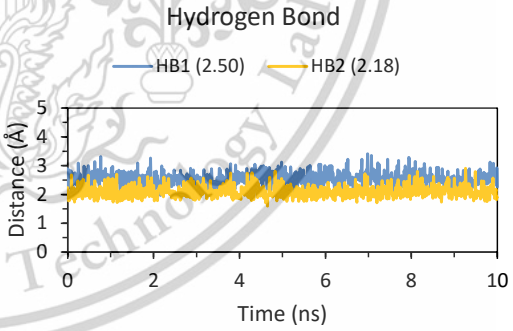

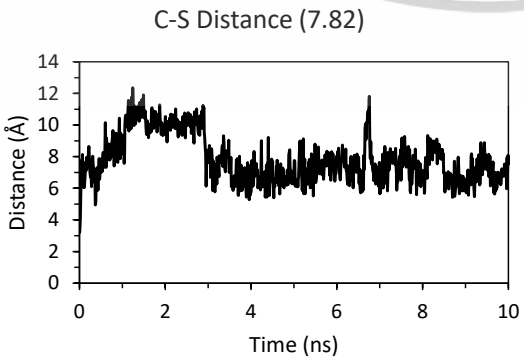

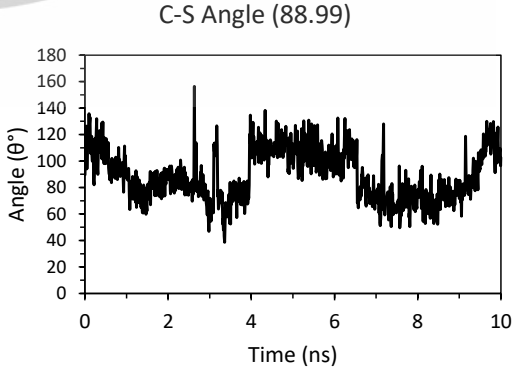

MD Simulation of 40

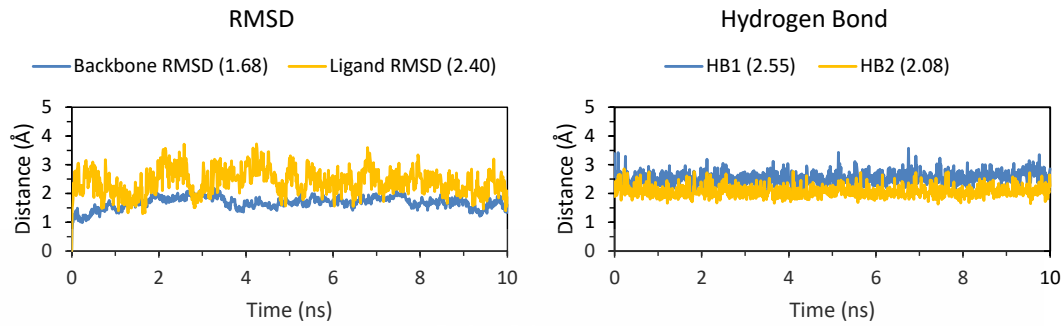

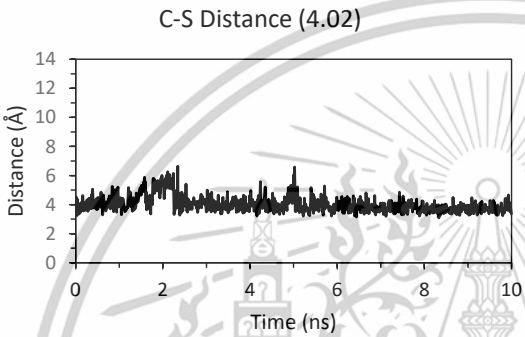

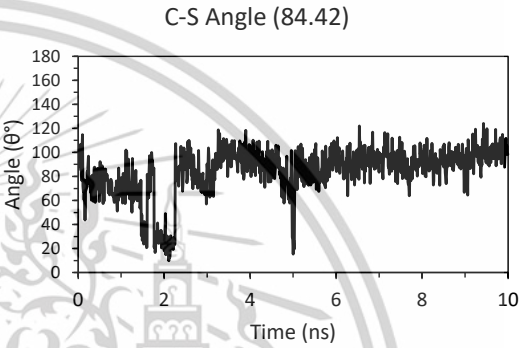

MD Simulation of 42

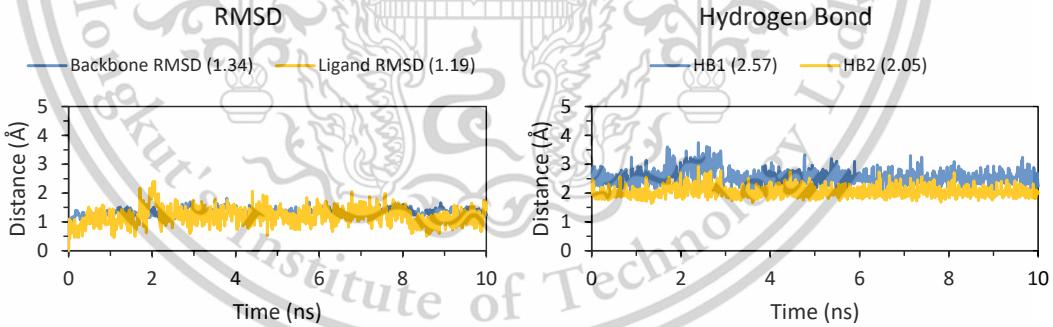

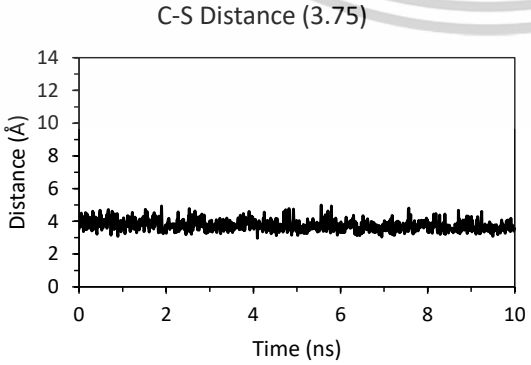

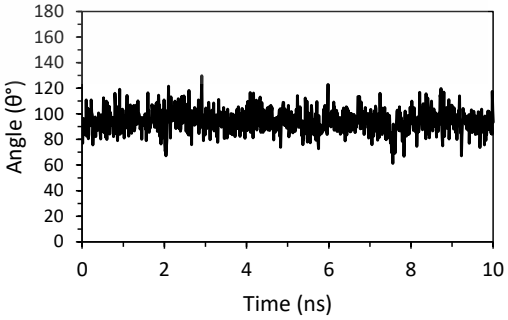

MD Simulation of 44

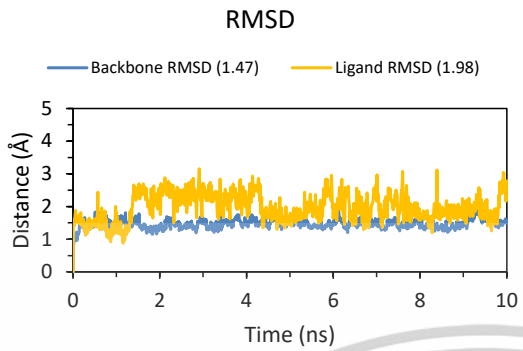

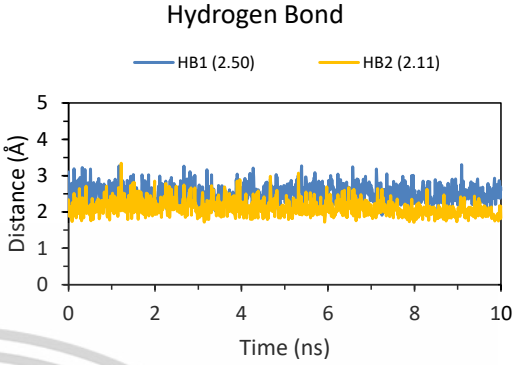

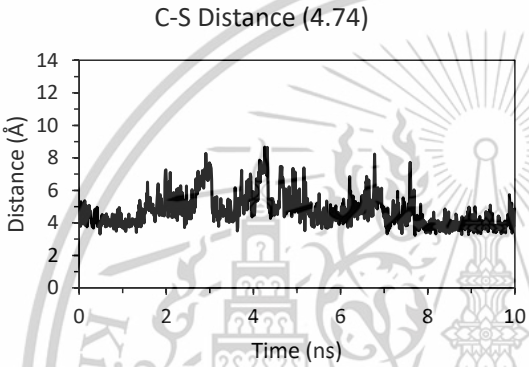

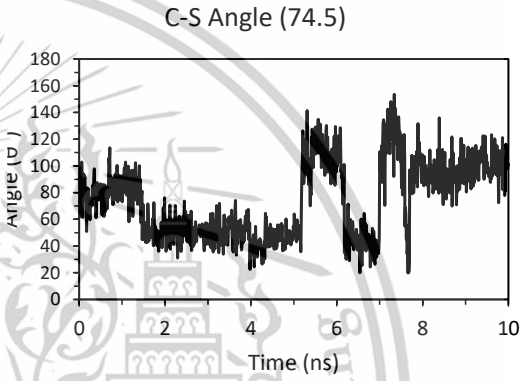

MD Simulation of 46

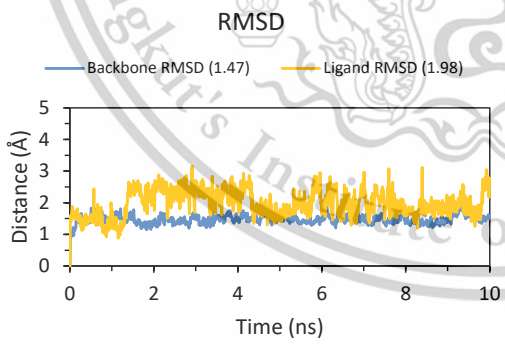

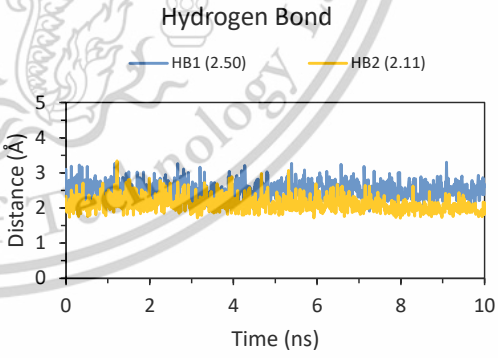

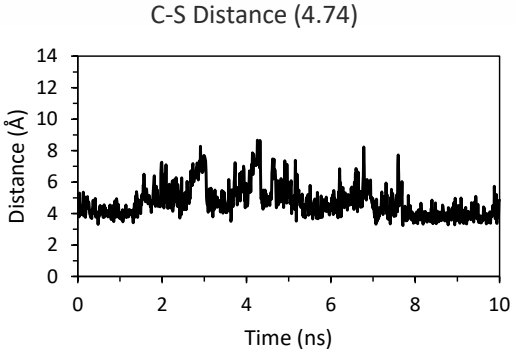

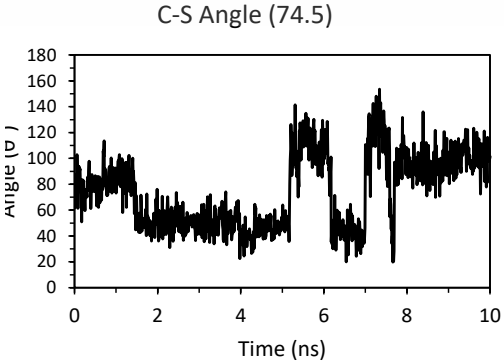

MD Simulation of 4Z16 original inhibitor

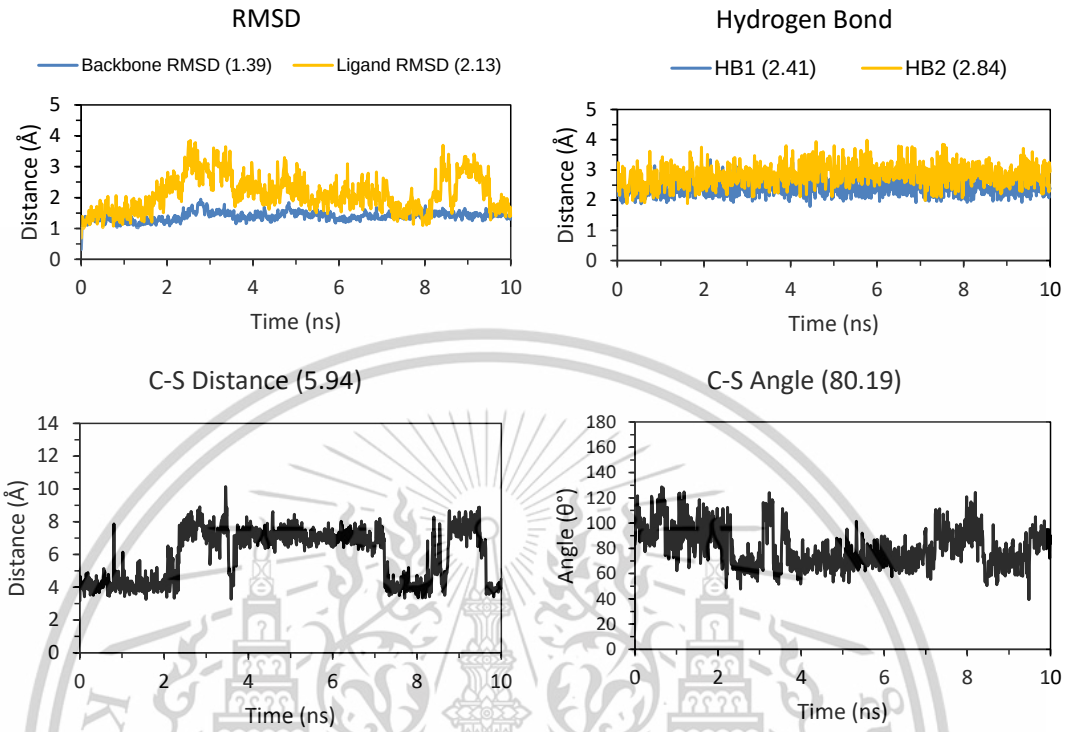

Appendix B

CHARACTERIZATION DETAILS

Compound 22: 1-[(3R)-3-[[2-[4-(4-methylpiperazin-1-yl)anilino]thieno[3,2-d]pyrimidin-4-yl]amino]pyrrolidin-1-yl]prop-2-en-1-one

Following the general procedure compound **8** (1 equivalent) was reacted with Acryloyl chloride (1.75 equivalent) under condition 1. 24 mg of white solid obtained with Yield 14%. HPLC analysis RT 2.520 min, Purity 96%. LCQTOF for $C_{24}H_{30}N_7OS$ $[M+H]^+$ Calc: 464.22217, found: 464.2237. ^{1}H-NMR (500 MHz, DMSO-d6) δ 8.73, 7.89, 7.60, 7.07 (d, J = 3.2 Hz), 6.82 (d, J = 5.5 Hz), 6.15 – 6.08 (m), 5.70 – 5.59 (m), 4.66 (m, J = 24.3, 7.6, 3.7 Hz), 3.74 (m, J = 10.3, 5.0 Hz), 3.01, 2.82 – 2.69 (m), 2.49 (d, J = 2.3 Hz), 2.44 (d, J = 1.1 Hz), 2.20 (d, J = 4.6 Hz), 2.03 – 1.93 (m).

Compound 23: 1-[(3R)-3-[[2-[4-(4-methylpiperazin-1-yl)anilino]thieno[3,2-d]pyrimidin-4-yl]amino]pyrrolidin-1-yl]but-2-yn-1-one

Following the general procedure compound **8** (1 equivalent) was reacted with 2-butynoic acid (1.75 equivalent) under condition 2. HPLC analysis RT: 2.500, purity 96.8%. LCQTOF for $C_{25}H_{30}N_7OS$ $[M+H]^+$ calc: 476.22271, found: 476.2247. ^{1}H-NMR (500 MHz, DMSO-d6) δ 8.73 (d, J = 7.1 Hz), 7.92 – 7.89 (m), 7.73 (dd, J = 8.0, 3.7 Hz), 7.60 (d, J = 4.3 Hz), 7.07 (dd, J = 3.1, 1.9 Hz), 6.82 (d, J = 5.5 Hz), 4.71 – 4.62 (m), 3.03 – 3.00 (m), 2.22, 1.99, 1.91, 1.87, 1.19. ^{13}C-NMR (125 MHz, DMSO-d6) δ 172.69, 161.75, 158.71, 157.19, 152.32, 145.75, 134.51, 133.28, 123.84, 120.17 (d, J = 31.7 Hz), 116.55, 107.05, 88.34, 75.00, 55.02, 53.17, 49.34, 46.49, 45.91, 43.93, 30.99, 30.13, 29.52, 21.62.

Compound 24: 1-[(3R)-3-[[2-[4-(4-methylpiperazin-1-yl)anilino]thieno[3,2-d]pyrimidin-4-yl]amino]pyrrolidin-1-yl]propan-1-one

Following the general procedure compound **8** (1 equivalent) was reacted with Propionyl chloride (1.75 equivalent) under condition 1. HPLC analysis RT: 2.500 min, purity: 98%. LCQTOF for $C_{24}H_{32}N_7OS$ $[M+H]^+$ calc: 466.23836, found: 466.23700. ^{1}H-NMR (500 MHz, DMSO-d6) δ 8.69, 7.89 (t, J = 2.9 Hz), 7.67 (dd, J = 10.8, 3.7 Hz), 7.60 (t, J = 4.7 Hz), 7.06 (dd, J = 3.3, 1.5 Hz), 6.81 (d, J = 5.5 Hz), 4.64 – 4.58 (m), 3.77 (ddd, J = 45.1, 6.7, 3.9 Hz), 3.64 – 3.51 (m), 3.51 – 3.44 (m), 3.01 – 2.98 (m), 2.41 (t, J = 3.1 Hz), 2.26

– 2.19 (m), 2.18, 2.01 (ddq, J = 27.5, 8.0, 3.9 Hz), 1.32 – 1.08 (m), 0.95 (dt, J = 6.9, 4.3 Hz). ^{13}C-NMR (125 MHz, DMSO-d6) δ 171.83, 171.77, 161.70, 158.70, 157.21, 145.93, 134.47, 133.12, 123.87, 120.20, 120.06, 116.51, 116.46, 55.26, 51.53, 49.58, 46.28, 44.79, 44.19, 31.68, 30.02, 27.48, 27.10, 9.43.

Compound 25: 1-[(3R)-3-[[2-[(1-methylpyrazol-4-yl)amino]thieno[3,2-d]pyrimidin-4-yl]amino]pyrrolidin-1-yl]prop-2-en-1-one

Following the general procedure compound 9 (1 equivalent) was reacted with Acryloyl chloride (1.75 equivalent) under condition 1. HPLC analysis RT 2.553 min, purity 97.5% LCQTOF for $C_{17}H_{20}N_7OS$ $[M+H]^+$ calc: 370.14446, found: 370.14390. ^{1}H-NMR (500 MHz, DMSO-d6) δ 8.78, 7.89 (d, J = 5.5 Hz), 7.85, 7.69 (d, J = 5.0 Hz), 7.43, 7.07, 6.56 (ddd, J = 21.5, 10.1, 6.2 Hz), 6.12 (dd, J = 9.8, 4.3 Hz), 5.64 (t, J = 6.9 Hz), 4.68 (ddq, J = 25.2, 6.9, 3.7 Hz), 3.80 – 3.76 (m), 3.74, 3.73 – 3.70 (m), 3.64 (t, J = 4.3 Hz), 3.59 – 3.52 (m), 2.21 (ddq, J = 28.4, 7.8, 4.3 Hz), 2.04 (ddq, J = 26.5, 8.2, 3.9 Hz). ^{13}C-NMR (125 MHz, DMSO-d6) δ 163.96, 158.26, 133.08, 130.19, 129.98, 129.66, 127.33, 124.83, 123.90, 120.41, 51.68, 51.31 45.01, 44.46, 39.15, 31.66, 29.88.

Compound 26: 1-[(3R)-3-[[2-[(1-methylpyrazol-4-yl)amino]thieno[3,2-d]pyrimidin-4-yl]amino]pyrrolidin-1-yl]but-2-yn-1-one

Following the general procedure compound 9 (1 equivalent) was reacted with 2-butynoic acid (1.75 equivalent) under condition 2. HPLC analysis RT 2.573 min purity 97.8%. LCQTOF for $C_{18}H_{20}N_7OS$ $[M+H]^+$ calc: 382.4446, found: 382.1447. ^{1}H-NMR (500 MHz, DMSO-d6) δ 8.83, 7.90 (dd, J = 3.2, 2.3 Hz), 7.73, 7.43 (d, J = 1.1 Hz), 7.08 (t, J = 3.0 Hz), 4.69 (dp, J = 8.0, 3.9 Hz), 3.96 (dd, J = 6.6, 3.8 Hz), 3.75 (d, J = 1.1 Hz), 3.74 – 3.65 (m), 2.27 – 1.97 (m), 1.93 (d, J = 1.6 Hz). ^{13}C-NMR (125 MHz, DMSO-d6) δ 161.71, 158.16, 157.33, 155.11, 152.29, 133.23, 130.10, 124.73, 123.82, 120.50, 88.09, 75.01, 53.13, 50.72, 46.44, 43.91, 39.15, 3.51.

Compound 27: 1-[(3R)-3-[[2-[(1-methylpyrazol-4-yl)amino]thieno[3,2-d]pyrimidin-4-yl]amino]pyrrolidin-1-yl]propan-1-one

Following the general procedure compound 9 (1 equivalent) was reacted with Propionyl chloride (1.75 equivalent) under condition 1. HPLC analysis RT: 2.540 min, purity: 98%. LCQTOF for $C_{17}H_{22}N_7OS$ $[M+H]^+$ calc: 372.16011, found: 372.15970. ^{1}H-NMR

(500 MHz, DMSO-d6) δ 8.76, 7.89 (d, J = 5.5 Hz), 7.85 (d, J = 2.3 Hz), 7.68 – 7.61 (m), 7.43 (d, J = 2.3 Hz), 7.07, 4.64 (dp, J = 27.2, 3.4 Hz), 3.75, 3.47 (td, J = 8.1, 3.8 Hz), 2.27 – 2.22 (m), 2.16 (dt, J = 13.5, 4.3 Hz), 2.05 (dt, J = 7.8, 4.0 Hz), 1.96 (h, J = 4.0 Hz), 0.96 (t, J = 4.6 Hz).

Compound 28: 1-[(3S)-3-[[2-[4-(4-methylpiperazin-1-yl)anilino]thieno[3,2-d]pyrimidin-4-yl]amino]pyrrolidin-1-yl]prop-2-en-1-one

Following the general procedure compound 10 (1 equivalent) was reacted with Acryloyl chloride (1.75 equivalent) under condition 1. HPLC analysis RT 2.667 min, purity 98%. HRMS for $C_{24}H_{30}N_7OS$ $[M+H]^+$ calc: 464.2227, found: 464.2200. ^{1}H-NMR (500 MHz, DMSO-d6) δ 8.73, 7.90 (dd, J = 4.3, 2.5 Hz), 7.72 (dd, J = 12.8, 4.9 Hz), 7.63 – 7.59 (m), 7.07 (dd, J = 4.3, 1.7 Hz), 6.82 (dd, J = 7.4, 2.0 Hz), 6.56 (ddd, J = 32.0, 13.4, 8.2 Hz), 6.12 (ddd, J = 13.4, 4.3, 2.0 Hz), 5.64 (ddd, J = 12.9, 8.2, 1.9 Hz), 4.68 (dq, J = 28.1, 4.8 Hz), 3.78 – 3.72 (m), 3.63 (ddd, J = 8.1, 6.3, 4.7 Hz), 3.60 – 3.53 (m), 3.49 (dd, J = 8.4, 4.4 Hz), 3.00, 2.46, 2.21, 2.19 – 2.11 (m), 2.10 – 1.99 (m).

Compound 29: 1-[(3S)-3-[[2-[4-(4-methylpiperazin-1-yl)anilino]thieno[3,2-d]pyrimidin-4-yl]amino]pyrrolidin-1-yl]but-2-yn-1-one

Following the general procedure compound 10 (1 equivalent) was reacted with 2-butynoic acid (1.75 equivalent) under condition 2. HPLC analysis RT 2.520 min, purity 95.4%. LCQTOF for $C_{25}H_{30}N_7OS$ $[M+H]^+$ calc: 476.22217, found: 476.2232. 1H-NMR (500 MHz, DMSO-d6) δ 8.73 (d, J = 6.9 Hz), 7.90 (t, J = 2.7 Hz), 7.73 (dd, J = 8.2, 3.7 Hz), 7.59 (d, J = 5.0 Hz), 7.08 – 7.05 (m), 6.82 (d, J = 5.5 Hz), 4.66 (q, J = 3.7 Hz), 3.00, 2.43, 2.20, 1.99, 1.91, 1.87, 1.19.

Compound 30: 1-[(3S)-3-[[2-[(1-methylpyrazol-4-yl)amino]thieno[3,2-d]pyrimidin-4-yl]amino]pyrrolidin-1-yl]prop-2-en-1-one

Following the general procedure compound 11 (1 equivalent) was reacted with Acryloyl chloride (1.75 equivalent) under condition 1. HPLC analysis RT 2.733 min, purity 97%. LCQTOF for $C_{17}H_{20}N_7OS$ $[M+H]^+$ calc: 370.14446, found: 370.1424. ^{1}H-NMR (500 MHz, DMSO-d6) δ 8.78, 7.89 (dd, J = 3.2, 1.8 Hz), 7.85 (d, J = 1.6 Hz), 7.69 (d, J =

5.5 Hz), 7.43 (d, J = 1.1 Hz), 7.07 (t, J = 2.6 Hz), 6.56 (ddd, J = 21.1, 10.1, 6.2 Hz), 6.12 (ddd, J = 10.1, 2.9, 1.5 Hz), 5.64 (ddd, J = 7.8, 6.2, 1.4 Hz), 4.68 (dq, J = 25.6, 3.5 Hz), 3.99 (q, J = 4.3 Hz), 3.75, 2.31 – 2.16 (m), 2.15, 2.04 – 1.95 (m).

Compound 31: 1-[(3S)-3-[[2-[(1-methylpyrazol-4-yl)amino]thieno[3,2-d]pyrimidin-4-yl]amino]pyrrolidin-1-yl]but-2-yn-1-one

Following the general procedure compound 11 (1 equivalent) was reacted with 2-butynoic acid (1.75 equivalent) under condition 2. HPLC analysis RT: 2.567 min, purity 97.7% LCQTOF for $C_{18}H_{20}N_7OS$ $[M+H]^+$ calc: 382.14446, found: 382.14380. ^{1}H-NMR (500 MHz, DMSO-d6) δ 8.81, 7.89, 7.84, 7.70, 7.43, 7.08, 4.68 (dt, J = 8.5, 4.2 Hz), 3.96 (dd, J = 6.6, 3.9 Hz), 3.75, 2.22 (dq, J = 7.8, 3.5 Hz), 1.99, 1.93 (d, J = 2.3 Hz), 1.87, 1.19. ^{13}C-NMR (125 MHz,) δ 172.66, 161.75, 158.17, 157.34, 155.07, 152.32, 133.21, 130.10, 124.72, 120.52, 88.15, 74.99, 53.14, 50.73, 46.45, 43.92, 30.18, 21.58.

Compound 32: 1-[(3R)-3-[[[2-[4-(4-methylpiperazin-1-yl)anilino]thieno[3,2-d]pyrimidin-4-yl]amino]methyl]pyrrolidin-1-yl]prop-2-en-1-one

Following the general procedure compound 12 (1 equivalent) was reacted with Acryloyl chloride (1.75 equivalent) under condition 1. 17 mg of white solid obtained with yield of 16%. HPLC analysis: RT 2.527 min, purity 97.9%. LCQTOF for $C_{25}H_{32}N_7OS$ $[M+H]^+$, Calcd: 478.23836, found: 478.2349. ^{1}H-NMR (500 MHz, DMSO-d6) δ 8.63 (d, J = 2.7 Hz), 7.88 (d, J = 3.2 Hz), 7.67 (dt, J = 6.6, 3.4 Hz), 7.59 (t, J = 4.8 Hz), 7.06 (d, J = 3.2 Hz), 6.80 (dd, J = 5.5, 2.3 Hz), 6.52 (ddd, J = 9.8, 6.3, 3.7 Hz), 6.08 (ddd, J = 10.1, 2.7, 1.4 Hz), 5.60 (tt, J = 3.7, 1.5 Hz), 3.63 (q, J = 5.7 Hz), 3.51 (p, J = 4.5 Hz), 3.43 (dt, J = 7.8, 3.7 Hz), 3.20 (dd, J = 7.3, 3.9 Hz), 3.02 – 2.96 (m), 2.63 (dp, J = 30.9, 4.1 Hz), 2.43 – 2.39 (m), 2.18, 1.97 (ddq, J = 22.7, 7.6, 4.1 Hz), 1.77 – 1.61 (m). ^{13}C-NMR (125 MHz, DMSO-d6) δ 163.85, 161.57, 158.91, 157.65, 145.90, 134.61, 132.78, 130.16 (d, J = 55.1 Hz), 126.99, 123.94, 120.23, 116.46, 106.92, 55.29, 50.12, 49.65, 46.31, 45.83, 45.28, 43.01, 39.13, 37.25, 29.67, 27.94.

Compound 33: 1-[(3R)-3-[[[2-[4-(4-methylpiperazin-1-yl)anilino]thieno[3,2-d]pyrimidin-4-yl]amino]methyl]pyrrolidin-1-yl]but-2-yn-1-one

Following the general procedure compound 12 (1 equivalent) was reacted with 2-butynoic acid (1.75 equivalent) under condition 2. HPLC analysis RT: 2.540 min, purity: 99% LCQTOF for $C_{26}H_{32}N_7OS$ $[M+H]^+$ calc: 490.23836, found: 490.23760. ^{1}H-NMR (500 MHz, DMSO-d6) δ 8.66, 7.88 (d, J = 3.2 Hz), 7.70 (d, J = 5.5 Hz), 7.59 (d, J = 5.5 Hz), 7.06, 6.80 (d, J = 5.5 Hz), 3.72 – 3.61 (m), 3.54 – 3.40 (m), 3.13 (dd, J = 7.4, 4.0 Hz), 3.01 – 2.96 (m), 2.69 – 2.57 (m), 2.46, 2.43 – 2.39 (m), 2.17, 1.96, 1.93, 1.76 – 1.63 (m). ^{13}C-NMR (125 MHz, DMSO-d6) δ 161.58, 158.88, 157.65, 152.21, 145.89, 134.59, 132.81, 123.96, 120.15, 116.49, 106.89, 87.78, 75.13, 55.27, 51.61, 49.64, 48.96, 47.37, 46.29, 44.71, 42.90, 38.38, 37.76, 29.01, 28.32, 3.75.

Compound 34: 1-[(3R)-3-[[[2-[(1-methylpyrazol-4-yl)amino]thieno[3,2-d]pyrimidin-4-yl]amino]methyl]pyrrolidin-1-yl]prop-2-en-1-one

Following the general procedure compound 13 (1 equivalent) was reacted with Acryloyl chloride (1.75 equivalent) under condition 1. HPLC analysis: RT 2.553 min, purity 97.4%. LCQTOF for $C_{18}H_{22}N_7OS$ $[M+H]^+$, Calcd: 384.16011, found: 384.1595. ^{1}H-NMR (500 MHz, DMSO-d6) δ 8.70, 7.91 – 7.81 (m), 7.65, 7.43 (d, J = 2.5 Hz), 7.07 (d, J = 3.2 Hz), 6.52 (ddd, J = 10.3, 6.3, 4.0 Hz), 6.11 – 6.06 (m), 5.60 (dt, J = 6.2, 1.9 Hz), 3.75, 3.68 – 3.60 (m), 3.52 (dd, J = 7.4, 4.2 Hz), 3.44 – 3.41 (m), 3.19 (dd, J = 7.4, 4.0 Hz), 2.69 – 2.54 (m), 1.96 (ddt, J = 23.3, 7.6, 3.7 Hz), 1.78 – 1.61 (m). ^{13}C-NMR (125 MHz, DMSO-d6) δ 163.90, 161.77, 158.46, 157.81, 132.68, 130.13 (d, J = 51.7 Hz), 127.05, 124.97, 124.02, 120.32, 50.08, 49.67, 45.83, 45.24, 37.13, 29.70, 27.89.

Compound 35: 1-[(3R)-3-[[[2-[(1-methylpyrazol-4-yl)amino]thieno[3,2-d]pyrimidin-4-yl]amino]methyl]pyrrolidin-1-yl]but-2-yn-1-one

Following the general procedure compound 13 (1 equivalent) was reacted with 2-butynoic acid (1.75 equivalent) under condition 2. HPLC analysis RT 2.540, purity 99% LCQTOF for $C_{19}H_{22}N_7OS$ $[M+H]^+$ calc: 396.16011, found: 396.16000. ^{1}H-NMR (500 MHz, DMSO-d6) δ .73, 7.87 (d, J = 3.2 Hz), 7.67, 7.43, 7.07, 3.75, 3.71 – 3.60 (m), 3.54 – 3.40 (m), 2.70 – 2.59 (m), 1.94 (d, J = 8.2 Hz), 1.75 – 1.65 (m), 1.57 (dd, J = 5.5, 2.5 Hz), 1.24

– 0.96 (m). ^{13}C-NMR (125 MHz, DMSO-d6) δ 161.77, 158.42, 157.79, 157.17, 152.15, 132.71, 129.98, 124.95, 124.01, 120.29, 87.98, 74.95, 51.60, 47.36, 44.69, 33.88, 28.31, 25.85, 3.74.

Compound 36: 1-[(3S)-3-[[[2-[4-(4-methylpiperazin-1-yl)anilino]thieno[3,2-d]pyrimidin-4-yl]amino]methyl]pyrrolidin-1-yl]prop-2-en-1-one

Following the general procedure compound 14 (1 equivalent) was reacted with Acryloyl chloride (1.75 equivalent) under condition 1.HPLC analysis RT: 2.527 min, purity 98% LCQTOF for $C_{25}H_{32}N_7OS$ $[M+H]^+$ calc: 478.23836, found: 478.22470. ^{1}H-NMR (500 MHz, DMSO-d6) δ 8.65, 7.88 (d, J = 3.2 Hz), 7.69 (d, J = 6.2 Hz), 7.59 (d, J = 7.8 Hz), 7.06 (d, J = 3.2 Hz), 6.81 (d, J = 5.3 Hz), 6.57 – 6.43 (m), 6.12 – 6.04 (m), 5.63 – 5.56 (m), 3.72 (t, J = 3.3 Hz), 3.63 (q, J = 4.9 Hz), 3.52 – 3.48 (m), 3.00 (t, J = 3.1 Hz), 2.71 – 2.62 (m), 2.58 (q, J = 4.2 Hz), 2.44 (t, J = 3.0 Hz), 2.20, 2.03 – 1.88 (m), 1.69 (dt, J = 25.2, 4.6 Hz).

Compound 37: 1-[(3S)-3-[[[2-[4-(4-methylpiperazin-1-yl)anilino]thieno[3,2-d]pyrimidin-4-yl]amino]methyl]pyrrolidin-1-yl]but-2-yn-1-one

Following the general procedure compound 14 (1 equivalent) was reacted with 2-butynoic acid (1.75 equivalent) under condition 2. HPLC analysis RT: 2.540 min, purity: 96%. LCQTOF for $C_{26}H_{32}N_7OS$ $[M+H]^+$ calc: 490.23836, found: 490.23850. ^{1}H-NMR (500 MHz,) δ 8.68, 7.88 (d, J = 3.9 Hz), 7.71 (d, J = 4.8 Hz), 7.60 (d, J = 4.6 Hz), 7.07 – 7.04 (m), 6.82 (d, J = 5.5 Hz), 3.72 – 3.59 (m), 3.51 (d, J = 6.6 Hz), 3.29 – 3.21 (m), 3.15 – 3.09 (m), 3.03, 2.68 – 2.58 (m), 2.55, 2.27, 1.96, 1.93, 1.75 – 1.63 (m).

Compound 38: 1-[(3S)-3-[[[2-[(1-methylpyrazol-4-yl)amino]thieno[3,2-d]pyrimidin-4-yl]amino]methyl]pyrrolidin-1-yl]prop-2-en-1-one

Following the general procedure compound 15 (1 equivalent) was reacted with Acryloyl chloride (1.75 equivalent) under condition 1. HPLC analysis RT: 2.547 min, purity 98%. LCQTOF for $C_{18}H_{22}N_7OS$ $[M+H]^+$ calc: 384.16011, found: 384.15970. ^{1}H-MR (500 MHz, DMSO-d6) δ 8.72, 7.93 – 7.80 (m), 7.67, 7.43 (d, J = 2.7 Hz), 7.07 (d, J = 3.2 Hz), 6.58 – 6.47 (m), 6.13 – 6.04 (m), 5.64 – 5.56 (m), 3.75, 3.68 – 3.58 (m), 3.49 (t, J =

3.9 Hz), 3.26 (t, J = 4.2 Hz), 2.67 (d, J = 11.2 Hz), 2.62 – 2.54 (m), 2.14 (t, J = 4.8 Hz), 1.97 (ddq, J = 23.6, 7.6, 4.0 Hz), 1.86 (p, J = 4.6 Hz), 1.80 – 1.62 (m). ^{13}C-NMR (125 MHz,) δ 174.32, 163.87, 161.76, 158.42, 157.79, 132.68, 130.10 (d, J = 68.9 Hz), 127.07, 124.95, 124.02, 120.29, 50.06, 49.67, 49.01, 45.82, 30.64, 17.75.

Compound 39: 1-[(3S)-3-[[[2-[(1-methylpyrazol-4-yl)amino]thieno[3,2-d]pyrimidin-4-yl]amino]methyl]pyrrolidin-1-yl]but-2-yn-1-one

Following the general procedure compound 15 (1 equivalent) was reacted with 2-butynoic acid (1.75 equivalent) under condition 2. HPLC analysis RT: 2.547 min, purity 97%. ^{1}H-NMR (500 MHz, DMSO-d6) δ 8.73, 7.92 – 7.81 (m), 7.68, 7.43, 7.07, 3.75, 3.72 – 3.59 (m), 3.54 – 3.36 (m), 3.12 (dd, J = 7.4, 4.0 Hz), 2.70 – 2.58 (m), 1.95 (d, J = 8.0 Hz), 1.69 (q, J = 4.6 Hz). ^{13}C-NMR (125 MHz,) δ 161.76, 158.42, 157.79, 152.20, 132.72, 129.99, 124.94, 124.01, 120.30, 87.83, 75.11, 51.60, 48.96, 47.36, 44.69, 37.64, 29.00, 28.31, 3.74.

Compound 40: 1-[(3R)-3-[[2-[4-(4-methylpiperazin-1-yl)anilino]thieno[3,2-d]pyrimidin-4-yl]amino]piperidin-1-yl]prop-2-en-1-one

Following the general procedure compound 16 (1 equivalent) was reacted with Acryloyl chloride (1.75 equivalent) under condition 1. HPLC analysis RT 2.540 min, purity 97% LCQTOF for $C_{25}H_{32}N_7OS$ $[M+H]^+$ calc: 478.23836, found: 478.23810. ^{1}H-NMR (500 MHz, DMSO-d6) δ 8.65 (d, J = 5.3 Hz), 7.89 (d, J = 3.2 Hz), 7.55 (d, J = 5.3 Hz), 7.43 (d, J = 4.8 Hz), 7.06 (d, J = 3.2 Hz), 6.77 (d, J = 3.4 Hz), 6.05 (dd, J = 38.3, 8.6 Hz), 5.57 (dd, J = 65.2, 6.9 Hz), 4.16, 4.01 (t, J = 6.6 Hz), 3.46 (d, J = 8.7 Hz), 3.18 – 3.08 (m), 2.96, 2.41, 2.18, 1.99 (d, J = 7.6 Hz), 1.79 (d, J = 7.1 Hz), 1.67 – 1.57 (m), 1.40.

Compound 41: 1-[(3R)-3-[[2-[4-(4-methylpiperazin-1-yl)anilino]thieno[3,2-d]pyrimidin-4-yl]amino]piperidin-1-yl]but-2-yn-1-one

Following the general procedure compound 16 (1 equivalent) was reacted with 2-butynoic acid (1.75 equivalent) under condition 2. HPLC analysis RT: 2.560 min, purity 98% LCQTOF for $C_{26}H_{32}N_7OS$ $[M+H]^+$ calc: 490.23836, found: 490.23740. ^{1}H-NMR (500 MHz, DMSO-d6) δ 8.67 (d, J = 5.9 Hz), 7.90 (t, J = 3.3 Hz), 7.60 (d, J = 5.5 Hz), 7.54 (d,

J = 5.5 Hz), 7.44 (dd, J = 8.4, 4.5 Hz), 7.10 – 7.04 (m), 6.82 – 6.76 (m), 4.14 (d, J = 6.6 Hz), 3.49 – 3.41 (m), 2.99, 2.42, 2.18, 2.01, 1.88 – 1.77 (m), 1.67, 1.49 – 1.14 (m). ^{13}C-NMR (125 MHz, DMSO-d6) δ 161.80, 158.80, 157.09, 152.75, 145.90, 134.45, 133.19, 123.82, 120.35, 120.06, 116.53, 106.97 (d, J = 68.9 Hz), 89.57, 73.56, 55.26, 50.78, 49.65, 46.29, 41.39, 30.75, 30.09, 25.18, 23.50.

Compound 42: 1-[(3R)-3-[[2-[(1-methylpyrazol-4-yl)amino]thieno[3,2-d]pyrimidin-4-yl]amino]piperidin-1-yl]prop-2-en-1-one

Following the general procedure compound 17 (1 equivalent) was reacted with Acryloyl chloride (1.75 equivalent) under condition 1. HPLC analysis RT: 2.580 min, purity 97% LCQTOF for $C_{18}H_{22}N_7OS$ $[M+H]^+$ calc: 384.16011, found: 384.15960. ^{1}H-NMR (500 MHz, DMSO-d6) δ 8.72 (d, J = 5.9 Hz), 7.88 (d, J = 3.2 Hz), 7.38 (d, J = 18.5 Hz), 7.06, 6.05 (dd, J = 27.2, 10.1 Hz), 5.57 (dd, J = 54.6, 7.0 Hz), 4.19 – 3.94 (m), 3.70, 3.13 (d, J = 3.2 Hz), 3.04 – 2.57 (m), 2.00 (d, J = 7.8 Hz), 1.79 (d, J = 8.2 Hz), 1.71 – 1.56 (m), 1.49 – 1.37 (m). ^{13}C-NMR (125 MHz, DMSO-d6) δ 164.96, 162.05, 158.40, 157.17, 133.02, 130.14, 129.01, 127.94, 124.79, 123.92, 120.54, 50.08, 49.14, 46.79, 45.87, 42.27, 25.64, 24.10.

Compound 43: 1-[(3R)-3-[[2-[(1-methylpyrazol-4-yl)amino]thieno[3,2-d]pyrimidin-4-yl]amino]piperidin-1-yl]but-2-yn-1-one

Following the general procedure compound 17 (1 equivalent) was reacted with 2-butynoic acid (1.75 equivalent) under condition 2. HPLC analysis RT 2.633 min, purity 97%. LCQTOF for $C_{19}H_{22}N_7OS$ $[M+H]^+$ calc: 396.16011, found: 396.1583. ^{1}H-NMR (500 MHz, DMSO-d6) δ 8.78, 7.89 (t, J = 3.1 Hz), 7.38 (d, J = 16.9 Hz), 7.06, 4.23 – 4.10 (m), 3.74, 3.09 (t, J = 8.5 Hz), 2.96 – 2.88 (m), 2.68 (t, J = 6.7 Hz), 2.01, 1.92, 1.87, 1.58 – 1.54 (m). ^{13}C-NMR (125 MHz, DMSO-d6) δ 172.66, 161.88, 158.27, 157.23, 152.74, 133.14, 129.86, 124.81, 120.54, 90.11, 73.38, 50.77, 48.05, 47.02, 45.68, 33.84, 25.82, 24.99, 21.59.

Compound 44: 1-[(3S)-3-[[2-[4-(4-methylpiperazin-1-yl)anilino]thieno[3,2-d]pyrimidin-4-yl]amino]piperidin-1-yl]prop-2-en-1-one

Following the general procedure compound 18 (1 equivalent) was reacted with Acryloyl chloride (1.75 equivalent) under condition 1. HPLC analysis RT: 2.467 min, purity: 95% LCQTOF for $C_{25}H_{32}N_7OS$ $[M+H]^+$ calc: 478.23836, found: 478.23940. ^{1}H-NMR (500 MHz, DMSO-d6) δ 8.66 (d, J = 5.3 Hz), 7.89 (d, J = 3.2 Hz), 7.56 (d, J = 5.5 Hz), 7.43 (d, J = 4.6 Hz), 7.06 (d, J = 3.2 Hz), 6.77 (d, J = 3.4 Hz), 6.27 – 5.91 (m), 5.75 (dd, J = 42.9, 6.1 Hz), 5.44 (dd, J = 12.1, 7.6 Hz), 4.20 – 4.12 (m), 4.01 (t, J = 8.5 Hz), 3.25 – 3.03 (m), 2.96, 2.83 – 2.59 (m), 2.41, 2.18, 2.00 (d, J = 10.3 Hz), 1.80 (d, J = 10.5 Hz), 1.62 (h, J = 7.8 Hz), 1.45 – 1.26 (m). ^{13}C-NMR (125 MHz, DMSO-d6) δ 165.08, 161.82, 158.80, 156.98, 145.83, 134.48, 133.03, 128.94, 127.77, 123.87, 120.21, 116.34 (d, J = 100.0 Hz), 55.24, 50.11, 49.63, 46.83, 46.26, 45.82, 42.27, 40.62, 39.52, 30.95, 25.61, 24.10.

Compound 45: 1-[(3S)-3-[[2-[4-(4-methylpiperazin-1-yl)anilino]thieno[3,2-d]pyrimidin-4-yl]amino]piperidin-1-yl]but-2-yn-1-one

Following the general procedure compound 18 (1 equivalent) was reacted with 2-butynoic acid (1.75 equivalent) under condition 2. HPLC analysis RT: 2.540 min, purity 97%. ^{1}H-NMR (500 MHz, DMSO-d6) δ 8.67 (d, J = 5.7 Hz), 7.90 (t, J = 3.3 Hz), 7.60 (d, J = 5.5 Hz), 7.54 (d, J = 5.5 Hz), 7.44 (dd, J = 8.6, 4.5 Hz), 7.06 (dd, J = 3.3, 2.2 Hz), 6.79 (dd, J = 5.4, 3.8 Hz), 4.14 (d, J = 6.9 Hz), 3.45 (dd, J = 7.6, 5.0 Hz), 3.14 – 3.07 (m), 2.99, 2.43, 2.18, 2.01, 1.87 – 1.77 (m), 1.66, 1.47 – 1.31 (m). ^{13}C-NMR (125 MHz, DMSO-d6) δ 161.87, 158.80, 157.09, 156.83, 152.55, 145.88, 134.57, 133.07, 123.82, 120.36, 120.07, 116.54, 106.99 (d, J = 62.0 Hz), 89.87, 89.58, 73.49, 55.43, 50.78, 49.61, 47.48, 46.22, 30.08, 25.17, 23.50, 3.49.

Compound 46: 1-[(3S)-3-[[2-[(1-methylpyrazol-4-yl)amino]thieno[3,2-d]pyrimidin-4-yl]amino]piperidin-1-yl]prop-2-en-1-one

Following the general procedure compound 19 (1 equivalent) was reacted with Acryloyl chloride (1.75 equivalent) under condition 1. HPLC analysis RT: 2.573 min, purity: 96%. LCQTOF for $C_{18}H_{22}N_7OS$ $[M+H]^+$ calc: 384.16011, found: 384.15990. ^{1}H-NMR

(500 MHz, DMSO-d6) δ 8.75 (d, J = 5.7 Hz), 7.88 (d, J = 3.2 Hz), 7.38 (d, J = 19.2 Hz), 7.07, 6.90 – 6.73 (m), 6.05 (dd, J = 26.9, 10.6 Hz), 5.57 (dd, J = 53.1, 7.1 Hz), 4.16 (t, J = 8.2 Hz), 4.06 – 3.96 (m), 3.71, 3.05 (dt, J = 46.7, 7.3 Hz), 2.70 (dt, J = 50.8, 7.6 Hz), 2.00 (d, J = 7.8 Hz), 1.79 (d, J = 3.2 Hz), 1.65 (q, J = 7.1 Hz), 1.51 – 1.36 (m). ^{13}C-NMR (125 MHz, DMSO-d6) δ 164.94, 162.05, 158.40, 157.18, 133.03, 130.13, 128.99, 127.97, 127.61, 124.79, 123.92, 120.54, 50.08, 46.79, 45.87, 42.27, 25.65, 24.11.

Compound 47: 1-[(3S)-3-[[2-[(1-methylpyrazol-4-yl)amino]thieno[3,2-d]pyrimidin-4-yl]amino]piperidin-1-yl]but-2-yn-1-one

Following the general procedure compound 19 (1 equivalent) was reacted with 2-butynoic acid (1.75 equivalent) under condition 2. HPLC analysis RT: 2.620 min, purity 97%. LCQTOF for $C_{19}H_{22}N_7OS$ $[M+H]^+$ calc: 396.16011, found: 396.19560. ^{1}H-NMR (500 MHz, DMSO-d6) δ 8.74, 7.89 (t, J = 3.2 Hz), 7.38 (d, J = 18.3 Hz), 7.06 (t, J = 3.7 Hz), 4.23 – 4.06 (m), 3.94 (d, J = 10.3 Hz), 3.73, 3.09 (t, J = 8.6 Hz), 2.99 – 2.87 (m), 2.68 (t, J = 7.1 Hz), 1.81 (d, J = 8.9 Hz), 1.49 – 1.36 (m), 1.18. ^{13}C- NMR (125 MHz, DMSO-d6) δ 172.73, 162.01, 158.33, 152.75, 133.15, 129.88, 124.83, 123.85, 120.53, 89.76, 73.38, 50.78, 47.03, 45.69, 41.38, 33.84, 29.98, 21.69, 3.88.

Compound 48: N-[4-[[[2-[4-(4-methylpiperazin-1-yl)anilino]thieno[3,2-d]pyrimidin-4-yl]amino]methyl]phenyl]prop-2-enamide

Following the general procedure compound 20 (1 equivalent) was reacted with Acryloyl chloride (1.75 equivalent) under condition 1. HPLC analysis RT: 2.733 min, purity 96%. LCQTOF for $C_{27}H_{30}N_7OS$ $[M+H]^+$ calc: 500.22271, found: 500.2232. ^{1}H-NMR (500 MHz, DMSO-d6) δ 10.13, 8.65, 8.17 (t, J = 3.5 Hz), 7.91 (d, J = 3.2 Hz), 7.68, 7.53 (d, J = 4.8 Hz), 7.44 (d, J = 5.5 Hz), 7.23 (t, J = 4.7 Hz), 7.05 (dd, J = 13.2, 4.0 Hz), 6.71 (d, J = 5.5 Hz), 6.39 (dd, J = 10.2, 6.1 Hz), 6.21 (dd, J = 10.2, 1.3 Hz), 5.71 (dd, J = 7.3, 1.4 Hz), 4.66 (d, J = 3.7 Hz), 3.01 – 2.91 (m), 2.40 (t, J = 3.1 Hz), 2.18. ^{13}C-NMR (125 MHz, DMSO-d6) δ 158.87, 153.35, 141.01, 140.06, 134.53, 132.87, 128.99, 123.90, 121.09, 120.04, 117.17 (d, J = 55.1 Hz), 116.44, 79.45, 55.29, 49.63, 46.29, 43.94, 40.28 (d, J = 51.7 Hz), 39.78 (d, J = 48.3 Hz), 28.65.

Compound 49: N-[4-[[[2-[4-(4-methylpiperazin-1-yl)anilino]thieno[3,2-d]pyrimidin-4-yl]amino]methyl]phenyl]but-2-ynamide

Following the general procedure compound 20 (1 equivalent) was reacted with 2-butynoic acid (1.75 equivalent) under condition 2. LCQTOF for $C_{28}H_{30}N_7OS$ $[M+H]^+$ calc: 512.22271, found: 512.22270. ^{1}H-NMR (500 MHz, DMSO-d6) δ 10.60, 8.64 (d, J = 4.1 Hz), 7.90 (dd, J = 6.3, 3.1 Hz), 7.63, 7.53 (d, J = 5.5 Hz), 7.42 (t, J = 5.0 Hz), 7.21 (t, J = 4.7 Hz), 7.05 (dd, J = 12.6, 3.9 Hz), 6.76 (d, J = 5.3 Hz), 6.70 (d, J = 5.5 Hz), 6.53 – 6.36 (m), 4.63 (d, J = 3.7 Hz), 4.56 (d, J = 3.7 Hz), 2.97, 2.41, 2.18, 1.99. ^{13}C-NMR (125 MHz, DMSO-d6) δ 161.65, 158.80, 157.46, 151.08, 149.09, 145.74, 141.15, 139.12, 134.41, 132.90, 129.21, 123.87, 122.59, 119.87, 118.26, 116.38, 115.03, 112.81, 106.85, 84.63, 76.40, 55.29, 49.60, 46.31, 43.89, 3.73.

Appendix C

STATISTICAL ANALYSIS

CHIRALITY

Variable	Analysis of Variance (tmp) Marked effects are significant at p < .05000							
	SS	df	MS	SS	df	MS	F	p
pIC50	0.006380	1	0.006380	7.811713	15	0.520781	0.012250	0.913337

Chiral	2-Way Tables of Descriptive Statistics (tmp) N=17 (No missing data in dep. var. list)		
	pIC50	pIC50	pIC50
R	8.067278	8	0.933598
S	8.106090	9	0.462395
All Grps	8.087826	17	0.699021

R1

Variable	Analysis of Variance (tmp) Marked effects are significant at p < .05000							
	SS	df	MS	SS	df	MS	F	p
pIC50	0.092837	1	0.092837	7.725256	15	0.515017	0.180260	0.677177

R1	2-Way Tables of Descriptive Statistics (tmp) N=17 (No missing data in dep. var. list)		
	pIC50	pIC50	pIC50
Piperazine	8.009444	8	0.457754
Pyrazole	8.157498	9	0.884483
All Grps	8.087826	17	0.699021

R2

Variable	Analysis of Variance (tmp) Marked effects are significant at p < .05000							
	SS	df	MS	SS	df	MS	F	p
pIC50	0.009378	1	0.009378	7.808715	15	0.520581	0.018014	0.895016

R2	2-Way Tables of Descriptive Statistics (tmp) N=17 (No missing data in dep. var. list)		
	pIC50	pIC50	pIC50
Acrylamide	8.102986	12	0.835694
2-Butynamide	8.051440	5	0.177821
All Grps	8.087826	17	0.699021

L

Variable	Analysis of Variance (tmp) Marked effects are significant at p < .05000							
	SS	df	MS	SS	df	MS	F	p
pIC50	2.850220	2	1.425110	4.967872	14	0.354848	4.016114	0.041830

L	2-Way Tables of Descriptive Statistics (tmp) N=17 (No missing data in dep. var. list)		
	pIC50	pIC50	pIC50
pyrrolidine	7.466442	5	0.953592
met-pyrrolidine	8.485313	4	0.040118
piperidine	8.277447	8	0.435184
All Grps	8.087826	17	0.699021